Addis Ababa University

Addis Ababa Institute of Technology

School of Civil and Environmental Engineering

Addis Ababa, Ethiopia

INVESTIGATION OF WATER SUPPLY SOURCES SUSTAINABILITY THE CASE OF HARAR TOWN, ETHIOPIA

By

Bedasa Abrahim Mummed

A Dissertation Submitted to Addis Ababa Institute of Technology, Addis Ababa University

Presented in Partial Fulfillment of Ph.D. Degree in Civil Engineering, Hydraulic Engineering Specialization, in the School of Civil and Environmental Engineering

Supervisor: Professor Yilma Seleshi

September, 2024

DECELERATION

I, the undersigned, declare that this dissertation is based on my original work and that it has not been presented for a degree in any other university. All sources of materials have been duly acknowledged.

Submitted by

Bedasa Abrahim	___________	**05/09/2024**
Student	**Signature**	**Date**

This dissertation has been submitted for examination with my approval as supervisor of the dissertation.

DOCTORAL DISSERTATION APPROVAL SHEET

Addis Ababa University, Addis Ababa Institute of Technology, School of Civil and Environmental Engineering

This is to certify that the dissertation presented by Bedasa Abrahim Mummed entitled: "**Investigation of Water Supply Sources Sustainability the Case of Harar Town, Ethiopia**" and submitted in partial fulfillment of the requirements for the degree of Doctor of Philosophy in Civil Engineering (Hydraulic Engineering) complies with the regulations of the University and meets the accepted standards with respect to originality and quality.

By:

Bedasa Abrahim	**Date**

Signed by the Examining Committee:

Prof. Yilma Seleshi, Supervisor	**Date**
Prof. Tirusew Asefa, External Examiner	**Date**
Dr. Agizew Nugussie, Internal Examiner	**Date**
Dr. Abrham Gebre, Dan SCEE	**Date**
Chair, Examining Committee	**Date**

ACKNOWLEDGEMENTS

First of all, I would like to thank Almighty Allah for his never-ending love and care in my life. This study would not have been possible without appropriate supervision, care, and motivation from different people and organizations. I want to express my genuine appreciation to my supervisor Prof. Yilma Seleshi for his great support, kind supervision, and encouragement during my Ph.D. studies. I have been extremely lucky to have supervisor who cared so much about my research work, and who responded to my questions and queries so promptly for the accomplishment of my Ph.D. study work. My acknowledgments are also extended to Ministry of Water and Energy of Ethiopia (MoWEE), the National Meteorological Agency (NMA), Mapping Agency of Ethiopia, Ministry of Agriculture (MOA), Harar Water Supply and Sewerage Authority (HWSSA) and US Geological Survey for the LANDSAT imagery and Digital Elevation Model), and the Food and Agriculture Organization (FAO) of the United Nations me for providing hydro-meteorological, soil map and geo-spatial data and important information from their Library resources and websites including for the study area. Moreover, I acknowledge the Ethiopian Ministry of Water and Energy staff that participated in field data collection year-round without any frustrations during all stream flow data recording time at any weather conditions. I am grateful to Addis Ababa University, Addis Ababa Institute of Technology (AAIT) for their follow up and great contribution and motivation to quickly finalize my Ph.D. study work. I appreciate all experts that participated for responding My questioners on time and contribution of their experience and knowledge in their field to My study. I am very grateful to colleagues at Haramaya University. I indebted many thanks to all my parents for their continuous inspiration during the research duration. Last but not least, I would like to thank my mother Qemeriya Beker and my wife Derartu Mehadi for their consistent dearest, attention and help throughout the study period.

DEDICATIONS

To My respected mother and father for showing me the pathway to success and always dedicated for my education My very kind and upright wife Derartu Mehadi and my lovely daughters Ihisan, Umran, Nemira, Iqama, Urwa and Newal for assisting me with your specific efforts and endurance towards achievement.

LIST OF ACRONYMS

AHP - Analytical Hierarchy Process

AR5 - Fifth Assessment Report

AWWA - American Water Works Association

CFSR - Climate Forecast System Reanalysis

CMhyd - Climatic Model Data for the Hydrologic Modeling Tool

CI - Consistency Index

CR - Consistency Ratio

CORDEX - Coordinated Regional Climate Downscaling Experiment

CSA - Central Statics Agency

CV – Coefficient of Variation

DEM - Digital Elevation Models

DMs - Decision Makers

EC - Evaluation Criteria

FAO - Food and Agriculture Organization

GCMs – Global Climate Models

GHGs - Greenhouse Gases

GIS - Global Information System

HWSSA - Harar Water Supply and Sewerage Authority

HRUs - Hydrologic Response Units

LULC - Land Use/Land Cover

LULCC - Land Use/Land Cover Change

IPCC - Intergovernmental Panel on Climate Change

ICP - Inter-Censual Population

ICPS - Inter-Censual Population Survey

IWA - International Water Association

MCDA - Multi-Criteria Decision Analysis

MERRA-2 - Modern-Era Retrospective Analysis for Research and Applications, version 2

MVPF - Medium Variant Population Forecast

MOWR - Ministry of Water Resources

NCEI - National Centers for Environmental Information

NSE - Nash-Sutcliffe Efficiency

NetCDF – network Common Data Form

NMA - National Meteorological Agency

NMIE - National Meteorological Institute of Ethiopia

NMSA – National Meteorological Statics Agency

NASA - Aeronautics and Space Administration

PBIAS – Percent Bias

POWER - Prediction of Worldwide Energy Resources

RCMs - Regional Climate Models

RI - Random Index

RCMs – Regional Climate Models

RCPs - Regional Concentration Pathways

SCS - Soil Conservation Services

SD - Sustainable Development

SUFI-2 - Sequential Uncertainty Fitting Index-2

SWAT - Soil and Water Assessment Tool

SWAT - CUP- Soil and Water Assessment Tools Calibration and Uncertainty Program

UN- United Nations

UNICEF - United Nations International Children's Emergency Fund

UTM - Universal Transverse Mercator

WAMM - Weighted Arithmetic Mean Method

WCED -World Commission on Environment and Development

WCRP - World Climate Research Program

WGS – World Geodetic System

WHO - World Health Organizations

WMO – World Meteorological Organization

ABSTRACT

In the present era sustainable water system is a concept that consuming the provided water sufficiently for a given need by preserving for future needs. In this research the water supply sources sustainability of Harar town was investigated in a more comprehensive approach. using the main and evaluation criteria that determine the sustainability of water supply sources. The sustainability analysis was performed from the experts' preferences in the field of water sectors by distributing questioners to respond on the preferences of main criteria, evaluation criteria and alternative scenarios. The average aggregation of the experts' preferences was used to attain final decision of influential evaluation criteria. The influential evaluation criteria used to examine the relative importance of the alternative water supply sources for the town.

The water supply sources sustainability were affected by various driving factors such as population increase, climate change and LULC change and it is important to quantify these effects for better understanding of their impacts on the water resources. The water supply sources effects due increasing population in the future is determined by analyzing the demand and supply data until the end of the water supply sources identification period of 2070. On the other hand, the climate change effects also have a considerable effect on the sustainability of water supply sources and that needs special attention to determine the extent of the effects. Similarly, LULC change effects on water supply sources sustainability was quantified. In this research climate change impacts on the water supply sources from historical (1979-2014) to future (2024-207) periods were identified using hydrological model under two emission scenarios. The climate models (CORDEX RCMS) were used in this research to generate the climate variables used for hydrological model simulation. The LULC change effects on the water supply sources were examined under LULC data for period (2001 to 2020). The LULC map that used for this research was developed from Landsat image by employing supervised image classification under ArcGIS software. The quantification of climate change and LULC change process were taken place by SWAT model that requires various spatial and temporal data. During SWAT model setup process the study area watershed of the upper Erer subbasin (466 km^2) were produced using the watershed delineation process. Nevertheless, hydrometeorological required for SWAT model are scarce and no continuous data. Despite the inadequacy of hydrometeorological data especially the rainfall distribution is variable both in amount and existence. The occurrence of rainfall on the stations with in a time gap probably affecting the areal rainfall estimation. Hence, in this research the spatiotemporal rainfall distribution implications on areal rainfall estimation characteristics were examined using more comprehensive method that involves the spatiotemporal rainfall distribution and mutual rainfall occurrence for the stations. Moreover, stream flow data were inadequate and continuous data are unavailable in the region. To fill the data gap, the streamflow data was measured on site for the year 2020 to 2021 using the installed staff gauge. The discharge was estimated from stream flow records using the rating curve.

The water supply sources sustainability investigation output indicates that most influential evaluation criteria were capital cost (12.33 %), political (7.48 %), seasonality of sources (6.16 %), and availability (5.99 %). The alternative scenario analysis showed that the advanced potable water supply sources scenario was the best, followed by potable water supply and the business as usual is the least preference. The population estimation of the town using the United Nations Medium Variant Population Forecast indicates that the current population of the town was 127,854 and it becomes 929,418 by the year 2070. The daily water demand was higher than supply each year. In the region the increase of population along with other driving factors will deteriorate the future condition of the water supply sources. In this study autocalibration for SWAT model was used to identify sensitive parameters in the study area and manual calibration used to calibrate and validate. The SWAT model performance measures was within satisfactory range of PBIAS ≤ (±25%), R^2 > 0.8 and NSE > 0.5. The calibrated and validated SWAT model output indicates that monthly mean temperature varies from 0.04 to 6.25^{0}C under RCP-4.5, and varies from 0.03 to 6.59^{o}C under RCP-8.5. The monthly mean precipitation to be decline by 90.71 mm and rise by 211. 22 mm under RCP-4.5 and decline by 84.97 mm and rise by 235.62 mm under RCP-8.5. The LULC change and their effect examination indicates that agricultural lands (3.97%) forest lands (3.99 %), and water bodies (0.60 %) were decreased and settlements (2.30%), shrub land (3.07%) and bare land (3.19) were increased. The LULC change impacts on hydrological response such as surface runoff, ground water flow, and water yields were increased by 6.03, 8.22, and 10.39 %, respectively. While, evapotranspiration was decreased by 3.34%. In this research the climate change and LULC change have significantly affect the hydrological component of the sub basin.

In the study area the average annual rainfall amount for Dire Dawa, Harar and Haramaya, Girawa, and Gursum stations are found to be 647, 816, 801, 958, and 840 mm with coefficients of variation of 23, 20, 20, 19 and 31%, respectively. The rainfall distribution at the gauging stations varies significantly both temporally and spatially. The joint probability of rain days estimation approach analysis output indicates that the monthly time step has better performance than daily, decadal and seasonal. The joint probability approach is used along with rainfall amount under monthly rainfall for areal rainfall estimation assessment in rainfall-runoff modelling. The efficiency of the hydrological model simulation highly dependent on the accuracy of data used during calibration and validation periods. The rating curve model performance measure values were in acceptable ranges of coefficient of determination of (0.98), root mean square error (4.49) and Nash–Sutcliffe Efficiency (0.97). This indicates that rating curve model was reasonably used to estimate the discharge in the upper Erer subbasin. The overall discoveries from this research can be used as valuable information for regional water authorities and decision-makers including planners in sustainable water resources management.

Keywords: Sustainable, Water supply sources, Climate change, LULC change, Water balance components, Rainfall distribution, Streamflow measurement, Upper Erer subbasin, Rating curve; Harar town

LIST OF ORIGINAL MANUSCRIPTS

This dissertation is based on the following five original manuscripts, which are listed as follows.

Manuscripts Published:

Manuscript 1: Abrahim Mummed, B., & Seleshi, Y. (2024). The implication of spatiotemporal rainfall distribution on the estimation of areal rainfall characteristics in Upper Erer Sub-basin, Ethiopia. *Water Practice & Technology*, wpt2024057 (https://doi.org/10.2166/wpt.2024.057) (Published).

Manuscript 2: Bedasa Abrahim Mummed, Yilma Seleshi (2024). Assessment of the effects of climate change on water balance components in the upper Erer subbasin, Ethiopia. Heliyon, 2024, e30297, ISSN 2405-8440Heliyon, Elsevier https://doi.org/10.1016/j.heliyon.2024.e30297 (Published)

Manuscripts Under review and ready:

Manuscript 1: Bedasa Abrahim Mummed, Yilma Seleshi (2024). Assessing sustainable water supply source using scenario's analysis in Harar Town, Ethiopia. Climate Resilience and Sustainability Journal, Wiley's Publisher (Under Review).

Manuscript 2: Bedasa Abrahim Mummed, Yilma Seleshi (2024). Assessment of the effects of land use land cover change on water balance components in the upper Erer subbasin, Wabishebele Basin, Ethiopia (Under Review).

Manuscript 3: Bedasa Abrahim Mummed, Yilma Seleshi (2024). Estimation of discharge using rating curve under data scarce region of upper Erer subbasin, Wabisheble River Basin, Ethiopia (Under Review).

TABLE OF CONTENTS

LIST OF FIGURES

LIST OF TABLES

1. INTRODUCTION

1.1. Background

The concepts of sustainable development and sustainability are the basis for understanding and defining sustainability criteria. Sustainable development was first described in 1987 by the Brundtland Commission as ‘development that meets the needs of the current without affecting the ability of upcoming generations to meet their own needs’ (WCED, 1987). Sustainable use of the water resources is highly significant as their disregard leads to severe financial, environmental, and social problems. In this regard, there have been serious challenges to achieve the objectives of sustainability, because of institutional, financial and technical aspects on one hand (Haider et al., 2016) and their social and environmental impacts on the other hand. Sustainability of water supply sources in meeting the water demands for future needs attention. The complexity of the decision-making problems and sustainability analysis in water supply systems requires the integration of multiple criteria, models and data sources (Eggimann et.al, 2017), which confirms that the use of multi-criteria decision analysis (MCDA) in a suitable approach for addressing water resources planning problems, including the identification and selection of new water supply sources Kang, M.-G.; Lee, 2011). In addition, scholars over the past 30 years quantify the extent of water supply to satisfy the human and environmental needs. A diverse set of water availability indicators has been developed among them major categories of indexes include water crowding indexes and various demand-to-supply ratios.

The United Nations (UN, 2006) stated that “the right to safe drinking water and sanitation is a human right crucial to the full delight of life and all human rights”. Accessibility of drinking water is a worldwide challenge probably due to non-functionality of water supply sources, high water use, expansion of cities, topographical setup of the city, populations increase, climate change and land use land cover change are most problematic to water supply sectors (Domene, E.; Sauri, 2006; WHO and UNICEF, 2006; Luck, M.; Landis, M.; Gassert, F., 2015). Nevertheless, the contribution of human activity to climate change has significantly disturbing the availability of water resources by increasing the concentration of greenhouse gases (GHGs) in the atmosphere (IPCC, 2014). Developing countries are likely to be affected by the increasing problem of water shortage and Ethiopia is one of the most susceptible countries (Cherie and Fentaw 2015). In the eastern region of Ethiopia, the water supply shortage was severe particularly in the upper Erer subbasin, which is the proposed and existing water supply sources of the Harar town (Harar Water Supply and Sewerage Authority (HWSSA, 2014). Currently, the town is facing serious problems regarding its water supply sources in addition to the large increasing population from rural and nearby small towns, watershed deterioration and its associated river flow reduction, rainfall decreases and illegal water collection. In this context highlights the necessity for introducing alternative water supply sources to achieve water supply sources sustainability in the region. The assessment of global environmental challenges that the world faces today are climate and land use land cover change effects (Canadell et al., 2023) on the availability of water sources in the subbasin is highly significant to well recognize their effects. In developing countries, the water resources are tough due to the diverse distribution of hydroclimatic gauging stations and unviability of continuous rainfall and runoff data (MoWR, 2004; NMA, 2015). Accurate estimation of rainfall over the region is critically important (Gebere et a., 2015). This suggests rainfall variability distribution analysis is required in the subbasin. In addition, the estimation of discharge of streamflow were vital for hydrological modeling and water resource analysis in the region.

1.2. Scope of the Research

1.2.1. Assessing sustainable water supply source using scenario's analysis

In the late years of the 20th century the dominant paradigm of development was challenged. People became aware that the development of the economy might be compatible with environmental conservation and economic development could only be likely happen if environment protection and social attachment were addressed. These ideas are associated with the concept of sustainable development. The concept of sustainability is always associated with the concept of sustainable development (SD). There are various methods have been developed to assess the sustainability of water resources. MCDA is the mostly used approach as a decision-support tool, and may consider multiple criteria (Hajkowicz & Collins, 2007; Pannu et al., 2009). Multi criteria decision analysis has been used in diverse scientific fields for different purposes such as optimization and decision making (Sohani et al., 2017). Huimin Li., et al., 2019, analyzes the sustainability water environment by using five dimensions such as economy, society, resources and environment, engineering, and project management. The discrete MCDA techniques have the potential to provide well structured, rational, consistent, transparent and objective solutions to complex decision problems in water supply system (Lai et al., 2008).

Selecting a proper MCDA method based on criteria in literature and observing current recognized restrictions, the selection of MCDA techniques is itself a multi criteria problematic (Abrishamchi et al., 2005). Normally, selecting a suitable MCDA technique reliable on the decision problem at hand, knowledge, practice and the preference of the expert or decision maker (DM). Rather, the simpler technique should be selected for the decision investigation. Various scholars have currently resolved water resources problems by application of different MCDA methods like Analytical Hierarchy Methods (AHP) (Wang et al., 2011). In the AHP method, alternatives are listed and then compared pairwise according to their influence to reaching each objective or criterion (Langemeyer et.al., 2016). This method is one of the widespread pplication to find weight of criteria (Saaty, 1980).

In this process the definition of criteria was compulsory that depend on every particular situation. However, a common method has been to consider social, technical, environmental, and economic aspects as the main criteria (Abrishamchi et al., 2005; Okeola et.al, 2012; Lu, Y.P. et.al, 2013). The process of AHP followed the following main steps as recommended by Saaty, T.L., 2010; Castillo, M. et.al., 2006, the process of the AHP as first set of pairwise comparisons is made among the main criteria to reproduce the preference of a decision maker regarding the importance of each criterion toward resolving a decision problem. The values attained from the first set of pairwise comparisons will be useful as the weight of each criterion. The second set of pairwise comparisons is a comparison of sub criterion concerning a specific criterion. The third comparison involves multiplying the result of the second set of pairwise comparison by that of the first set of pairwise comparisons and ranking the results. The alternatives that can possibly satisfy the problem would be defined. Each alternative, or choice, must characterize a possible and appropriate determination to the problem of the water supply, considering the financial, social, and environmental limitations (Gregory, R., et.al, 2012).

For every decision, good or bad influences to consider are usually emotionally understood in the form of benefits (gains) and costs (losses) (Saaty, T.L., 2005). The assessment of a decision according to these features is not directly accomplished, (Saaty, R.W., 1987) that suggests producing a cost hierarchy to paired comparisons with decisions using a measure of 1 to 9. The AHP requires numerous pairwise comparisons, a shared problem is constancy in the choices. To resolve this problematic (Saaty, 1987) suggested a consistency ratio to measure the consistency in the judgements of decision makers. Ratios higher than 0.1 often require re-examination. Based on this classification, the relative weights of the criteria and alternatives can be predictable by a scientific method that is known as estimation of eigenvalues (Saaty, T.L., 2005). An indicator for sustainability criteria is tools used to check and assess the fulfillment of sustainability criteria, as well as development to sustainability. An evaluation criteria or indicator is a parameter which points to deliver evidence about and designate the state of a phenomenon (Sahely et al., 2005). The indicator or evaluation criteria should be clearly formulated and relatively simple to apply.

1.2.2. Assessment of water balance components consequences of changing climate

Climate change is expected to worsen the present pressures on water resources consequential from population growth, economic influences and land use changes, expansion of industrialization (Raneesh KY., 2014). As detailed by the Intergovernmental Panel on Climate Change (IPCC), 2013, since 1750 human activities have critically enlarged the global atmospheric absorptions of greenhouse gases. Bates et al., 2008, review IPCC and confirmed that water resources are particularly susceptible to, and strongly obstructed by, climate change. The hydrological cycle will be straight forward exaggerated by the influences of climate change, subsequently affect the local water resource accessibility in most regions in the world (Dile, Y.T. t al, 2013; Faramarzi et al., 2013; Awal et al., 2018). However, the investigation and thoughtful of how climate changes continue to interrelate and interrupt the catchment hydrology fluctuates from worldwide to regional and regional to local scale. The Regional Climate Models (RCMs) were recognized that significantly rises the truthful simulation of the temperature and precipitation at the scale of subbasin level (Wangpimool et al., 2013). The doubt due to the selection of release scenario is less important for the near term, because most scenarios show very similar levels of emissions over the 2050s and it takes time for the atmosphere to respond (Wilby and Harris, 2006). Nevertheless, the future scenarios that based on Representative Concentration Pathways (RCPs) from the IPCC fifth assessment report (AR5) were better address the climate change status (IPCC, 2013). The RCPs include four different scenarios from low forcing level (RCP-2.6), moderate emission scenarios (RCP-4.5/RCP-6.0), and high emission scenarios (RCP-8.5) that based on with different combinations of economic, technological, demographic, policy, and institutional futures (Moss et al., 2010).

1.2.3. Assessment of water balance components owing to changing land use land cover

The main human induced activities that alter the hydrological scheme are land use land cover changes (Homdee et al., 2011; Tekleab et al., 2014). In this respect the land use land cover changes and population growth are the most common problems in developing countries such as Ethiopia since their economic growth mostly reliable on farming (Tufa, D. F, et. al., 2014). Assessing the present land use land cover changes and understanding the relation between humans and the natural environment are vital (Leta et al., 2021) but complex. Remote sensing plays a substantial role in the analysis of the Earth’s surface studies by providing spatiotemporal evidence on LULCC (Gregrio & Jansen, 2000). The land use land cover information was determined by the use of remote sensing data of Landsat Image using a collection of pixels. Now a days different image classification methods were under use, such as supervised, unsupervised, and hybrid, as well as innovative methods such as artificial neural networks (Taye, H., 2016). These suggests the importance of quantifying the LULCC changes and their impacts on local scale and needs the use of specific hydrological modeling techniques. The soil and water assessment tool (SWAT) model has been widely used to assess the effects of LULCC on the hydrological cycle (de Oliveira et al., 2022).

1.2.4. Spatiotemporal rainfall distribution characteristics

The onsite record of rainfall was measured using rain gauge (Nair et al., 2009) installed at the stations. Accurate estimations of rainfall are vital for numerous water resource related studies including agricultural water use, water supply for human consumption and industrial use, and for thoughtful of hydrological response of the subbasin (Mirshahi et al., 2008). Ground stations are rare and sparsely distributed to estimate precise rainfall in space and time (Negreiros et al., 2011). However, the number and distance of rain gauge stations were influencing the distribution of observed rainfall (Buytaert et al., 2006; Villarini, 2010). In mountainous regions, rainfall is highly variable (Villarini, 2010) and this affects the rainfall distribution over short distances and within short periods of time (Anders et al., 2006). The rain gauges that provide accurate local information (Yilmaz et al., 2010) are usually limited to characterize areal rainfall estimation.

1.2.5. Estimation of discharge and modelling the rating curve in data scarce region

Streamflow data is required for planning and design of various hydraulic structures and water resource projects and assessment of water resources potential (Muzzammil et al., 2018) and consistent and continuous record of streamflow data is highly important. In addition, peak flow conditions in river discharge data measurement are required for several hydrological analysis including for calibration and validation of rainfall–runoff models, flood frequency analysis and others (Di Baldassarre et al., 2011). Despite the important of stream flow direct measurement of discharge at the station is costly. As a result, the stage–discharge rating curve methods are used to transform the measured stage into discharge. The rating curves for hydrometric stations in Ethiopia has not updated for couple of decades that restricts the output of recent climate change influences and water resources inconsistency (Goshime et al., 2021). In country wise Donauer et al., (2022) and Haile et al. (2022) recommended the need for stream flow monitoring across the country. Such data gaps need cross relative between data provider and data users (Taye et al., 2021). So, on site recording of streamflow records at the gauging site helps to estimate the discharge at a specific cross section.

1.3. Problem of the statement

The upper Erer subbasin that used and proposed water supply sources of Harar town and used as a water source for irrigation development in the region has not get cross attention of the researchers. In the subbasin understanding on water supply sources sustainability and factors that affect its sustainability are limited. In addition, unavailability and quality of hydro-climatic data need urgent attention. Most of the studies such as (; Bichai, Françoise, et al., 2015; Marques et al., 2015; Sofiane Boukhari, 2018; Zhou et. al.m 2018; Alemu et.al., 2020; Khan, et al., 2020) used limited criteria without considering uncertainties (Henry A. et.al., 2019). Therefore, in this study the sustainable water supply sources assessment was designed using the integrated multi criteria such as economic, environmental, social, governance & institutional, technical & functional, water supply yield.

Sustainability of water supply sources were affected more by climate change and land use land cover changes. The hydrometeorological process could change in occurrence and strength due to climate change, but also due to local land use/land cover change (Dibaba et al., 2020). Recently studies such as (Ashofteh et al., 2017; Workuet al., 2018; Moghadam et al., 2019; Dioha et al., 2020; Musie et al., 2020; Demissie et al., 2021; Golfam et al., 2022; Moghadam et al., 2023) were conducted on climate change influences on various water schemes but most of them used coarser data on basin scale (Geleta et al., 2022). Hence, in this study uses the refined ensemble average regional climate model (RCM) to minimalize uncertainties on climate change impacts at local conditions. The assessment of recent land use land cover change mostly has not considered local scale hydrological condition and not include the aggregate impacts of the changes (Negese, 2021). The LULC change on water balance components were indeterminate and needs a refined spatiotemporal examination to well understand the changes and its impacts on local hydrological responses.

The assessment of climate and land use land cover change and their impacts on water balance components were implemented by using hydrological models that need the hydroclimatic data. In Ethiopia unavailability of uniform distribution of hydroclimatic gauging site and continuous record of rainfall-runoff data is always a problem (MoWR, 2004; NMA, 2015; Abebe et al., 2020). This is severe in the upper Erer subbasin (Wudineh et al., 2021). The river flow data has affected the study focused on water resources analysis (Negatu et al., 2022). So, appropriate measurement of stream flow data is required for various hydrological studies (Goshime et al., 2021). In this study the steam flow discharge was estimated by employing rating curve equation using on site record steam flow data. In addition to the steam flow data analysis, rainfall distribution also an issue in various hydrological studies. The spatiotemporal variability affects the distribution of rainfall with in small distances (Oettli, P., & Camberlin, P., 2005; Terink et al., 2018). The dispersed spreading of gauging sites disturbs rainfall distribution and amounts with in the gauging stations. The accuracy of point and areal rainfall estimations are significantly affected by the number and locations of existing rain gauges stations (Cho et al., 2017; Al-Timimi et al., 2020) with in the entire area of the study.

The studies conducted in the past are typically focused on rainfall amount and its distribution analysis (Nandargi, S., & Mulye, S. S., 2012; Al-Ozeer et al., 2020; Ayehu et al., 2021 Hafizi and Sorman, 2022). Those studies were not considered the mutual spatiotemporal rainfall distribution at the gauging stations. In this study the comprehensive method that considers the joint spatiotemporal rainfall distribution of the gauging stations was introduced as a new approach.

1.4. Research Questions

The following questions need to be answered with respect to water supply sources sustainability for Harar town and upper Erer subbasin water sources.

1. How can main criteria and evaluation criteria affect water supply sources sustainability in the study area? How can sustainability analysis using alternative scenarios determine the alternative scenarios of water supply sources in the region? What are the most influential evaluation criteria that affect the sustainability of water supply sources alternatives?
2. Why the population project trends increase in the region? Do the water supply and demand analysis determine the current and future water supply status? How can be determined the dependable water supply sources in the region?
3. Does climate change affect the water supply sources sustainability and accessibility of water resources? How can be determine the extent of impacts of climate change on hydrological response?
4. Why the exiting water supply sources in the region was affected by land use land cover change? How can be determined the impacts of land use land cover change on water balance components?
5. Do SWAT hydrological model well simulated for the assessments of climate and land use land cover changes in the study area.

6. Why the spatiotemporal rainfall distribution in the study area is nonuniform both in amount and existence with in the gauging stations?
7. Why the estimation of areal rainfall characteristics depends on the mutual spatiotemporal rainfall distribution of the gauging stations.
8. Can unavailability of stream flow data gap be estimated using onsite record of stream flow data is using rating curve viable in the region?

1.5. Research Objectives

In an effort to deliver answers to the research questions of the present study the following specific research objectives are developed.

a) To evaluate the sustainability of water supply sources
b) To investigate the impact of climate change on water balance components.
c) To assess land use land cover change effects on the hydrological responses.
d) To analyze the amount and occurrence of spatiotemporal rainfall distribution with in the gauging stations implication for estimation of areal rainfall characteristics.
e) To estimation the steam flow in data scarce region using on site records of stream flow data.

1.6. Conceptual Framework

In this study work the water supply sources sustainability was evaluated using the main criteria, sub criteria under alternative water sources scenarios. After identifying the water supply sources sustainability is completed, the assessment of factors that affect the accessibility of water resources were examined in this research. Climate change and LULCC impact analysis were performed using the SWAT model and the model uses various input data. In this study the ground observed rainfall and stream flow data were used as input for the model.

The rainfall distribution among the stations were evaluated to determine the spatiotemporal rainfall distribution for the time series. In the region the stream flow data was not continuous and there are no recent records of stream flow data and the steam flow data gap was filled using on site records employing the rating curve equation.

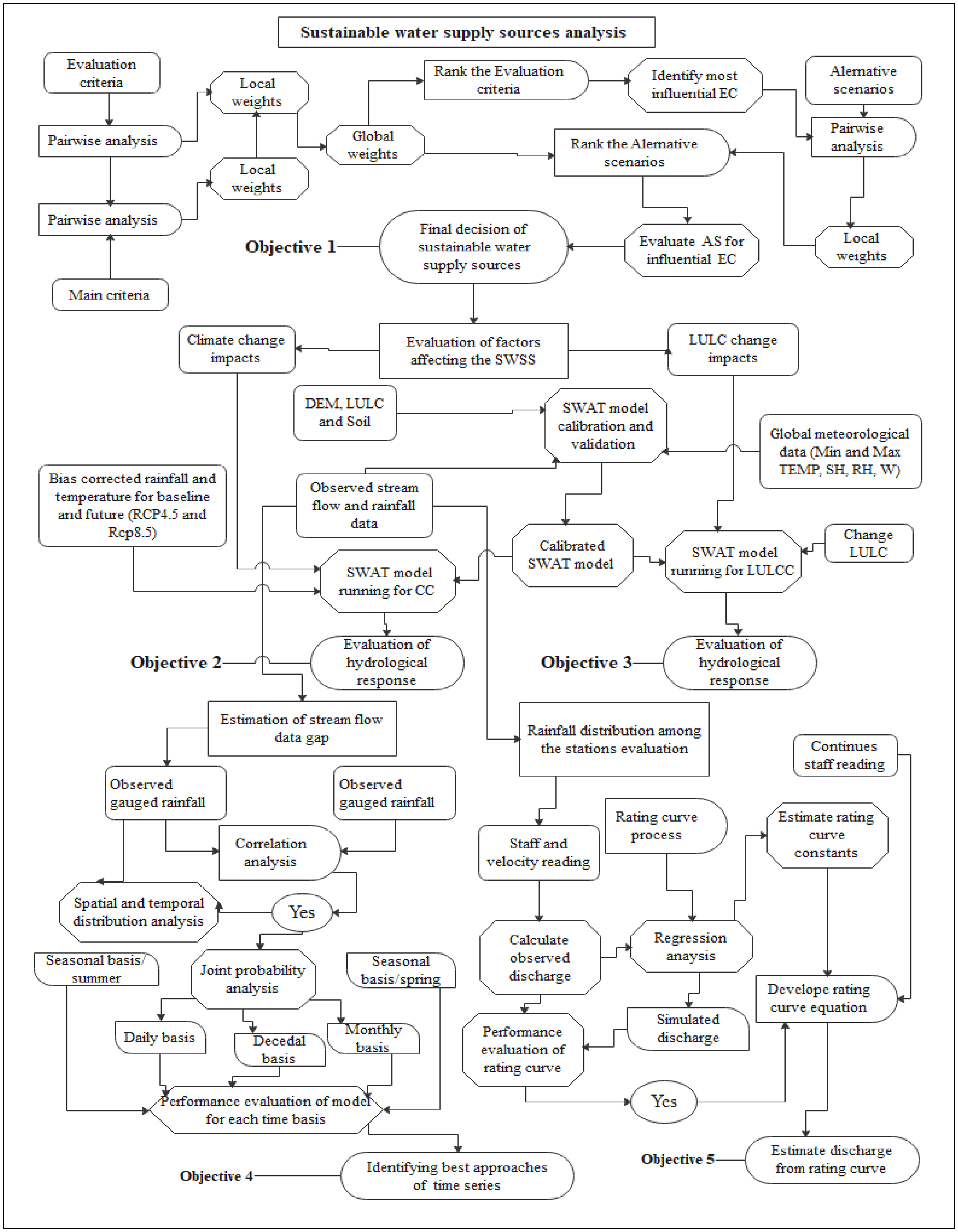

Figure 1.1. The conceptual framework (SWAT= Soil and Water Assessment Tool, DEM= Digital Elevation Model, LULC= Land Use Land Cover, LULCC= Land Use Land Cover Change, CC= Climate Change), AS= Alternative water sources, EC= Evaluation criteria, SWWS= Sustainable water supply sources

1.7. Organization of the Dissertation

The dissertation is organized into eight chapters, which consists of five research outputs from chapters 3 to 7. A brief description of the outline of the contents is presented to simplify the understanding of the connection between the chapters.

1st chapter: presents an overview of the dissertation: the research background, the scope of the research, the problem of the statement, the research questions, the research objectives, and the conceptual framework.

2nd chapter: presents the synthesis chapter that links each chapter to the topic

3rd chapter: presents the water supply sources sustainability assessment.

4th chapter: Focuses on the impacts of climate change on hydrological response.

5th chapter: Presents the impact of land use land cover change on hydrological responses.

6th chapter: Investigate the spatiotemporal rainfall distribution with in the station's implication on areal rainfall estimation characteristics.

7th chapter: Upper Erer river discharge data gap filling using on site records stream flow measurement.

8th chapter: Presents a conclusion and recommendation

2. COMPREHENSIVE OUTLINE OF THE STUDY

In this study five main chapters were organized that represent the research outputs. The study output basis the contents of the chapters paper by paper presentation. The sustainability of the water supply sources is a broad concept that integrates various key factors and indicators. Firstly, the water supply sources sustainability was assessed using the main and evaluation criteria. Sustainable water supply sources availability was affected by various circumstance such as the climate change, land use land cover change, socio-demographic features, water efficient devices, and population changes and others. The climate change impact on the availability of sustainable water supply sources ranks among the first. So, the second part of the study output focuses on the impact of climate change on the water resources is quantified under projected period (2024-2070). The other external driving factors that affect the availability of sustainable water supply sources is land use land cover charge. Including the previous water supply sources in the region and present water supply sources were affected by land use land cover change in addition to climate change. Thirdly, the research output basis on the impact of land use land cover change on water supply sources was quantified for the last two decades.

In this study both the climate change and land use land cover change impacts were quantified using SWAT hydrological model. The model uses the spatial data and temporal data. In the region the temporal data like; climatic data especially rainfall data from ground gauging stations are not representative of the areal rainfall as the distribution of ground rain gauge stations is not uniform. The scattered distribution of gauging stations affects both rainfall distribution and intensities in the gauging stations. Hence, the fourth part of the study focuses on the assessment of temporally and spatial distribution of rainfall to determine the likely characteristics of areal rainfall estimation in the region. Moreover, the steam flow records in the region were neglected and no continuous records and the rating curves was not updated regularly. Therefore, lastly the study focuses on the estimation of discharge using on-site records of stream flow data to fill the data gap.

3. ASSESSING SUSTAINABLE WATER SUPPLY SOURCE USING SCENARIO'S ANALYSIS IN HARAR TOWN, ETHIOPIA

Abstract

The sustainability of regional water resources can only be achieved through a comprehensive consideration of different criteria and scenario analysis. The Analytical Hierarchy Process (AHP) was used for the decision-making process in water resource analysis in this study. The data collection processes were implemented using questioners distributed to the experts' involved in different fields including professionals, managers and scientists. The study indicates that the current population of the town was 127,854 and it becomes 929,418 by the year 2070. The evaluation criteria output shows the most influential evaluation criteria were capital cost (12.33 %), political (7.48 %), seasonality of sources (6.16 %), and availability (5.99 %). The alternative scenario analysis showed that the advanced potable water supply sources scenario was the best, followed by potable water supply and the business as usual is the least preference. The daily water demand was higher than the supply for all years under consideration. In the region the population increased along with other driving factors will deteriorate the future condition of the water supply sources. In this regard, to solve the current problem and mitigate the future worst situation; the local water sector, concerned government authorities and local communities will have to do intensive work.

Keywords: Sustainable; evaluation criteria; water demand and supply; advanced potable water; potable water; business as usual; scenarios.

3.1. Introduction

Providing access to drinking water is a global challenge that assurances the excellence of life and economic development. The full enjoyment of life and all human rights were achieved through the provision of safe drinking water (United Nations 64/292, 2016) and, hence, international organizations sates that it is a must to provide the necessary financial resources for securing them, UNICEF and the World Health Organization (UNICEF; WHO, 2015). The pressure on the water resource increases, and substantially more difficult to satisfy an increasing demand of water (Santos et al., 2009). Globally, urbanization increases the demand for high-quality of water for domestic and industrial use (Serageldin, I., 1995). Fresh water resources are limited and continue to decline around the world. Water stress due to climate change, population and water demand increase, urbanization, agricultural, and industrial activities result implies in finding of alternative solutions and adaptation of water management activities (Nazli, 2014). Conducting a sustainability assessment for regional water resources makes the quantification possible (Yu, Haijiao et.al, 2020).

Sustainability can be defined by different scholars some defines as the management of financial, technological, institutional, natural, and social resources to guarantee the needs of present and future generations (Valenti et al., 2018). The others define as the sustainability of regional water resources can only be achieved through a comprehensive consideration of the regional social, economic, environmental, and water systems and climate changes (Yu, Haijiao et.aal, 2020). In this regard the sustainability of the water supply sources was achieved by assessing the multicriteria decision analysis (MCDA) that has potential to provide well-structured, rational, consistent, transparent, and objective solutions to complex decision problems in water resources management and planning (Hajkowicz, 2007; Nazli, 2014). Several studies used MCDA in order to evaluate sustainable development in the water supply (e.g., Kang, M.-G.; Lee, 2011; Marques et al., 2015). The most widely used methods of MCDA in decision making studies are the Analytic Hierarchy Process (AHP), Elimination and Choice Translating Reality (ELECTRE), Preference Ranking and Organization Method for Enrichment Evaluation (PROMETHEE), Technique for Order Performance by Similarity to Ideal Solution (TOPSIS), Measuring Attractiveness by a Categorical Based Evaluation Technique (MACBETH) and (vi) Fuzzy Set Analysis.

Among the MCDA methods AHP is extensive applications in water resources problem decision analysis. Jaber, J.; Mohsen, M., (2001), used the AHP to evaluate non-conventional water resources supply alternatives to ensure water availability and sustainability in Jordan and got a good result. Okeola and Sule, (2012) used the AHP to evaluate alternative sources for urban water supply. Recently, many researchers have solved water resources problems by the application of AHP such as (Kiker, Gregory A., et al., 2005; Abed et al., 2011; Lade et al., 2012). In the assessment of sustainability of water resources various indices may be considered such as population, climate change, urbanization, economic development and others (Nazli, 2014; Alemu et.al., 2020; Yu, H et al., 2020). Major categories of indexes include water supply-to-demand ratio. Harar is one of the towns with water stress in the region (Atlas of changing environment, 2008). Many countries face major problems in maintaining reliable water supplies, and this is expected to continue in upcoming years (Kassa, 2017). Variations in scenarios are also important that enable one to address all possibilities for the future and to model more accessible probability distributions or deterministic models, and to conduct sensitivity analysis (Varum and Melo 2010).

Mostly, the studies were focused in developed countries and some of them not included the uncertainty conditions that probably affect the water supply source sustainability (Henry A. et.al., 2019) and some of them used limited criteria for the analysis. In addition, the studies conducted on sustainability of water resources not used AHP methods (Marques et al., 2015). The sustainable development is dynamic process which passes in time and reliable on numerous parameters, up-to-date no equivalent conception of sustainability and the indicators were not unambiguously qualified (Li, Huimin, et al., 2019). This context highlights the need for assessing sustainability of water supply source. in this context the research is focused to assess sustainable water supply sources in Harar town using the integration of multi criteria like; economic, environmental, social, governance & institutional, technical & Functional, and water supply yield under alternative scenarios. The study output used to guide policy framework developer for sustainable water supply sources evaluation in the town and other cities.

3.2. Materials and methods

3.2.1. Description of study area

The proposed research was applied to Harar town, Ethiopia. Harar is one of the oldest and historical towns of Ethiopia and the capital city of Harari region and East Hararghe Zone. It is found in the eastern part of Ethiopia located at 9° 19' N latitude and 42° 7' E longitude (Figure 3.1). The town lies on a hill side that slopes roughly in the direction west to east and at an elevation approximately between 1800 and 2200 meters above sea level. The existing water supply sources of Harar town is from different sources; Haramaya Well Field, Hassaliso Well Field, Errer Well Field, and small hand dug wells and Springs (Atlas of changing environment, 2008).

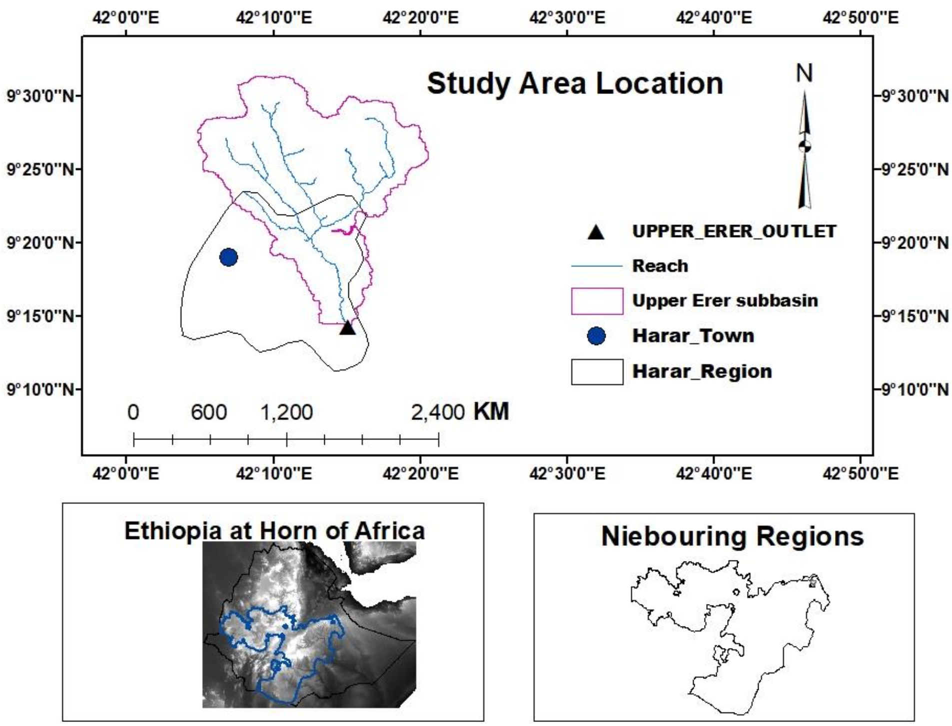

Figure 3.1. Location map of the study area for evaluation of sustainable water supply sources

3.2.2. Data sources

The population data for Harar town were collected from the central statistics agency (CSA, 1984; CSA, 1994; CSA, 2007) using the United Nations (UN) Medium Variant Population Forecast (MVPF) (UN, 2019) for the population growth estimation of town. The existing water supply sources and demand information were collected from HWSSA (Harar water supply and sanitation authority), Ministry of Water and Energy of Ethiopia (MWE). The minimum per capita water supply demand for the town were adapted from the Ministry of Water and Energy (MWE) and the United Nations. The complication of the decision-making problems in water supply sources needs the incorporation of multiple criteria and data sources

(Eggimann et al., 2017). Additionally, data used for sustainability analysis was collected through the questionnaires shown (Appendix 1) from the experts' preferences as suggested by (Cornelis J. et.al., 2013).

3.2.3. Demand and supply analysis

The demand and supply sides were considered along with the sustainability analysis. In estimating domestic water demand, general design standards were adopted: 30 to 50 L/c/d for urban centers for the short term, 40 L/c/d for medium term, and 50 L/c/d for long term (MoWR, 2004). But the estimated per capita demand at this stage was more than this and the future per capita demand was adapted from updated government policy. Likewise, the economic growth (urbanization) and population growth rate and other relevant data were adapted from updated government policy. Taking the government policy indicates that the existing water supply coverage in the town during the million-development goal (MDG) Ethiopian water supply access coverage increased from 14% to 57% (43%-point increase) (WHO; UNICEF, 2006). Provide urban water supply access with GTP-2 minimum service level of 100 l/c/day for category-1 towns/cities, 80 l/c/day for category-2 towns/cities, 60 l/c/day for category-3 towns/cities, 50 l/c/day for category-4 towns/cities, up to the premises and 40 l/c/day for category-5 towns/cities within a distance of 250m with piped system for 75% of the urban population (MoWIE, 2019). The daily demands were estimated using per capita demand and population size for the year under consideration and using urban water supply policy and guideline, official statistics and reports, growth and transformation plan 1 and 2 (GTP-2).

3.2.4. Generation of dimensions, evaluation criteria and driving factors affecting the sustainable water supply sources

As suggested by (Nazli, 2014; Dibaba et al., 2020), there were various factors that can influence the water consumption per person, such as climate, socio-demographic features, water efficient devices, and water resource availability, and population changes. Population growth, increased food production, and industrial growth in conjunction with improved living standards lead to increased water demand, while climate change and environmental pollution affect the availability of water resources to meet this growing demand (Domene, E.; Sauri, 2006). The climate change effect in Ethiopia have shown increasing stresses on water resources availability (IPCC, 2013; Gadissa et al., 2018). Luck et al., 2015 study indicates that in some areas of sub-Saharan Africa there is ever-increasing needs of the growing population, inappropriate land management practices and overuse of land and water exist.

The main criteria and the evaluation criteria were derived from (Alegre et al., 2006; AWWA 2009 and other studies). Based on the local situation and data availability, adequate indicators and indices can be selected to quantify the sustainability characteristics in a certain area as proposed by (Kools et al., 2019). The AHP were structured in to 6 merged main criteria, 28 evaluation criteria and three water supply sources alternative scenarios. Both the global and the local weights of the goal (the root of the tree) sum up to 100%, and both the global and local weights of the main criteria coincide. Global weight of any sub criterion is calculated from the product of its local weight and its parent criterion. From the final global weights, the rank of the evaluation criteria was identified. The evaluation criteria that most affect water supply sources sustainability have been identified through the analysis of pairwise comparisons and ranking as per the final result of global weights. Thus, using the most influential evaluation criteria the importance of each alternative scenario was examined.

3.2.5. Scenario analysis

Scenario development is defined as a tool to improve the decision-making process and to deal with uncertainty due to the application of different strategies (Varum and Melo 2007). Developing scenario alternatives needs understanding of the likely water supply sources to be considered, such as; Baseline, Potable water supply and Advanced potable water supply sources. The water supply sources considered for the future are surface water sources as the proposed water supply sources in the other studies in the region were from surface sources (HWSSA, 2014). The alternative scenarios selected were expected to address the existing water scarcity and assurance the sustainable water supply sources for the coming 50 years for the town. To create the scoring of the scenarios, each scenario was accumulated and weighed throughout the hierarchical structure.

1. Baseline scenario: This is also named as business-as-usual scenario. In this case, all important assumption and other factors are assumed to remain the same as in the base year except socioeconomic and demographic factors which expected to raise at the official projected rate. This scenario also helped as a reference for comparison of the results of the remaining scenarios.
2. Potable water supply scenario: This includes the water supply sources from surface water in the upper Erer sub basin.
3. Advanced potable water supply scenario: This is the water supply sources including the potable water supply sources that need intensive water collection structures such as hydraulic structures including dam.

3.2.6. Analytic hierarchy process (AHP) approaches

In the AHP process the response from a group of experts are required to avoid bias in their preferences as groups are accepted to be more familiar than individuals (Sofiane Boukhari, 2018; Henry A. et al., 2019). All discrete criteria are paired with each other and the results accumulated in matrix system (Kiker, Gregory A., et al., 2005). In this study the rank of arrangement of the criteria and sub criteria uses 9 values of classification from 1 to 9 based on the pairwise comparison measure given by (Saaty,1977).

The AHP used to split a complex decision-making problematic that were reduced to a series of pairwise comparisons between aspects of the decision hierarchy (Balyani et al., 2015). Questionnaires were distributed for the survey to gather the respondent's judgement (Sofiane Boukhari et al., 2018). Experts were requested to compare 6 main criteria and 28 evaluation criteria, and 3 alternative water supply scenarios using four level hierarchies.

In specific terms, the sustainability analysis for this study was followed four steps as suggested by (Saaty, 1977, Sofiane Boukhari, et al., 2018); first identify the problem definition, secondly, search for alternative scenarios and selection of main and sub criteria, thirdly, the matrix analysis main and sub criteria and alternatives, and finally, the evaluation of an alternative under most influential evaluation criteria identified. The hierarchical tree of four level were developed for this study that contains the goal, main criteria, evaluation criteria and the alternative scenarios as shown in Appendix 2. The methodologies proposed for the study were summarized in Figure 3.2. Each comparison of the experts preferences of the relative importance of the elements values were used as suggested by (Saaty 1977), whose meanings are indicated in Appendix 3.

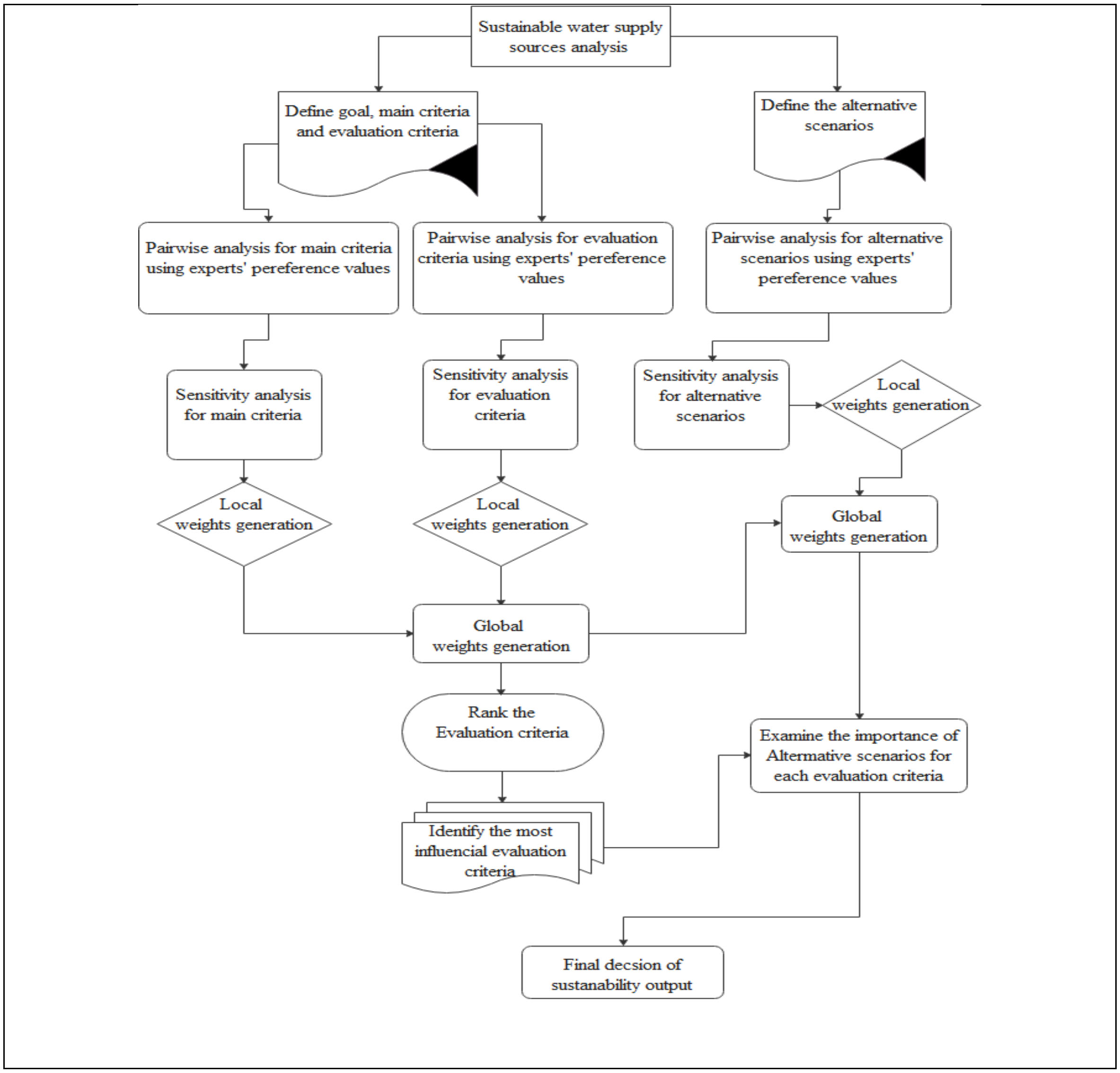

Figure 3.2. Conceptual framework for the study

The global weights can be derived by combining the weights through the hierarchy structure. To aggregate the opinion of all groups of DMs, it uses the weighted arithmetic mean method (WAMM) (Zyoud et al., 2016). The decision matrices for main criteria, evaluation criteria and alternatives are then calculated by averaging of each discrete priority for the two decision matrices. The AHP method then proposes confirming the dependability of the result by calculating the consistency ratio (CR), which enables us to detect faults in our calculation and assessment. The value of CI: the Consistency Index, which is calculated by Equation (2.1) is used to calculate the consistency ratio.

$$\mathrm{CI} = \frac{\lambda_{\max} - n}{n-1} \qquad \text{Equation (2.1)}$$

Where: n is the number of rows or columns of the square matrix of judgment and RI and $\lambda_{\max}$ is the principal eigenvalue. The CR is calculated by Equation (2.2)

$$\mathrm{CR} = \frac{\mathrm{CI}}{\mathrm{RI}} \qquad \text{Equation (2.2)}$$

Where RI: the Random Consistency Index, (RI) as can be determined using the data on Appendix 4 (Saaty, 1977) and CI: the Consistency Index, which is calculated by Equation (2.1). If CR $\leq$ 0.1, the decision is considered adequately coherent; otherwise, the assessment may require some modification to decrease discrepancies (Saaty, 1977). After the local weights of the aspects of the levels are calculated, the global weight is calculated by simply multiplying the weights of the lowermost level.

3.3. Results and discussion

3.3.1. The pairwise comparison of the elements

Based on the questionnaires distributed to experts from professionals, managers and scientist determined their opinion on the main criteria and evaluation criteria on the basis of their information, practice, and background in water supply sources problem analysis (Sofiane Boukhari et al., 2018). Each expert made their judgment using the Saaty scale (Saaty, 1977) as shown in Appendix 3. In this study the aggregation process of the individual/group preferences works in such a trend that the whole groups become a new individual by merging individual opinions to obtain a single opinion in which the priorities are computed and then combined using the arithmetic mean method.

Appendix 5 shows the global and local weights and ranks of evaluation criteria compared to each other's. The result shows that the most influential evaluation criteria were capital cost

(12.33 %), political (7.48 %), seasonality of sources (6.16 %), availability of sources (5.99 %), policy (5.50 %) and performance of the source (5.54 %). The capital cost and political are categorized under the economic and social main criteria, respectively. While, seasonality of sources, availability of sources, policy and performance of the source evaluation criteria were categorized under the environmental, water yields, management & institutional, and technical & functional main criteria, respectively.

In this study the minimum weightages were given to environmental impact (environmental main criteria), resilience (technical & functional main criteria) and vulnerability (technical & functional main criteria) with the weights of 0.80 and 0.90 and 0.93 %, respectively. This confirmed that the environmental impact, resilience, and vulnerability had less importance for sustainable water supply sources in the region. Other study suggested (Nnaji & Banigo, 2018) water quality, risk of contamination, sustainability, maintainability, and public acceptance were the most important criteria which were found to affect the ranking of water sources for domestic water supply. Nevertheless, the subjectivity of the experts remains a limitation in the pairwise comparisons as confirmed by (Szabo et al., 2021). Overall weights of all evaluation criteria that were obtained by AHP were shown in Appendix 6.

3.3.2. Population, supply and demand analysis

Demand and supply projection targets for 2050 and 2070 are key years of interest using the years 1994, 2007, and 2012 for the past and year 2023 currently existing references for alternative scenario analysis. The driving factors that affect the demand and supply are dependent on different situations during various time periods. Table 3.1 indicates population, water supply and demand trends for period 1994-2070. The result indicates that Population for the town was established by (CSA, 2007) and having a population of nearly 99,368 population census data (CSA, 2007). During the period, there is not enough drinking water available to meet the demands of the people for most of the years. Using medium variant population forecast the daily water balance data were evaluated in terms of demand and supply based on the data from Harar Water Supply and Sewerage Authority (HWSSA).

Currently (2023) the population of the town is 127,854. The supply is lower than the demand and the supply-to-demand ratio is estimated as 0.78 at the year 2023. By 2050, the population is expected to be 234,855, this is nearly double of the current population. Similarly, by 2070, the total population in the town will exceed 929,418. Hence, ti is expected that the town is able to provide water supply to a population more than sevenfold of existing population (2023) at the end of half century. The rural growth rates were higher than the corresponding urban growth rates in the region during 1994-2007. This may have occurred due to the influx of migrants into the rural areas and new settlements coming up just outside the urban limits, which are basically an expansion of the urban areas that are yet to be recognized as urban (CSA, Inter-Censual Population Survey (ICPS), 2012). It is expected that in Harar town urbanization may increase in the future due to either or both of following; first, the emergence of new urban areas which are currently rural and secondly, the inclusion of the population just outside the periphery of the existing towns into the urban limits. The population growth was 30% from 1994 to 2007 for about 13 years period and 32 % from 2007 to 2012 for only 5 years period. This indicates that the population increase for the last 15 years were highest growth

Table 3.1. Existing and projection of population, water demand and supply description

Years	**Total urban population**	**Per capita demand (l/c/d)**	**Demand (m^3/day)**	**Supply (m^3/day)**	**Remarks**
1994	76,378	50	3,819	1,500	Population census 1994, CSA, 1994
2007	99,368	65	6,459	4,092	Population census 2007, CSA, 2007
2012	117,125	85	9,956	7,488	Projection ICP 2012, CSA, 2012
2023	127,854	100	12,785	9,988	Projection from graph, CSA, 2012
2030	135,188	110	14,871	-	UN, CSA, Population Projections
2050	234,855	120	28,183	-	UN, CSA, Population Projections
2070	929,418	150	139,413	-	UN, CSA, Population Projections

In the town the population was in an increasing trend for the last 27 years. Contrary, the supply had not met the required demands for the last period. Population increase and per capita demand (increased living standard) increase brings a reduction of water security in the town. Thus, there was a need for better collaboration between the two desirable's goals of water security and population increase along with living standard increase. On the other hand, the supply sides were not increased to satisfy the existing situations of the requirements.

Figure 3.3 indicates the time series analysis of the average daily water demand and supply. The average daily water demand was higher than supply each year. The daily average water demand (3819 m^3/day) and supply (1500 m^3/day) for the year 1994 and at the year 2023. But, it became 12785 m^3/day for demand and 9988 m^3/day for supply. Previously, the water supply sources of the town were from Lake Haramaya treatment plant and the Haramaya Lake dried up because of local climate change, change in land use in its basin, and increased irrigation (Atlas of changing environment, 2008). The current source of water supply of Harar town was ground water sources such as well fields and small hand dug wells and from natural springs that owned by the community itself as stated by Harar Water Supply and Sewerage Authority (HWSSA) Managers during the interview.

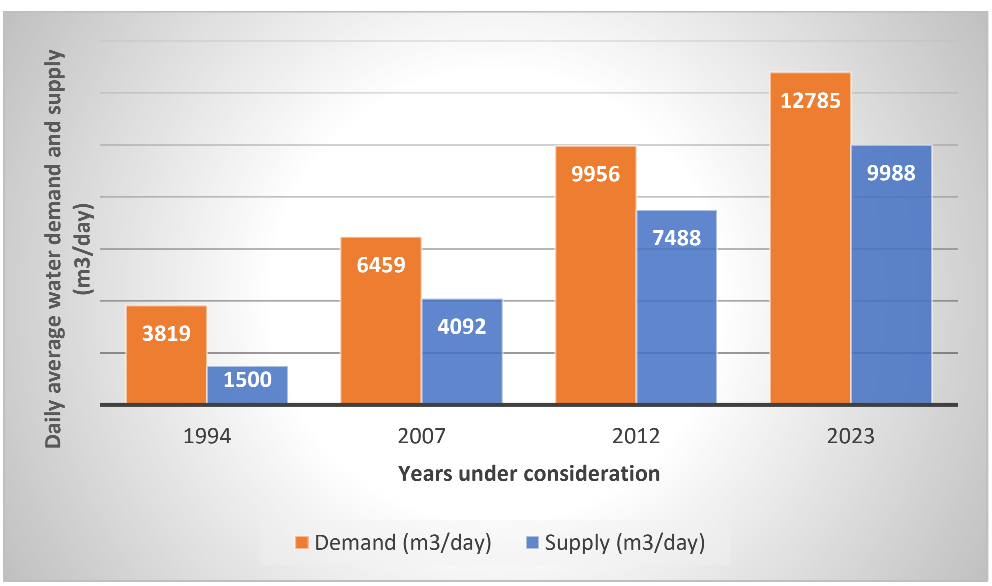

Figure 3.3. Daily average water demand and supply

The population projections indicated on Table 3.1 shows that the population size at years 2023, 2050, and 2070 is to be 127,854, 234,855, and 928,418, respectively. The result showed that population will tend to increase dramatically mean while the per capita demand will also increase as per strategic plan of the country. The demand for water is in increasing, and this agrees with the suggestion by (Domene, E.; Sauri, 2006).

3.3.3. Evaluation of scenario alternatives under the most influential evaluation criteria

The rank the alternative scenarios are obtained from the matrix of alternative scenario and most influential evaluation criteria weightages. From Figure 3.4 shows the dimensions (main criteria) weightages. The result indicates that the economic (21.10%), environmental (17.01 %), social (18.24 %), governance & institutional (14.84 %), technical & functional (17.45 %) and water supply yield (11.37 %). The economic dimension was with the highest perefernces followed by social and technical & functional. The water yield was the dimension with minimum preferences. This is probably due to the subjectivity of the experts' preferences in their decision.

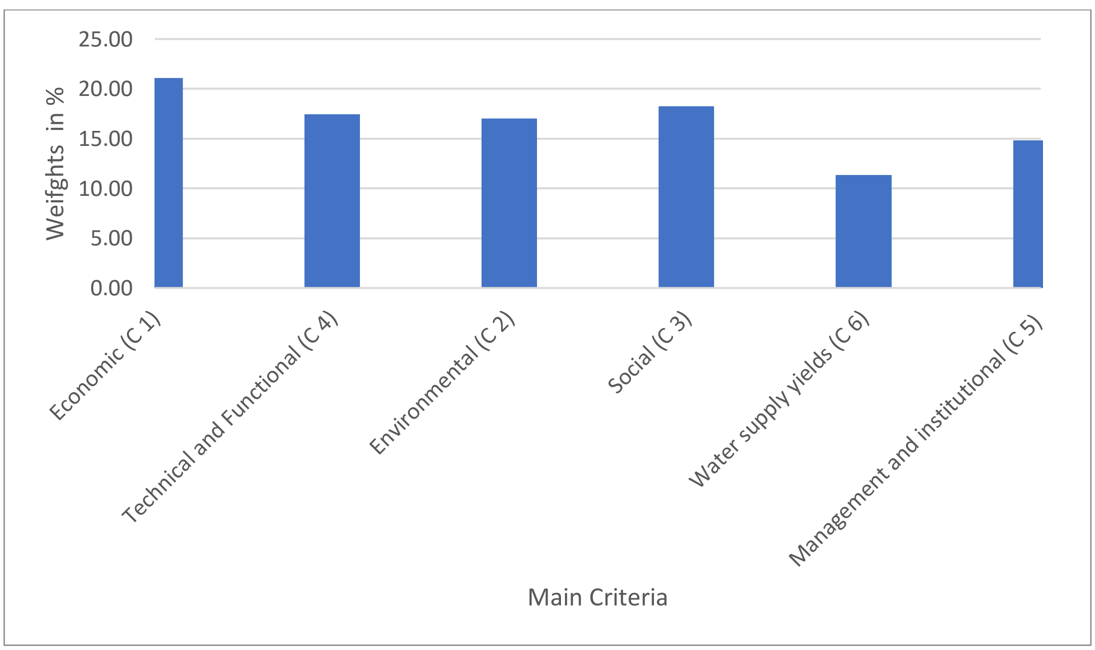

Figure 3.4. Weights of criteria obtained from pairwise comparison

The result shown in Appendix 5 revels that the capital cost was first, followed by political, availability, seasonality, performance, and policy were ranked from highest to lowest values in respective order that indicate the water resources and sustainability assessment was influenced by the highest value rank evaluation criteria (Zhou et. al., 2018). The most influential evaluation criteria output indicates high water supply source expansion in addition to the existing sources to explicitly fit the current population demands. And also, large capital investment and finding the alternative water source is vital to cope up the existing situation. This result agrees with the regional water authority's and the town water supply administration recommendation.

Table 3.2. Global weights and rank of the alternative scenarios the D1, D2, D3, D4, D5 and D6 denotes the Dimensions (main criteria) types used in this study (Economic, Social, Environmental, Governance & Institutional, Technical & Functional, and Water Supply Yield), respectively

Criteria weightage analysis	Dimensions	D1 (0.211)	D2 (0.170)	D3 (0.182)	D4 (0.174)	D5 (0.148)	D6 (0.113)	Overall priority	Rank
	Evaluation criteria	EC1.1 (0.584)	EC2.3 (0.352)	EC3.1 (0.410)	EC4.1 (0.317)	EC5.1 (0.370)	EC6.1 (0.541)		
	Global weights	0.1233	0.0599	0.0748	0.0554	0.0550	0.0616		
Alternative scenario global weightage analysis	Baseline	0.080	0.029	0.045	0.012	0.012	0.016	0.204	3
	Potable water	0.025	0.014	0.063	0.032	0.054	0.063	0.252	2
	Advanced potable water	0.010	0.080	0.014	0.079	0.056	0.044	0.283	1

In relation to environmental main criterion again the baseline scenario had the best performance and potable water supply sources scenario had the second-best performance. Regarding the social main criterion, the potable water supply source scenario was the best. Concerning the technical & functional and management and institutional main criteria, the advanced potable water supply sources scenario was the best.

3.4. Conclusions

The AHP methodology that treats the integration of multi criteria such as economic, environmental, social, governance & institutional, technical & functional and water supply yield were used. In this study around 28 sub criteria and three alternative scenarios were also selected for the evaluation of sustainable water supply sources. From the result, the most influential evaluation criteria identified were; capital cost, political availability, seasonality of the sources, and performance of the sources and policy.

Among the alternatives, the best is advanced potable water supply sources scenario, followed by potable water supply and the least preference is business as usual scenario. Moreover, as per the preference of the experts', the evaluation criteria having the highest effects for sustainable water supply sources in the region were also identified. The demand and supply was analysis in the town indicates the daily average water demand (3819 m^3/day) and supply (1500 m^3/day) for the year 1994 and at the year 2023 the demand became (12,785 m^3/day and supply (9,988 m^3/day). The population projection indicates that in the town population will tend to increase dramatically mean while the per capita demand will increase as per strategic plan of the country.

The current study showed slight direction and helps for policy makers, water authorities, government bodies, and stakeholders in the water sector including ordinary people to understand the likely situation that mostly affect the sustainability of water supply sources in the region.

A limited criteria weights regarding a possible future application is that the model (analytic hierarchy process) certainly requires re-weighting by experts. Moreover, future studies may use additional evaluation criteria such as health impact and more professional experts using additional main criteria and sub-criteria that may help to better understand and identify the qualitative benefits for the stakeholders.

4. ASSESSMENT OF THE EFFECTS OF CLIMATE CHANGE ON WATER BALANCE COMPONENTS IN THE UPPER ERER SUBBASIN, ETHIOPIA

Abstract

Eastern Ethiopia watersheds are located in transition zone from Arid to semi-humid climate and in expanding to westwards the west annual rainfall is highly declining. This paper explains future hydrological response impacts under changing climate using ensemble average of the CORDEX RCMs for historical (1979-2014) and future (2024-2070) periods. The result revels the monthly average temperature varies (0.04 to 6.25^{0}C) for RCP-4.5, while it varies (0.03 to 6.59^{o}C) for RCP-8.5. The monthly average rainfall to be decline by 90.71 mm and rise by 211. 22 mm for RCP-4.5, while it is going to decline by 84.97 mm and rise by 235.62 mm for RCP-8.5. The adjusted SWAT model was used to detect the changes of projected hydrological response from reference period. balance components of the baseline period was compared to future period. The result shows the change in decrease of annual mean surface flow (4.98% to 5.63%), groundwater flow (5.63% to 6.68%), evapotranspiration (2.45% to 2.57%) and water yield (5.54 % to 5.21 %) to be expected from RCP-4.5 to RCP-8.5. The findings of this paper provide valuable assistance to water resource planners by enhancing their comprehension of change in climate effects at local level.

Keywords: Water balance; Climate change; Scenarios; Historical; Projections; Rainfall; Temperature.

4.1. Introduction

The global warming contributes the change in surrounding atmosphere by increasing local temperature and variability in rainfall. Globally this situation is expected to affect the hydrological processes (Ashofteh et al., 2013; WG et al., 2013; Pachauri et al., 2014; Koneti et al., 2018; Pandey & Khare, 2018; Azadi et al., 2021; Dariane and Pouryafar, 2021). In recent years, the changing climate effects analysis conducted at different function of water sources worldwide for instance (Moghadam et al., 2019; Golfam et al., 2021; Golfam et al., 2022; Moghadam et al., 2023) indicate that their effect increases water shortage in the system. The increase in temperature and rainfall variability expected in the future (Dioha et al., 2020;

Anose et al., 2021; Musie et al., 2021; Geleta et al., 2022) aggravate the water resources stress. Hence, climate change studies are remarkable in the sustainability of water sources and the effects can touch different parts of the world (Cherie & Fentaw, 2015; Chen et al., 2020). In this regard, less developed countries are probably impacted mostly and Ethiopia stands in the first list (Frederick et al., 2013). The waters scarcity problem coupled with increasing climate change extremes affect the water supply sources of local communities in eastern Ethiopia. The Upper Erer subbasin of the eastern Ethiopia, which is the proposed and existing water supply sources for Harar town, has been suffering from water scarcity (Hurni, H., 1998; HWSSA, 2014). This implies conducting climate change impact studies in the country used for better understanding of their effect. Today many researchers such as (Giorgi et al., 2009; Wilby & Wood, 2012; Dile & Srinivasan, 2014) rank the importance of water resource challenge by climate change effects. But, most of these analyses were implemented on large basins with coarser data (Somorowska, 2017). So, high-resolution data are required to efficiently quantify climate change impacts at local scale. To cope up this problem various institutions developed high resolution climate models such as National Aeronautics and Space Administration (NASA), World Climate Research Program (WCRP) (Anose et al., 2021; Nikulin et al., 2012). The WCRP generated Coordinated Regional Climate Downscaling Experiment (CORDEX) Regional Climate 4 Models (RCMs) and easily accessible (Gutowski et al., 2016).

The CORDEX RCMs can capture at local scale for changing climate studies that could be affected by elevation difference (Gutowski et al., 2016; Worku et al., 2018; Dibaba et al., 2019). The CORDEX RCMs have been assessed in numerous studies on Africa that have well performance in simulating temperature and precipitation (Rathjens et al., 2016; Negewo et al., 2019; Demissie et al., 2021; Yeboah et al., 2022) are used in this study. The RCMs can be influenced by geographical location and the correctness of climate variables (Zhang et al., 2018). Using the RCMs data directly for climate models without bias correction make the output unreliable (Abdulahi et al., 2022; Mathewos et al., 2022). The performance of RCMs was strongly represented by the consequence of bias adjustments in RCMs simulation. The CMhyd models that defined as Climatic Model Data for the Hydrologic Modeling Tool have well performance in other watersheds (Chiew & Vaze, 2015; Schurz et al., 2019) in extracting and bias-correction of CORDEX RCMs for hydrological modelling. Several hydrological models have been in use to model hydrological processes using spatially distributed information and time series data (Gyamfi et al., 2016; Onyutha, 2016; Ashraf et al., 2017) under data scarce. The Soil and Water Assessment Tool (SWAT) model is implemented to quantify hydrological response and climate change studies under data scarce regions (Zhao et al., 2019; Yeboah et al., 2022) and also used in this study.

Climate change effects on hydrological response under RCMs studies are limited in this study area, but those studies conducted in the region used courser data that not favored hydrological models. Moreover, the studies conducted in this region only used single RCMs for their analysis. To understand climate change impact requires multiple ensemble average of RCMs (Kim et al., 2014). Most of the researches were carried out at large watershed and outside the Upper Erer subbasin study area. Not any climate change anlysis studies conducted on water balance components under CORDEX RCMs on Upper Erer subbasin. Hence, quantifying climate change at subbasin level and investigating its influence on hydrological processes indicates originality of the paper. This research explains the examination of climate change projection and its effects on hydrological response from historical period (1979-2014) to future period (2024-2070) in the Upper Erer subbasin.

4.2. Materials and methods

4.2.1. Study area description

The Upper Erer basin that drains from the Harar highlands to the Wabisheble River Basin are found at 15 km south east of Harar Town. Physically upper Erer subbasin located in between 9^{o}13’26.4” N to 9^{o}31’26.4” N latitude and 42^{o}4’40.8” E 42^{o}20’38.4” E longitude. The upper Erer river watershed area is 466 km^{2} having topographical ranges of 1306 to 3019 meters (Figure 4.1).

The daily mean maximum (26.72 °C) and minimum (12.78 °C) temperatures are recorded in the region (Hurni, H., 1998). The ecological climate zone and their elevation ranges were shown in Table 4.1 indicates in the region the dominant agroecological zone is Woinadega (cool subhumid) (Abebe, 2017). The population income mostly depends on agriculture (Mihertu, 2019).

Table 4.1. Ecological climate zone explanation

Ecological climate zone types	Elevation ranges	% coverage
Warm semiarid (Kolla)	500 to 1500 meters	13.06
Cool subhumid (Woinadega)	1500 to 2300 meters	73.98
Cool humid (Dega)	2300 to 3200 meters	12.96

4.2.2. Observed climate and climate models information

National Meteorological Institute of Ethiopia (NMIE) provided the recorded precipitation information for the period (1979-2014) (Appendix 7). The absence of long-period of observed climatic data has significant effect on climate change impact studies (Endris et al., 2106) in data scarce regions. In Ethiopia, the long-term meteorological time-series data is a challenge, even if the country is expanding the number of meteorological stations in various parts. In the absence of ground recorded climate information, the Climate Forecast System Reanalysis (CFSR) information was implemented in a data scarce condition that has good performance for various studies such as (Fuka et al., 2016; Andrade et al., 2021; Yeboah et al., 2022). In this study except precipitation all other meteorological data used for SWAT model input were generated from CFSR for the period (1979 to 2014).

The historical and future CORDEX RCMs climate variables (precipitation, minimum and maximum) generated from CORDEX RCMs were used. The historical and projected CORDEX (RCMs RCP-4.5 and RCP-8.5 that approximately represents the medium and maximum carbon release scenarios (Negewo et al., 2019; Liersch et al., 2108), respectively were selected that have been used in other studies (Tan et al., 2014) has good performance. To bias correct the RCMs the observed rainfall, maximum and minimum temperatures were used. It is strongly recommended by (Zewdu et al., 2020) to use a long overlapping period (i.e., two to three decades) for observed and original historical RCMs data. In this study two future periods were merged and produced the period (2024-2070) that used for the examination. The CORDEX dataset includes five RCMs for historical (1970-1999) and for future (2000-2099)

(Wilby & Wood, 2012). The historical period (1979-2014) and future period (2024-2070) are considered which aligned with the water supply source for the year 2070 target.

The RCMs used in this study includes: Fourth Generation Canadian Regional Climate Model version 4 (CanRCM4), Rossby Centre Regional Atmospheric Model version 4 (RCA4), Regional Atmospheric Climate Model version 2.2 (RACMO22T), High-Resolution Hamburg Climate Model 5 (HIRAM5) and Swedish Meteorological and Hydrological Institute-Rossby Centre Regional Atmospheric Model version 4 (SMHI-RCA4). Selection of five local's climate models' information depends on broadly application in regional changing climate effects researches in Eastern Africa. Table 4.2 shows explanation of the RCMs information implemented in this research.

Table 4.2. Explanation of RCMs information

Item	**RCMs (GCMs)**	**Data type/ sources/ time span**	**Resolution**	**References**
1	Can-RCM4 (Can-ESM2)	Maximum and minimum temperatures and rainfall information for references and projected periods: from CORDEX database (1979–2014) and future (2024–2070) under RCP-4.5 and 8.5	longitude 0.44° and latitude 0.44°	(Yeboah et al., 2022; Mathewos et al., 2022)
2	RCA-4 (MPI-ESM-LR)			(Dibaba et al., 2019; Nyembo et al., 2022)
3	RACMO-22T (EC-EARTH)			(Bates et al., 2008; Tumsa, 2021)
4	HIRHAM-5 (EC-EARTH)			(Mascaro et al., 2015; Demissie & Sime, 2021)
5	SMHI-RCA-4 (EC-EARTH)			(Liersch et al., 2108)

4.2.3. Extraction and bias correction

The RCMs data are not available in usable format for input in hydrological modeling. Hence, the data points were extracted by using the latitude and longitudes of stations considered. ArcGIS 10.7.1 software was employed for the extraction RCMs using NetCDF table view tool under multidimension tool of the ArcGIS interface. The RCMs information have bias due to various reasons (Graham et al., 2007; Schaefli, 2015). The correction for bias is performed to elevate the estimation of climate model output and to minimalize the inconsistency from recorded climate variables that probably affect hydrological parameters (Graham et al., 2007, Dibaba et al., 2019). The CMhyd tool were used in various application of bias-correction analysis (Lenderink et al., 2007; De Carvalho et al., 2021). The CMhyd tool was employed in this study to develop climate data for the SWAT model input (Schurz et al., 2019; Zewdu et al., 2020).

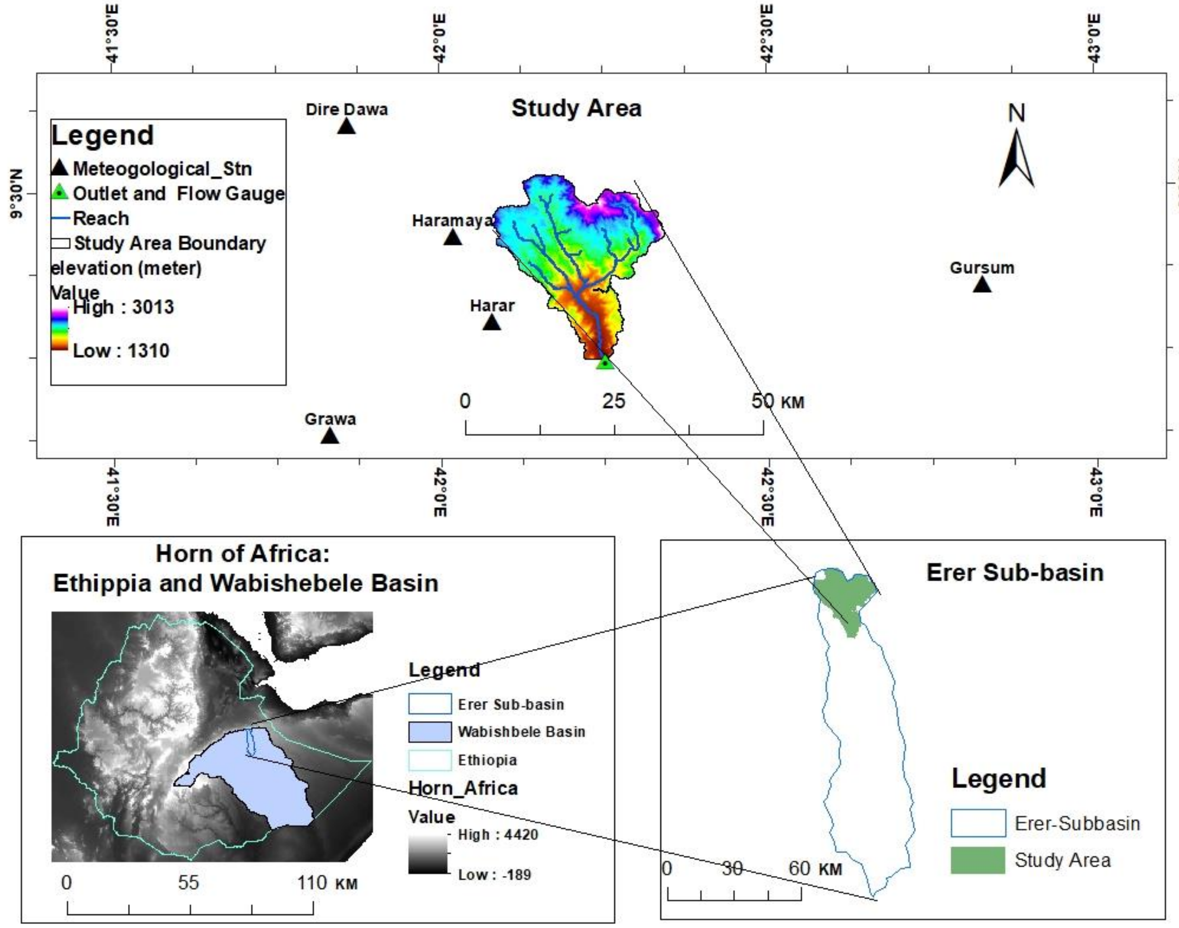

Figure 4.1. Study area location for assessing climate change impacts on water balances

The error adjustment was performed for temperatures using Equation (3.1) and for precipitation using Equation (3.2) (Teutschbein & Seibert, 2012).

$$T_{D,F,} = T_{RCM,Bias,D,F} + \left(meanT_{Obs,M} - meanT_{RCM,Obs,M}\right) \qquad \text{Equation (3.1)}$$

where, $T_{D,F,}$ is daily bias corrected climate model in projected duration, $T_{RCM,Biased,D,F}$ is daily bias raw RCM temperature in future period, and $meanT_{Obs,M}$ is mean monthly measured data in reference duration, and $meanT_{RCM,Obs,M}$ is bias mean monthly RCM in baseline period.

$$P_{D,F,} = P_{RCM,Bias,D,F}\, x\, \left(\left\lfloor\frac{meanP_{Obs,M}}{meanP_{RCM,Obs,M}}\right\rfloor\right) \qquad \text{Equation (3.2)}$$

where, $P_{D,F,}$ is daily bias corrected RCM precipitation in future period, $P_{RCM,Biased,D,F}$ is daily bias raw RCM precipitation in future period, and $meanP_{Obs,M}$ is mean monthly observed precipitation in baseline period, and $meanP_{RCM,Obs,M}$ is biased mean monthly RCM precipitation in baseline period. The ensemble average of RCMs performed well from of the discrete RCMs (Teutschbein & Seibert, 2010; Gadissa et al., 2018) and ensemble mean of five RCMs is used in this research.

4.2.4. Projections analysis for climate change

Several statistical approaches are used to evaluate the implementation of regional climate models simulation (Worku et al., 2018; Dibaba et al., 2019). Generated historical ensemble average RCMs of climate variables in reference duration (1979–2014) were evaluated in the study regions using observed stations. The statistical parameter used in this study is Coefficient of determination (R^2) shown Equation (3.5). The R^2 parameters 1 indicates high value with less inconsistency, and more than 0.5 was fall under recognized ranges. Moreover, ensemble average monthly climate variables of original and bias corrected RCMs were analyzed in the reference duration for considered stations. Figure 4.2 indicates summary of overall methodology and procedures used in this study.

4.2.5. Description of SWAT model arrangement and simulation

In this study the effects of climate change on water balance components of the watershed were examined by the application of SWAT model (Ashraf et al., 2017). The climate change effects were detected by varying error minimized climate model information between the reference and projected duration under two emission scenarios for SWAT model input without changing other climate, spatial and temporal input data.

Table 4.3 shows the description of data used for SWAT model. The information for SWAT input shown in Table 4.3. The procedures for linking climate and hydrologic models suggested by various scholars (e.g. Lafon et al., 2013; Neupane et al., 2015; Hendrik et al., 2016) have been followed for this study.

Table 4.3. Description of data used for SWAT model

Description	Sources of data	Resolution/ scale	References
Digital Elevation Model (DEM)	https://vertex.daac.asf.alaska.edu/	30 x 30 m	(Zhao et al., 2019)
Land use land cover (LULC)	Landsat 7; path/row= 166/54 for year 2001 from https://www.glovis.USGS.gov	30 x 30 m	(Ashraf et al., 2017)
Soil data	FAO-UNESCO Global Soil Map	1:5,000,000	(Ashraf et al., 2017)
Recorded climate (daily data)			
Reanalysis dataset	(CFSR) (1979-2014)	0.5^ox 0.5^o North to South and East to west direction	(Ficklin et al., 2009; Kim et al., 2014)
Ground observation data: Precipitation	Ethiopian Meteorological Institute (EMI) (1979-2014)		(Abebe, 2017)
Discharge	Ethiopian Ministry of Water and Energy (EMWE) (1984-1990) and (1993-1996)		(Balascio et al., 1998)

Water balance components for the SWAT model equation (Arnold et al., 1998) provided in Equation (3.3).

$$\mathrm{SW_D} = \mathrm{SW_o} + \sum_{i=1}^{t} (P_i - Q_{surf} - E_a - W_{Seep} - Q_{gw}) \qquad \text{Equation (3.3)}$$

Where SW_t represents final water in soil (millimeters), SW_o shows original water in soil (millimeters) on initial duration i, D represents the duration in days. While, P_i indicates rainfall in millimeters/day, Q_{surf} is the runoff in mm/day. And E_a revels the amount of evaporation and transpiration in millimeters/day, W_{Seep} represents water filtration from the soil layer in millimeters/day, and Q_{gw} represents the deep aquifer recharge in millimeters/day.

During the watershed delineation around 23 Hydraulic Response Units (HRUs) (Appendix 8)) and 146 HRUs were produced for the study sub-basin. The LULC information were produced from the Landsat image information with cloud-free (< 10%), dry season and the availability of Landsat image within average time range of historical period (1979-2014).

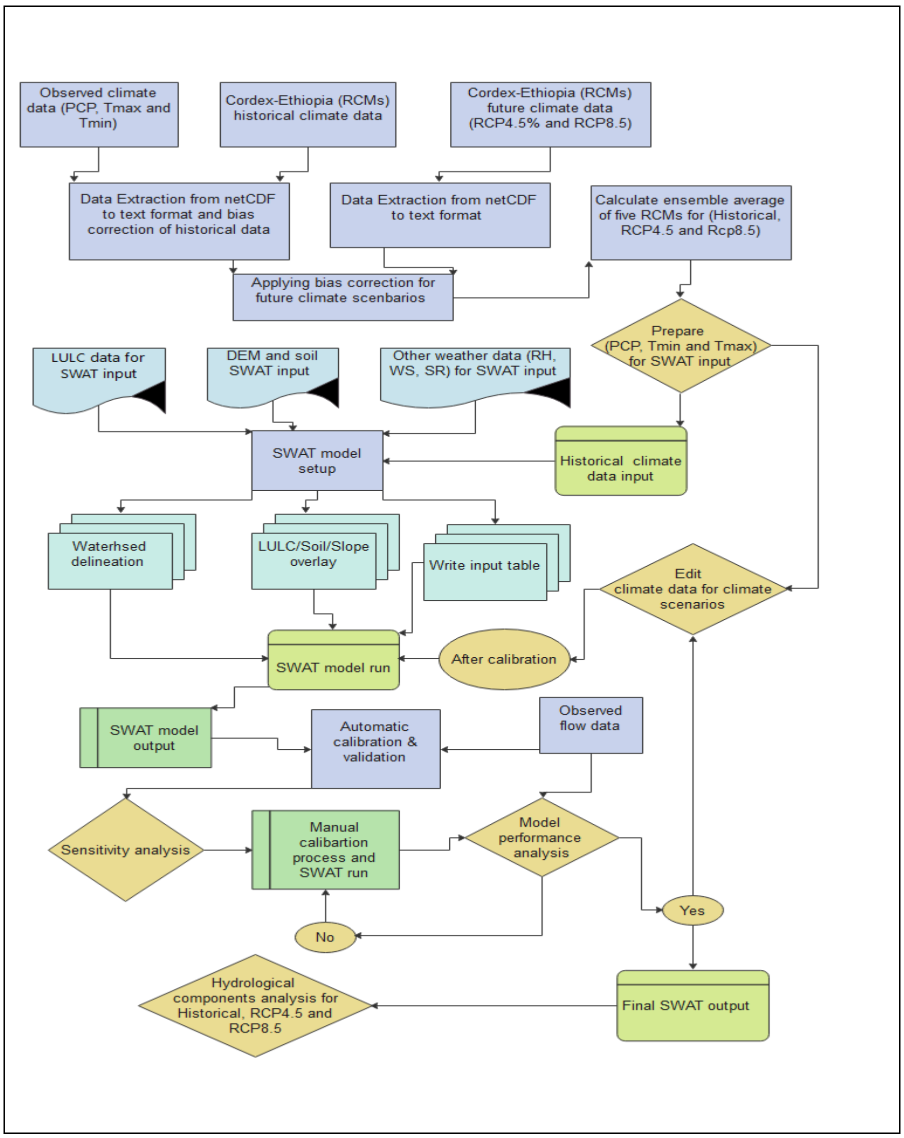

Figure 4.2. Conceptual framework for the study

The model databases were manually edited to make compatible with the FAO soil using database from MWSWAT of lookup table. In this process three soil group are generated (Appendix 9). The model simulation uses three years warm up duration were considered as suggested by (Balascio et al., 1998). In this study DEM data were used to generate slope classes as shown in Appendix 10. The image classification is conducted using ArcGIS interface under supervised image classification procedures. About six land use classes are identified during the image classification from Landsat 7 that prepared LULC map for the year 2001 (Appendix 11). The analysis of image classification accuracy was performed to identify the accuracy of the process of data generation. The soil information required for SWAT input produced from the Food and Agriculture Organization (FAO) and soil map of Ethiopia.

4.2.6. Hydrological model calibration and validation process

The measured daily discharge data at the outlet of upper Erer subbasin was collected. This daily discharge was transformed to monthly discharge was organized to the model input. In this research the duration (1984-1990) for calibration and (1993-1996) for validation were selected. The sensitivity analysis was implemented by employing SUFI-2 (sequential uncertainty fitting) algorithm. were used to identify sensitive parameters form selected parameters (Taylor, 2001). The calibration was performed both automatically and manually (Arnold et al., 1998). In this research manual calibration and validation was also implemented (Moriasi et al., 2007) after automatic calibration.

4.2.7. Investigation of sensitive parameters of hydrological model

In the SWAT model simulation stream flow is affected by high number of parameters. The calibration of entirely these parameters at once is tedious. In this regard sensitive parameters were identified using autocalibration. Initially, around seventeen flow parameters were identified form past studies. Then, employing the SUFI-2 the t stat and p values were produced. The minimum t-stat values stand for minimum sensitivity, whereas great values represent more sensitivity. Lesser p-values stands for more sensitivity, though higher values represent small sensitivity (Zhao et al., 2019).

4.2.8. Performance assessment of hydrological model

The performance measures were used to assess the performance of the model in simulating observed discharge. The performance of SWAT model was evaluated by Nash–Sutcliffe efficiency (NSE), percent bias (PBIAS), and the determination coefficient (R^2) (Ayugi et al., 2021). for the statistical measures Equations (3.4, 3.5, and 3.6) were used.

$$NSE = 1 - \left[\frac{\sum_{i=1}^{n}(Q_{oi} - Q_{si})^2}{\sum_{i=1}^{n}(Q_{oi} - \mathrm{Qoav})^2}\right] \qquad \text{Equation (3.4)}$$

$$R^2 = 1 - \left[\frac{\sum_{i=1}^{n}(Q_{oi} - Q_{sav})(Q_{oi} - Q_{oav})}{\sum_{i=1}^{n}(Q_{si} - Q_{sav})^2 \sum_{i=1}^{n}(Q_{oi} - Q_{oav})^2}\right] \qquad \text{Equation (3.5)}$$

$$PBIAS = 1 - \left[\frac{\sum_{i=1}^{n}(Q_{oi} - Q_{si})}{\sum_{i=1}^{n}(Q_{oi})}\right] \qquad \text{Equation (3.6)}$$

where; Q_{oi} and Q_{si}: the measured and estimated streamflow, Q_{oav} and Q_{sav} mean of the measured and estimated streamflow.

The model is in accepted for ($R^2 \geq 0.6$), (NSE ≥ 0.5) and (-25% ≤PBIAS ≥ +25%) according to (Moriasi et al., 2007). R^2 ranges (zero to one) and as R^2 closer to one represents small discrepancy. Whereas, NSE varies from negative infinity to one with the value approach to one indicates better simulation. While, PBIAS with zero value represents better performance. The PBIAS with "+" sign standards for underestimations, while a "- "sign indicates overestimations of model output (Moriasi et al., 2015).

4.2.9. Evaluation of changing climate effects

The calibrated SWAT model was used to simulate future hydrological response in this research The projection of the water balance components was estimated using the calibrated SWAT model (Kuma et al., 2021). The ensemble average of bias-corrected projected period

(2024–2070) of RCMs for two carbons release scenarios (RCP-4.5 and RCP-8.5) were implemented to simulate projected hydrological responses of the subbasin. The monthly and annual water balance components alteration between baseline and future duration was evaluated.

4.3. Results and discussion

4.3.1. Biased corrected RCMs evaluation under baseline period

The performance of RCMS in simulating the measured climate data at a small level represents a measure for assurance in the researches of climate change effect assessment (Ayugi et al., 2021). Observed climate information stands to measure model performance for bias correction output (Yeboah et al., 2022). The determination coefficient used to estimate the simulation status of RCM shown in Table 4.4.

Table 4.4. Results of statistical parameters to evaluate RCMs

Stations	Statistical parameter	
	Average temperature	Precipitation
	R^2	R^2
Dire Dawa	0.97	0.98
Girawa	0.96	0.64
Gursum	0.95	0.98
Haramaya	0.95	0.03
Harar	0.93	0.96

The result indicates that for all stations the coefficient of determination statistic for average temperature were greater than 0.93. This shows the correction for bias of average temperature indicates well performance (Mathewos et al., 2022). For precipitations, the determination coefficient was all > 0.64 except at Haramaya station. At this station, the value is much smaller than expected. Out of five possibilities only one coefficient of determination less than 0.5 that indicates satisfactory R^2 statistics for rainfall. These indicate a good relationship between the observed and simulated monthly climate variable. Bias correction for precipitation statistics in other study shows R^2 values ranges from 97-99% (Zhang et al., 2018). In this study, bias correction can efficiently minimize errors for average rainfall except for Haramaya station.

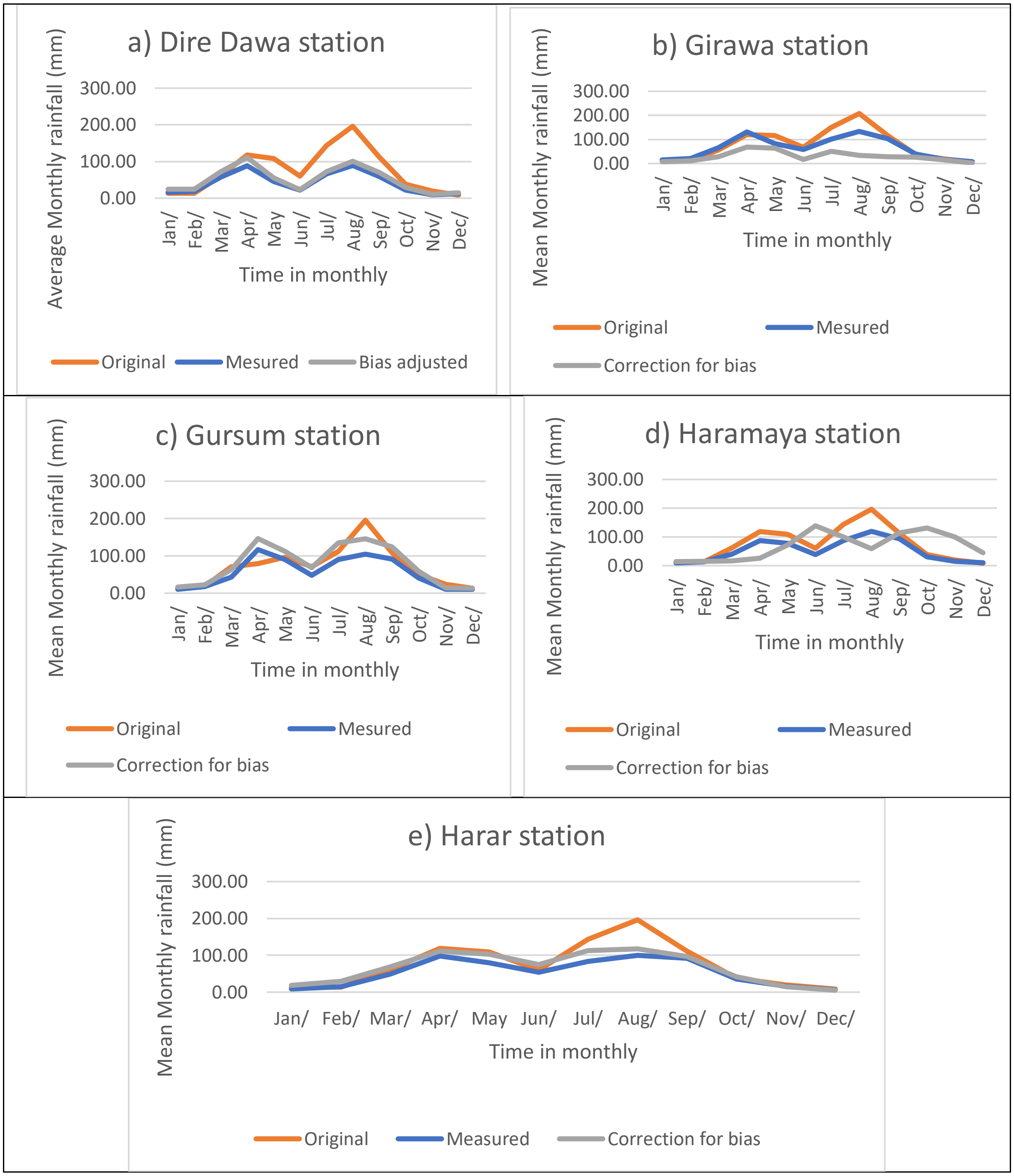

Figure 4.3 (a-e). Monthly average rainfall of observed, original historical CORDEX and bias corrected historical CORDEX for the stations

Figure 4.3 (a–e) indicates ensemble mean monthly rainfall series of original and bias corrected RCMs compared with the observed in the reference duration for stations under considerations.

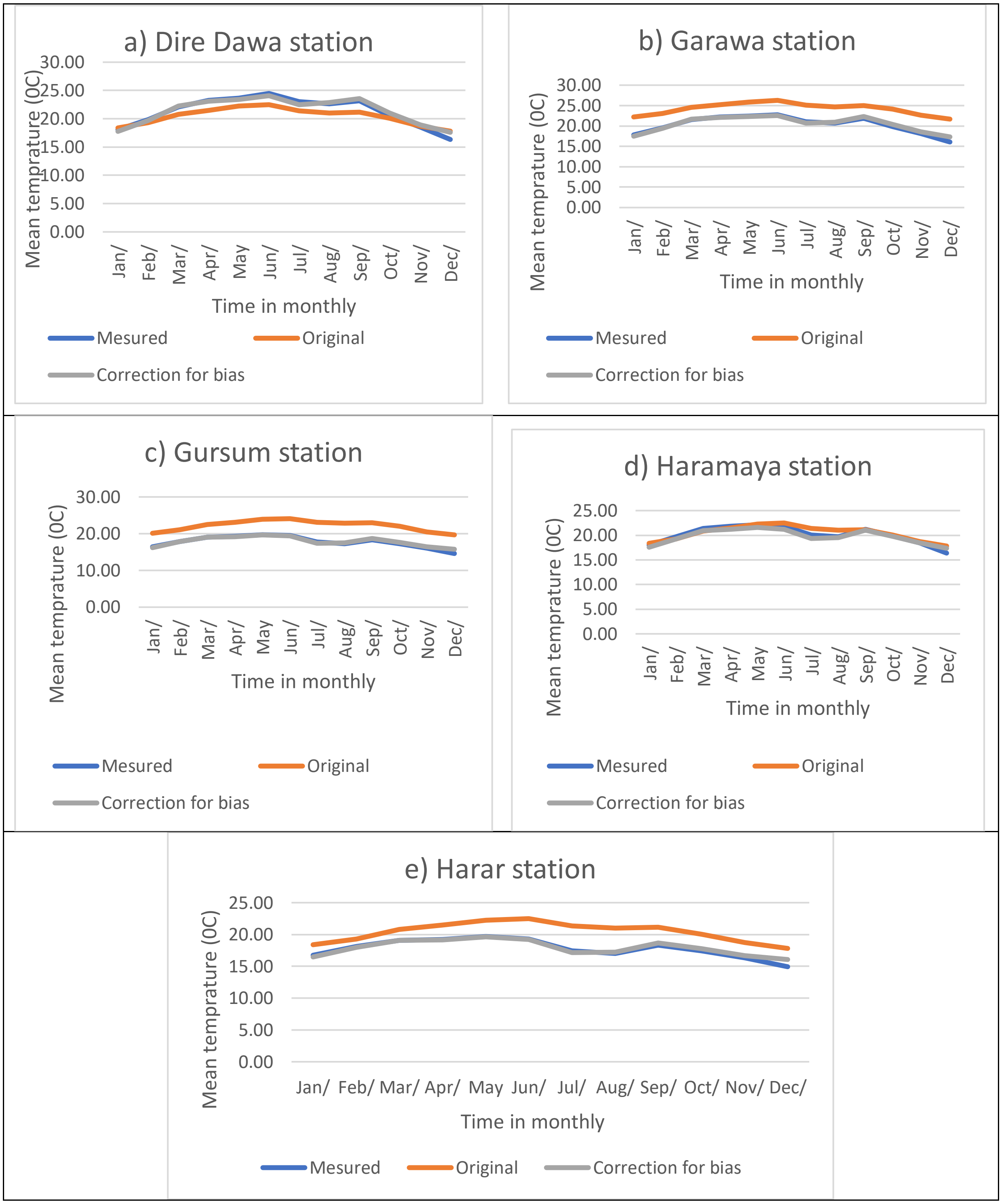

Figure 4.4 (a-e). Average monthly temperature of observed, original historical CORDEX and bias corrected historical CORDEX for the stations

The outcome revels original ensemble average of RCMs for precipitation series are not overlapped with the measured for entire months except (January - March) and (mid-October - December) for Dire Dawa station, (January - February) and (October - December) for Girawa station, (January - March) and (September - December) for Gursum station and (January - February) and (mid-October - December) for Harar station. But, at Haramaya station the precipitation series is not uniform throughout the year. This was perhaps associated with less effective model simulation in Haramaya gauging station or else the possibly due to its topographic characteristics during data record. After bias correction the overlap were significantly improved (Figure 4.3(a–e)).

Figure 4.4(a-e) depicts the ensemble average monthly cycle of original and bias corrected RCMs compared to the mean monthly observed temperature. The original ensemble average of the RCMs for mean temperature overestimated for Girawa, Gursum and Harar stations. While, the original RCM underestimated for Dire Dawa station. The output indicated that bias adjustment meaningfully enhanced model simulation and probably reduces the doubts happening during SWAT model running (Abdulahi et al., 2022). The average monthly values of ensemble average of bias corrected RCMs of temperature were 15.76 ^{0}C and 24.08 ^{0}C at Gursum and Dire Dawa stations, respectively. However, the average monthly observed mean monthly temperature was 14.59 ^{0}C and 24.88 ^{0}C at Gursum and Dire Dawa stations, respectively. At the months of August and September mean monthly ensemble average of biased corrected RCMs shows overestimation for average monthly surface temperature for all stations. But, at Haramaya station the model overestimated only for the months of October and December.

4.3.2. Rainfall projection analysis

Future rainfall for moderate as well as maximum carbon release scenarios were used to analyses rainfall change for the projection period (2024–2070) from reference period (1979–2014). Figure 4.5 (a-e) demonstrates mean monthly rainfall changes for projected period (2024-2070) for RCP-4.5 and RCP-8.5 scenarios of gauging stations. This result indicated that the future precipitation under these two scenarios will rise from May to December for Dire Dawa station, while expected to decline from January to April. At Girawa station, precipitation is expected to increase for entire months in both emission scenarios. But, projected rainfall at Gursum station expected to decrease in all months except in the months of March (RCP-8.5), June (RCP-8.5), August (RCP-4.5 as well as RCP-8.5) and November

(RCP-4.5 as well as RCP-8.5). At Harar and Haramaya stations, the rainfall will rise from July to September for (RCP-4.5 as well as RCP-8.5) scenarios.

Figure 4.5 (a-e). Mean monthly rainfall change for projected (2024–2070) for RCP-4.5 and RCP-8.5

In general, precipitation will rise for whole stations from July to August expect at Gursum station. In The future precipitation will rise for rainy season of June, July and August at higher rate than the rest of months (Ougahi et al., 2022) in Dire Dawa and Girawa stations. The output from Figure 4.5 (a-e) shows the rainfall projection in the Upper Erer subbasin are consistent with climate change impacts studies such as (Gadissa et al., 2018; Daba & You, 2020) that testifies the intra-annual rainfall change having decreasing and increasing monthly share. This indicates that rainfall changes are not uniform for all the stations (38) across the year. The maximum average monthly precipitation rise via 211.22 mm (for RCP-4.5) as well as 235.62 mm (for RCP-8.5) for the station stations. Whereas, the maximum decrease via 90.71 mm (for RCP-4.5) and 84.97 mm (for RCP-8.5). For moderate carbon release the maximum future precipitation alteration is expected at August (44.15 mm, 135.70 mm, 152.73 mm, 194.42 mm and 211.22 mm) for Gursum, Harar, Dire Dawa, Haramaya and Girawa stations, respectively. Nevertheless, the maximum future precipitation alteration is expected in the months of August (49.37 mm, 80.32 mm, 168.13 mm, 220.99 mm and 235.62 mm) for Gursum, Harar, Dire Dawa, Haramaya and Girawa stations, respectively under RCP-8.5. This indicates that the maximum changes in mean rainfall is expected to be happing in the month of August for all stations under both scenarios. The month of August is found in wet season, having highest precipitation in the region. Projected mean rainfall change in all five stations shows the highest mean rainfall change is predictable at Girawa station, but the minimum at Gursum station.

4.3.3. Temperature projection analysis

The comparison the future alteration of temperatures from reference duration (1979-2014) to future duration (2024–2070) for RCP-4.5 and RCP-8.5 v was performed. Figure 4.6 (a-e) revels projected average monthly temperature changes for period (2024–2070) for both carbon release scenarios in reference-to-reference period (1979–2014). The outcome revealed that the increase in monthly mean temperature for RCP-8.5 is more as related to RCP-4.5 for all stations except for Haramaya station in the month of November. Whereas, the temperature for RCP-4.5 is more than for RCP-8.5 scenario.

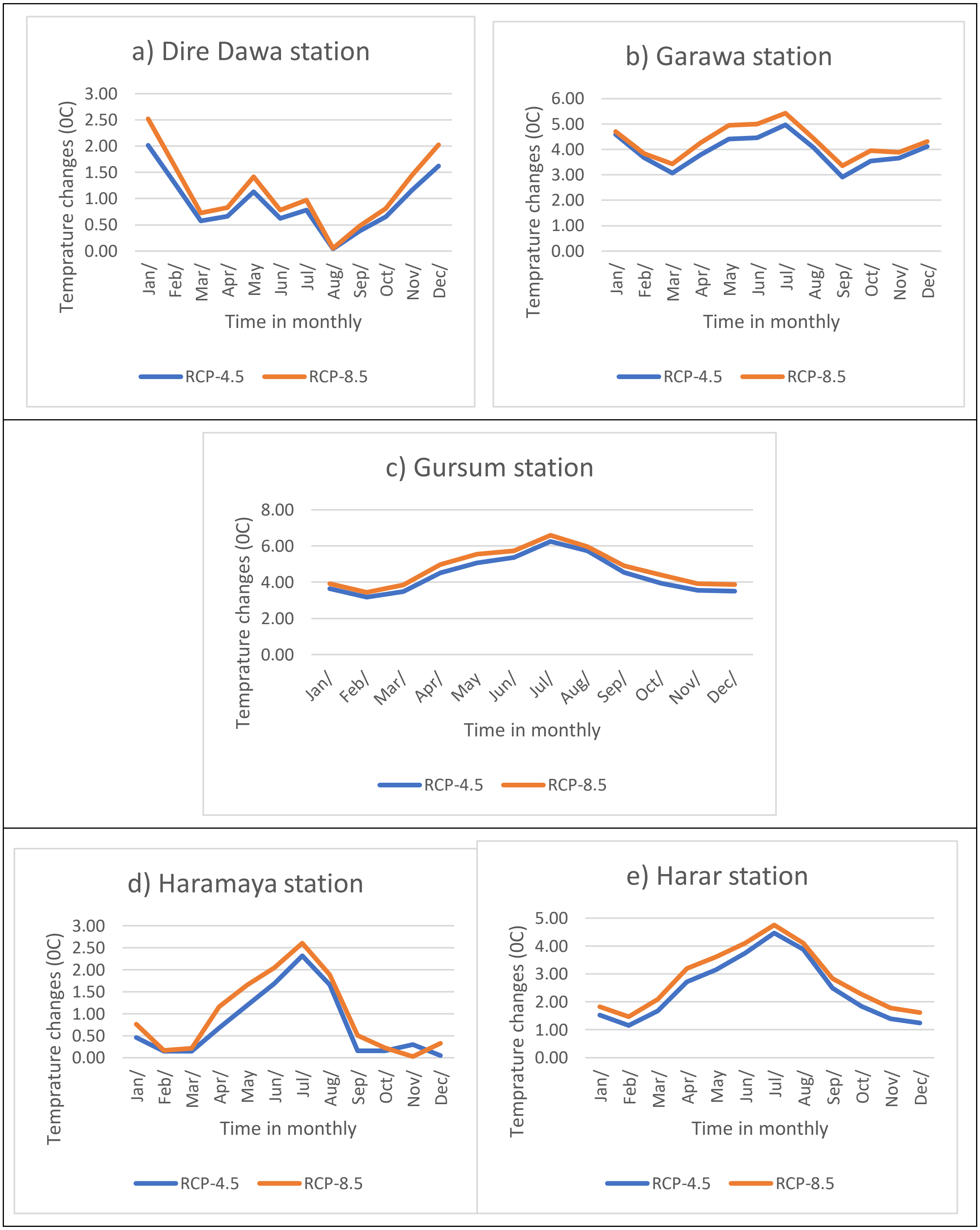

Figure 4.6 (a-e). Change in mean monthly temperatures of RCP-4.5 and RCP-8.5 scenarios for five stations

This shows monthly average temperatures will be expected to increases (Negewo et al., 2019) for projected duration in reference-to-reference duration for RCP-4.5 and RCP-8.5. The minimum alteration for average monthly temperature will rise by 0.04°C (Dire Dawa station) for RCP-4.5, while highest change in average monthly temperature be expected to rise by 6.5°C (Gursum station).

Nevertheless, under RCP-8.5 the minimum monthly change is expected to rise by 0.03°C (Haramaya station), while the maximum mean monthly temperature change is expected to rise by 6.59 °C at Gursum. This result indicates the predicted mean monthly temperature is expected to rise (Kebede et al., 2013; Kassie et al., 2014) for RCP-4.5 and RCP-8.5. Temperature increase is higher for RCP-8.5 than RCP-4.5 that indicates there is a high greenhouse gases concentration is expected for RCP-8.5, having a more global temperature increase.

The output shows that regional environment is warmer than the current duration for RCP-4.5 and RCP-8.5 scenarios (Ougahi et al., 2022). Maximum predicted average temperature change will happen for January (2.02 ^{0}C), July (4.97 ^{0}C), July (6.25 ^{0}C), July (2.32 ^{0}C) and July (4.47 ^{0}C) for Dire Dawa, Girawa, Gursum, Haramaya and Harar stations, respectively for RCP-4.5 scenarios. While, for RCP-8.5 scenario, maximum change will happen in the months of January (2.52 ^{0}C), July (2.6 ^{0}C at Dire Dawa), July (4.75 ^{0}C at Haramaya), July (5.43 ^{0}C- at Harar) and July (6.59 ^{0}C at Gursum).

The result indicates that the maximum change in average temperature change will be happening in July for all stations. But for Dire Dawa station, it is expected to be happening in January. This is probably due the effect of the topographical location of Dire Dawa gauging station (lowest topography) as compared to other stations (higher topography) (Appendix 7). Dire Dawa station location is categorized under warm semiarid ecological climate zone (Hurni, H., 1998).

The results for future mean temperature in all five stations shows an increasing in both emission scenarios. The maximum mean temperature to be predicted for Gursum station and minimum at Dire Dawa station. Lowest projected mean temperature is expected to occur in Dire Dawa, Haramaya, Harar, Girawa and Gursum stations in increasing order under both emission scenarios. Generally, the average temperature projection in two emission scenarios is in the range that predicted by IPCC and coincides with similar studies (Gyamfi et al., 2016; (Zhao et al., 2019). Most climate change studies in various areas of Ethiopia watersheds showed that the temperature is likely to rise, such as study conducted in southwest Ethiopia (Geleta et al., 2022).

4.3.4. Hydrological model sensitivity analysis and performance evaluation

Sensitive parameters were identified before the implementation of model simulation. Initially seventeen parameters were identified that used for sensitivity analysis by employing sufi2 algorithm in the SWAT-CUP model. The lowest p-value and the highest t-stat were considered to identify sensitive parameters. Using this process, ten most influential parameters were identified. Appendix 13 shows the sensitive parameters values from the autocalibration analysis.

The statistical measures NSE for calibration (0.65) and validation (0.53) found. While, R^2 for calibration (0.84) and validation (0.72) period. These showed that the model performance was well improved for calibration than the validation time. This is possibly credited to inappropriate stream flow records for the validation period or else inconsistency in hydroclimatic and spatial data. The PBIAS for calibration (-23.04 %) and validation (-14.16) for simulation indicated predicted discharge overestimated the measured discharge. Overall, statistical measures NSE, R^2 and PBIAS results shows measured and predicted monthly discharge were in good relation (Moriasi et al., 2015; Osima et al., 2018) as shown in (Appendix 15). This best relation among measured and predicted discharge revels that SWAT model used to simulate monthly stream flow in the region significantly.

4.3.5. Hydrological model calibration and validation

Autocalibration and manual-calibration process were used in this study. After the autocalibration process and identification of sensitive parameters manual calibration (Neitsch et al., 2011) were used to adjust the SWAT model sensitive parameters. During the processes sensitive parameters were identified for groundwater and surface runoff parameters (Appendix 13) using the observed streamflow records. To improve the performance of the model several simulations run (twenty-eight) by adjusting the parameters values within acceptable ranges. Finally, the parameters values range and associating good match values gotten are shown in Appendix 14. The model simulation was performed for entire period (1979- 2014) using three years warmup period (1979-1981). The calibration and validation process taken place using observed monthly stream flow for (calibration from 1984 to 1990) and (validation from 1993 to 1996).

The manual calibration process has been set in the order of sensitivity on the runoff and ground water flow parameters for instance surface CN2, GW_REVAP, REVAPMN and RCHRG_DP (Neitsch et al., 2011). During first SWAT model run output shows baseflow was too low and evaporation was too high. So, adjustments were made on the groundwater flow parameters, by decreasing the GWQMN and GW-REVAP and increasing the REVAPMN parameters successively until the model performance measures were reaching satisfactory values of (NSE, R^2 and PBIAS).

Then, baseflow became highest and the peak flows were lowest. Hence, adjustments were made to the surface runoff and baseflow parameters by increasing CN2 and decreasing the other flow parameters (SURLAG, ESCO and EPCO) slightly until reach reasonable statistical measures (R^2, NSE and BIAS. Then, the same adjustments were made to the soil parameters includes: Saturated hydraulic conductivity at layer 1 (SOL_K (1)), Soil water available capacity (SOL_AWC (1)) to reach the acceptable performance metrics values (Neitsch et al., 2011; Zhao et al., 2019).

Appendix 16 (a and b) shows monthly stream flow hydrograph of (calibration and validation). The output indicates during the calibration time model overestimated (January and from April to December). Whereas, the model overestimated for the months of (April and from September to January) during validation time. In this research peak monthly runoff was predicted for the both calibration and validation time (Appendix 16 (a and b)).

Therefore, SWAT model captured the monthly peak flow at model simulation time. This indicates, SWAT model is suitable to quantify the possible effects of change in climate as well as to understand hydrological response under refined hydro-meteorological data in the study subbasin.

4.3.6. Evaluation of hydrological balance variation for changing climate

The SWAT model predicted for hydrological balances of runoff, lateral flow, ground-water-flow, water-yields, evapotranspiration and potential-evapotranspiration by changing climatic variables. Climate change impacts on the hydrological balance of the upper Erer subbasin were evaluated using the temperature and rainfall changes for projected duration (2024-2070) in reference-to-reference duration (1979-2014) for RCP-4.5 and RCP-8.5 scenarios.

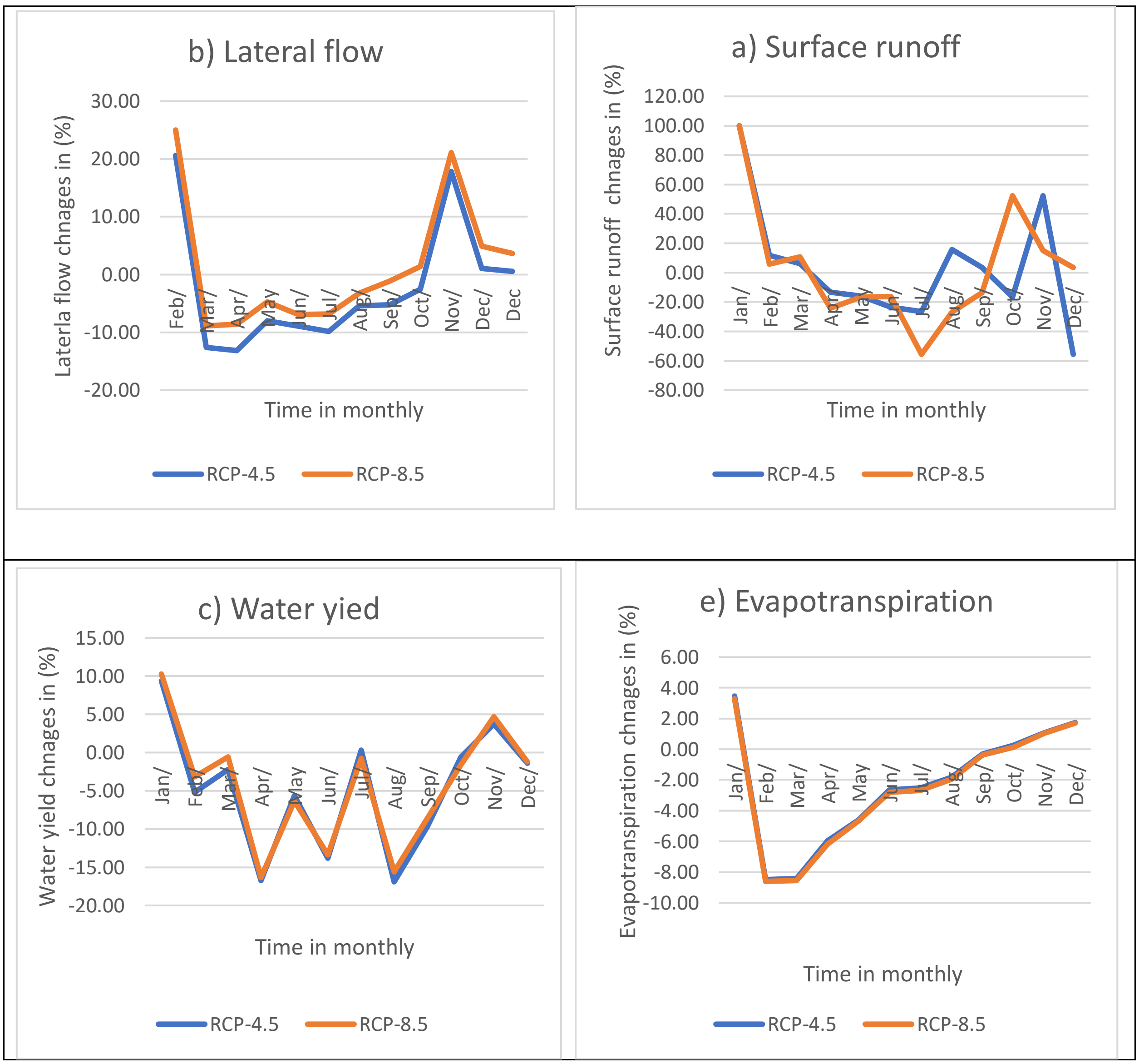

Figure 4.7 (a-d). Average monthly change of predicted surface-runoff, lateral-flow, water-yields and evapotranspiration in reference-to-reference duration for RCP-4.5 and RCP-8.5

Accordingly, Figure 4.7 (a-d) shows that monthly predicted change of surface-runoff lateral-flow, water-yields, evapotranspiration a potential-evapotranspiration in reference-to-reference duration RCP-4.5 and RCP-8.5. The result indicates that the projected surface runoff at (March, June, October and December) is lower under RCP-4.5 than RCP-8.5, but for the other months the surface runoff is expected to be more under RCP-4.5 than RCP-8.5. Nevertheless, lateral-flow change for entire is higher for RCP-8.5 than RCP-4.5. The water yield for entire months is expected to be lower for RCP-4.5 than RCP-8.5 excluding (May, July, October).

The mean annual change for all hydrological response shows a decrease under both emission scenarios except the potential evapotranspiration (Table 4.7). The monthly average flow fluctuates significantly throughout the year (Negewo et al., 2019). Hence, the predicted change in climate will decrease most of the water balance in the subbasin (Ougahi et al., 2022). The SWAT model output indicates that decrease of precipitation and rise of temperatures are expected in the region. This will probably drop in surface-runoff, lateral-flow, groundwater-flow and overall water-yields. The yearly surface-flow decreases probably happening due an increase of mean temperature in the study area. This is confirmed by (Zhang et al., 2018) that reported the temperature increase can result in a decrease of annual surface flow. The increment in temperature also caused an increase of Potential Evapotranspiration (PET). This shows that the temperature changes and PET are interrelated absolutely.

Table 4.5. Annual water balance component changes for RCP-4.5 and RCP-8.5

Hydrological response (unit)	Scenarios	
	RCP-4.5	RCP-8.5
Surface runoff (%)	-4.98	-5.30
Groundwater flow (%)	-5.63	-6.68
Evapotranspiration (%)	-2.45	-2.57
Lateral flow (%)	-3.64	-0.18
Water yields (%)	-5.54	-5.21
Potential Evapotranspiration (PET)	0.47	0.49

The result shown in Table 4.5 indicated that the predicted groundwater-flow to change via a higher amount and evapotranspiration via a minor amount. The amount change in surface runoff and lateral flow are low when compared with groundwater flow and water yield.

Nevertheless, the predicted surface runoff change is higher relative to lateral-flow, water-yields, evapotranspiration and potential-evapotranspiration for both emission scenarios.

Figure 4.8 shows that the mean annual projected change for RCP-4.5 and RCP-8.5 of surface-runoff, groundwater-flow, lateral-flow, water-yields, evapotranspiration and potential-evapotranspiration in reference-to-reference period. The result indicates that the highest decrease for mean annual surface runoff, ground waterflow and evapotranspiration will happen under RCP-8.5. But, the maximum decrease in mean annual water yield and lateral flow will happen under RCP-4.5. Nevertheless, the potential evapotranspiration is expected to increase under both scenario and maximum under RCP-8.5 scenario.

Generally, monthly change on water balance component will have varying intensity and surface-runoff is substantially changing than others for carbon release scenarios. However, annual climate change impacts will have maximum impacts on groundwater flow. Evapotranspiration and lateral flow are the minimum effects with the changing climate as compared to others for two scenarios. Average monthly precipitation for entire stations is variable, but at sub basin level the mean monthly rainfall is decreasing during wet season. The temperature is increasing and rainfall is decreasing (during wet season).

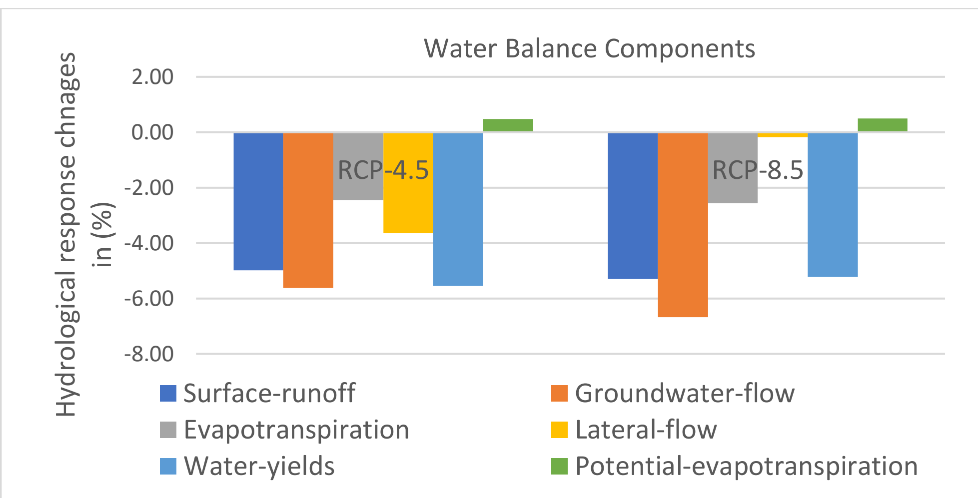

Figure 4.8. Mean annual projected percentage change of surface-runoff, groundwater-flow, evapotranspiration, lateral-flow, water-yield and potential-evapotranspiration for RCP-4.5 and RCP-8.5 scenarios in reference-to-reference duration

This will decrease the surface-runoff, groundwater-flow, water-yields and evapotranspiration. While, potential-evapotranspiration will rise. The decline of mean annual water yield over the subbasin possibly will happen due to the reduction of annual and seasonal (wet season) rainfall and increasing mean surface temperatures under both emission scenarios. But station wise the mean monthly rainfall is variable. Moreover, the incline in PET will happen due to the surface temperature increases and this aggravated the decrease in rainfall and affects the ecosystem. The likely reduction of water yields critically affects the accessibility of the water resources in the region.

4.4. Conclusions

Eastern Ethiopia watersheds are located in transition zone from Arid to semi-humid climate. The annual rainfall distribution is highly declining in expanding westwards in the watersheds including the upper Erer subbasin. This research is focused climate change impacts assessment on future hydrological response under daily bias corrected climate variables from CORDEX RCMs on upper Erer subbasin, located in Eastern Ethiopia. The performance of ensemble average of the baseline period (1979-2014) of five RCMs was evaluated using observed climate variables. The change from the past duration (1979-2014) to future duration (2024-2070) in ensemble average of RCMs determine the predicted change in climate variables. Extraction and bias correction were performed on RCMs before using the climate data for analysis to minimize bias. It is found that the mean monthly temperature is varied from (0.04 to 6.25^{0}C) and from (0.03 to 6.59^{o}C) for RCP-4.5 and RCP-8.5, respectively. However, average monthly precipitation will reduce and rises within the range of (90.71 mm to 211. 22 mm) and (84.97 mm to 235.62 mm) for RCP-4.5 and RCP-8.5, respectively.

SWAT model is employed to predict the hydrological balance of the reference duration and projected duration to quantify its changes. The output revels that the subbasin annual hydrological response will decrease in both scenarios having minimum value of 2.45% (evapotranspiration) and 0.18% (lateral-flow) and a maximum value of 5.63% (groundwater-flow) and 6.68 % (groundwater-flow) for RCP-4.5 and RCP-8.5, respectively. The mean monthly change of streamflow is running from a maximum increase of 100 % (January) to a maximum decrease of 55.6 % (December) under both scenarios. The mean monthly changes of lateral flow with maximum increase at January (20.6 %) and maximum decrease at February (13.1%) and having maximum increase at January (25%) and maximum decrease at March (8.9%) will happen for RCP-4.5 and RCP-8.5, respectively. The highest mean monthly increase and decrease in water-yields (9.4 % and 16.9%) for RCP-4.5 scenario and (10.3% and 16.3%) for RCP-8.5 scenario. However, the maximum average monthly evapotranspiration increase (3.5% and 3.33%) and maximum decrease (8.5% and 8.6 %) for RCP-4.5 and RCP-8.5 scenarios, respectively. The hydrological components vary significantly for all the months in the year and high values is expected to happen in (November, December and January) that concedes with dry season. While, lowest hydrological response change is expected in (March, April, May, June and August) that fall under wet season in the region. Moreover, the decreasing hydrological response is expected to be happening in the wet season (from March to July). But, surface-runoff is increasing in March only.

In general, the climate model prediction demonstrates high variation in model performance for one station. This is therefore, it is crucial to identify these deviations to examine change in climate effects on water sources systems. In addition, hydrological model simulation process indicates that the model prediction was better at calibration than validation time. This is probably due to poor quality of stream flow records and inconsistency in hydroclimatic and spatial data. Hence, future research may use refined hydrometric and spatial data for reasonable result.

5. ASSESSMENT OF THE EFFECTS OF LAND USE LAND COVER CHANGE ON WATER BALANCE COMPONENTS IN THE UPPER ERER SUBBASIN, WABISHEBELE BASIN, ETHIOPIA

Abstract

Land use change has a vital role in disturbing the hydrological response and assessing the LULC change and its impacts on the hydrological response is required for efficient water resource planning. The extent of LULC changes at the local level was uncertain and how the hydrological conditions were affected by LULC changes locally was a challenge. This study focused to assess the LULC change and its impacts on the hydrological components in the upper Erer sub basin using SWAT model from 2001 to 2020. The LULC change indicated that agricultural lands (3.97%) forest lands (3.99 %), and water bodies (0.60 %) were decreased and settlements (2.30%), shrub land (3.07%) and bare land (3.19) were increased. The model was calibrated and validated using monthly flow data indicates the performance was within satisfactory range of PBIAS ≤ (±25%), R^2 > 0.8 and NSE > 0.5. The surface runoff, ground water flow, and water yields were increased by 6.03, 8.22, and 10.39 %, respectively. While, evapotranspiration was decreased by 3.34%. In this study, the change in LULC has significantly affected the hydrological component of the sub basin. This implies the implementation of adaptation strategies for sustainable water resource management in the region.

Keywords: Surface runoff; Evapotranspiration; Hydrological component, Land use land cover change; Manual calibration;

5.1. Introduction

Land use change is highly affected by the population growth (Arnold & Allen, 1999; Tufa et al., 2014). The driving forces that affect hydrological situations are land use land cover (LULC) changes and climate change (Torabi et al., 2020). Land use change has a dynamic role in distressing the surface runoff and groundwater flow (Napoli et al., 2017; Pandey et al., 2021). The study conducted in Upper Nile Basin indicated LULC change affected the surface runoff and evapotranspiration (Berihun et al., 2019). Similar studies indicated that the development of agricultural land, intensification of bare land, and urbanization resulted in stream flow increase (Welde & Gebremariam, 2017; Belihu et al., 2019). In addition, the intensification of cropland and urbanization alters the soil moisture conditions and groundwater storage (Galata et al., 2020). The LULC changes due to the loss of forest affects the infiltration rate season (Belihu et al., 2019). Settlement lands were the largest contributor to water yield (Lu, Z. et al., 2015). The surface runoff and water yield were positively linked to variation in cropland and settlements. However, ground water flow and evapotranspiration were negatively linked to changes in cropland and settlement lands (Aragaw et al., 2021; Chemura et al., 2020). The increase in rainfall resulted in an increase in annual runoff (Daba, 2020). Other study in Wabishebele Basin indicated portion of forest coverage and population concentration was found negatively correlated with surface runoff (Wudineh et al., 2021). The output from similar study indicated that additional natural vegetation land cover changes to cropland or grazing lands, probably tends to decrease dry-season streams and exaggerate peak runoff (Mango et al., 2011). The surface runoff extent has high positive correlation with cropland and population density and a strong negative correlation with natural vegetation (Wudineh et al., 2022). Natural vegetation cover, expansion of agriculture and settlements were the main land use driver affecting the variation in hydrological components (Marhaento et al., 2018; Gebremicael et al., 2019; Kenea et al., 2021).

The LULC changes will have an impact on water resources (Koycegiz et al., 2019). Assessment of the hydrological impacts under LULC changes produced by different hydrological components (Gebre et al., 2022). So, related studies will be used to understand the hydrological processes of water resource administration and development (Ding et al., 2022). The continuous watershed situation assessment was vital for improved watershed management. The LULC change effects analysis is essential in watershed management at sub basin level (Wu, F. et al., 2015). The LULC change affects the hydrological cycle in complex ways with scale differences and different spatiotemporal scales under regional conditions (Ding et al., 2022). To mitigate this problem now adays there is high interest of using hydrological models in order to appropriately compute the diversified effects land use land cover changes (Tufa et al., 2014). The hydrologic models are likely to quantity and evaluate hydrological component. The hydrological component includes the amount of precipitation, actual evapotranspiration and water yield (Takala et al., 2016; Gebre et al., 2019). The interaction of land and water conservation practices were needed for the implementation of sustainable water resource management and planning under local and regional scale (Belihu et al., 2020). Sustainable water resource development was implemented by examining the land use land cover change effects on long-term changes in hydrological conditions and understanding the impacts of LULC change on hydrological components (Baker & Miller, 2013; Mohammad et al., 2016; Galata et al., 2020). The soil and water assessment tool (SWAT) hydrological model was successfully simulated for water balance component analysis under the LULC change (Abbaspour et al., 2007; Torabi et al., 2020; Getu et al., 2021).

Defining the characteristics of hydrological circumstances regionally and locally is a challenge under LULC changes (Aredo et al., 2021). This is more severe in developing countries where there is a shortage of data, the degree of LULC change is indefinite (Torabi et al., 2020). For this reason, it is important to conduct studies concerning the land use/cover change effect, especially in watersheds with low hydrometeorological data availability such as the upper Erer sub basin. As confirmed by (Weldu & Edo, 2020) in the Erer subbasin the land use land cover change has a substantial. Hence, determining the land use land cover changes and assessing their effects become particularly relevant for sustainable management of land and water resources in the long term in the upper Erer sub basin. Now a days Numerous studies were analyzing the impact of LULC changes on the hydrological process; eg (Moreira et al., 2018) and others. Researchers such as (Masood et al., 2023) computed the impacts of climate and land cover changes on the hydrological regime of a complex dam catchment area, Pakistan. Their discoveries showed that the complex dam catchment area is predictable to practice dangerous hydrological situations owing to the land-use and climatic circumstances of the river basin which depends on impacts on surface runoff. Similarly, (Zhang, Y., You et al., 2016) in Australia simulated water balance components to land-use change in the North Johnstone River catchment and found that land-use change affected hydrological components, with the most prominent effect presence on surface flow. Other research in Tanzania assessed land use land cover changes effects of the Wami sub-basin considered only a few hydrological parameters for their analysis, suggested to include other hydrological parameters in order to better understand the hydrology of the basin for the optimal use of water resources (Ngondo et al., 2022). Generally, in spite of their prominent results, these and many other studies are mainly focused to river sub-catchments/sub-basins using some or part of the hydrological components. Thus, mostly they have not address the capacity to deliver collective effects of land use land cover changes (LULCCs) on the hydrology at local scale especially in the study area region. Limited information is also available on the effects of land use and land cover change on soil and water resources in arid and semiarid areas of the country (Negese et al., 2021) including the upper Erer sub basin. It is important to evaluate the land use land cover change impact, mainly at the local level (Taye H. et al., 2016). Similarly, such problems are existed in the Upper Erer subbasin, which has multiple land uses and considerable land use land cover changes (Weldu & Edo, 2020). Nevertheless, the increase in multiple LULCCs and their impacts, only few hydrological studies have been conducted on the region. In Ethiopia the understanding of the challenge to LULC change effects need further investigation on ground water hydrology in particular and other hydrological components (Negese et al., 2021).

The present research has used more hydrological components in the equation that represent the actual pertaining situation of the catchment hydrology. This research objective is to assess the effects of LULC change on water balance, such as surface runoff, total water yield, groundwater flow, lateral flow, and evapotranspiration at subbasin scales employing SWAT model. The study used for better understanding of hydrological processes under changing LULC in the upper Erer subbasin.

5.2. Materials and Methods

5.2.1. Description of study area

The upper Erer subbasin, which is located physically in between $9^{o}13'26.4''$ N to $9^{o}31'26.4''$ N latitude and $42^{o}4'40.8''$ E $42^{o}20'38.4''$ E longitude found at the upper part of the Erer River Basin. The Erer River Basin is a tributary of Wabisheble Basin and found in the upper Wabishebele Basin, which drains from the Harar highlands. The Upper Erer Subbasin area is about 466.84 km2 with an elevation range from 1306 to 3019 meters as shown in (Figure 5.1).

The Upper Erer River Alluvial Valley Plain is found about 10 to 20 km east and south east of Harar Town.

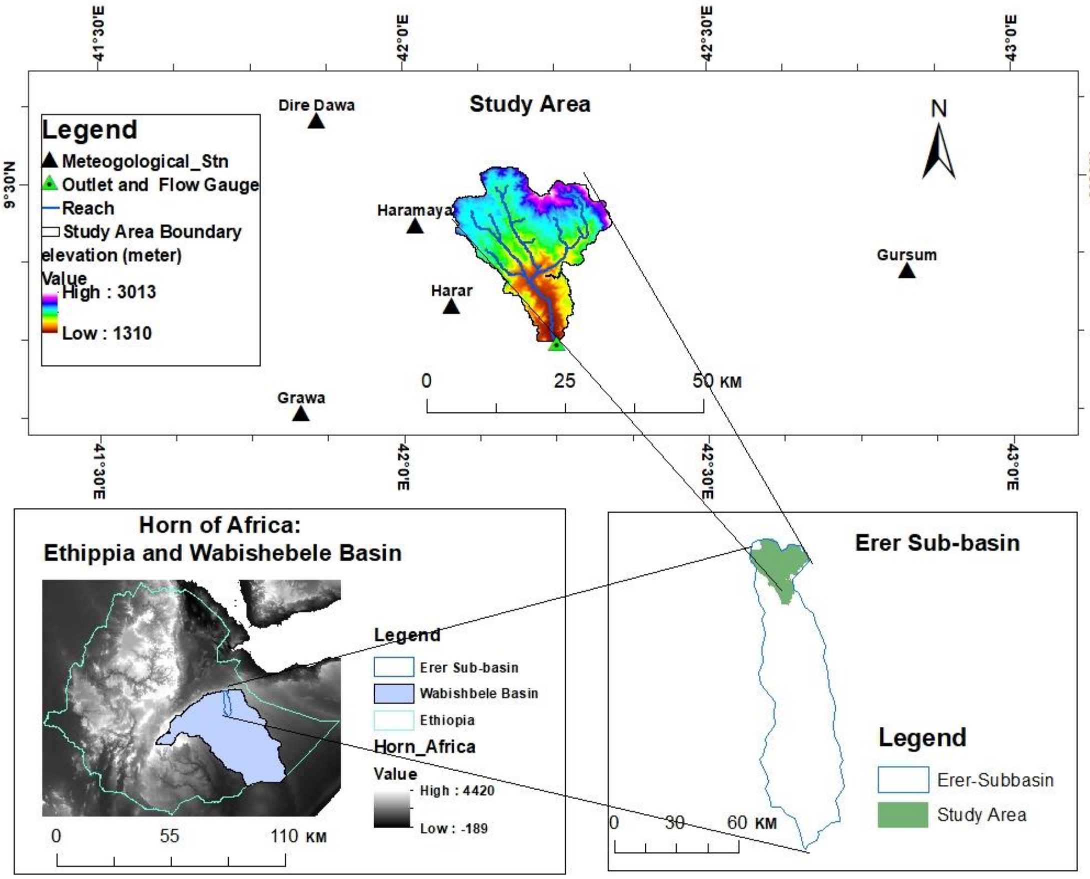

Figure 5.1. Study area location of the upper Erer subbasin for LULC change impacts on hydrological components

Ecologically, the upper Erer subbasin is categorized in to three climatic zones; Kolla (warm semiarid), varied from elevation 500 to 1500 meters, accounted for about 13.06 %, Woinadega (cool subhumid) varied from elevation 1500 to 2300 meters is accounted for 73.98 % and Dega (cool humid) varied from elevation 2300 to 3200 meters accounted for 12.97 % of the total drainage area (Hurni, H., 1998). The mean daily minimum and maximum temperatures were 12.78 and 26.72 °C, respectively (Abebe, 2017). The regional agroecological zone climate highly dominated by Woinadega (cool subhumid). The population income mostly depends on agriculture (Mihertu, 2019).

4.2.2. SWAT model setup and description

In this research SWAT hydrological model was employed for hydrological component assessment under LULC changes. Semi-distributed based modeling approaches are considered for a remote watershed that suffers from deficiency of continuous and good quality data (Addis et al., 2016). The user probably identifies the type of projection and the projection settings within the interface when creating a new project setup (Winchell et al., 2013). In this research the projected coordinate systems of UTM (Universal Transverse Mercator) were used. The suitable UTM zone of WGS 84-UTM zone 37 N have been identified during the process. The hydrologic response unit (HRUs) in which each HRUs had exceptional soil–land use combinations were generated in the sub basin. The hydrological cycle simulated by SWAT model is based on the water balance components indicated in Equation (4.1).

$$\mathrm{SW_t} = \mathrm{SW_o} + \sum_{i=1}^{t}(\mathrm{Pi} - \mathrm{Qsurf} - \mathrm{Ea} - \mathrm{Wseep} - \mathrm{Qgw}) \qquad \text{Equation (4.1)}$$

Where $\mathrm{SW_t}$ is the total soil water capacity (mm), $\mathrm{SW_o}$ is the original soil water capacity (mm) at initial time i, t is the time in days, Pi is rainfall in mm/day, Qsurf is the surface flow in mm/day, Ea is evapotranspiration in mm/day, Wseep is the water percolation from the soil profile in mm/day, and Qgw is the groundwater recharge in mm/day.

During SWAT model simulation the computation of evaporation from soil and plants were separately processed. Hence, in this research the Penman– Monteith potential evapotranspiration (Arnold et al., 2011) was selected for evapotranspiration calculation. The daily rainfall/CN/daily runoff (rainfall-runoff) parameters were selected for watershed parameters for the assessment of water balance. Soil Conservation Services (SCS) curve number method was chosen for surface runoff estimation (Winchell et al., 2013). In the SWAT model simulations various spatial and temporal data are required such as Digital Elevation Model (DEM), soil map, meteorological data, land use land cover data. The DEM data with a grid resolution of 30 m by 30 m is downloaded from United States of Geological Survey (USGS) Earth Explorer website: (http://earthexplorer.usgs. gov/) https://vertex.daac.asf.alaska.edu/and used to generate the topography and slope of the sub-basin (Her et al., 2015). Using the DEM data the SWAT model produces five slope categories. The soil data used for the research was created from United Nations Food and Agriculture Organization (FAO) website and clipped by FAO soil map of Ethiopia that collected from Ministry of Agriculture.

The FAO soil map of Ethiopia was prepared by the professionals considering the local circumstances of soil characteristics. SWAT soil map input data was prepared having soil map of the study area and lookup table. The soil map was linked to the model and used to indicate the soil type and the lookup table was used to describe the map using two columns arranged, one for the soil name and the other for soil values generated from the map (Winchell et al., 2013). In this study, the Map Windows in the MWSWAT database were used for the soil database in Arc SWAT database to make compatible the user soil map data with the ARC SWAT database.

The temporal data used for SWAT model simulation are daily meteorological data. Both observed daily observed and global data (CFSR) were used for this research. The rainfall data was collected from ground rain gauge observations from Dire Dawa, Girawa, Gursum, Haramaya, and Harar stations provided by the National Meteorological Institute of Ethiopia (NMIE) for the period (1979 to 2014). Whereas, others weather data (maximum and minimum temperatures, relative humidity, solar radiation and wind speed) were collected from Climate Forecasting System Reanalysis (CFSR) (Dile & Srinivasan, 2014; Nkiakaet al., 2017; NCEI, 2020) using the overlapping coordinate with the ground gauging stations.

Five meteorological ground stations were selected (Appendix 7) based on the quantity, quality, period, consistency, homogeneity, and their uniformity distribution around the Upper Erer subbasin. The missing data for the rainfall data were adjusted from the nearby stations using the arithmetic mean method and normal ratio method as recommended by (Egigu, 2020). The user weather databases were prepared and copied to the Arc SWAT database (Winchell et al., 2013). In this research the user edited the entire user-wgn manually using the weather generator program such as WGNmaker4.xlms that nun to calculate the value of different precipitation parameters used for weather generator. This program uses the EXCEL macro to calculate the weather station statistics used for weather generator for SWAT model input. The values of RAINHHMX (Maximum 0.5-hour rainfall in entire period of record for month*)* are 1/3 of the maximum daily rainfall of a month is taken as their values are not recorded locally (Winchell et al., 2013) cross ref: http://www-ssl.tamu.edu Texas A &M University.

The land use land cover map was prepared for SWAT input using the image classification by employing ArcGIS software under supervised image classification procedures. During image classification the accuracy of the prepared image were checked Image for its accuracy and image classification accuracy assessment was used to check the accuracy for the land use land cover map generated from Landsat image. Detail image classification procedures were presented in the following sub-section. After the completion of the image classification the produced map were a lookup table with unique land use code to link the grid values to SWAT LULC classes (Winchell et al., 2013).

During the SWAT model setup, the Hydraulic Response Units (HRUs) analysis was implemented by overlaying the classified LULC map, soil map, and slope map (generated from DEM). In this research the percentage values of LULC (10%), soil (15%), and slope (15%) were used as recommended by (Winchell et al., 2013).

4.2.3. Image classification

The extraction of Landsat image the cloud-free (< 10%) dry season, and image availability was considered for the periods. During the image extraction the seasonal differences in vegetation distribution were minimized by extracting uniform season image for different image extraction (Shanko & Camberlin, 1998) as shown in Table 5.1. The Satellite images for the years 2001 (Landsat 7) and year 2020 (Landsat-8) were obtained from United States Geological Survey (USGS) (https://www.glovis.USGS.gov). The downloaded images were analyzed using ArcGIS and following the supervised classification approach to make a land cover map for the region.

Image classification accuracy assessment was used to detect the image classification accuracy for the classified LULC map generated from Landsat data, and this was used to know the proximity of the images to the training sample on the classified images. Using the interactive supervised image classification, the LULC maps for 2001 and 2020 were produced. Due to a constraint of field data, Google Earth, a previously generated map of the region and the digitalized topographic map with 1:50,000 scale of 1st edition 2000 of Ethiopian Mapping Agency was used for the reference sample generation as suggested by (Shigute et al., 2022). The accuracy of the image classification was verified using the overall percentages of accuracy, user's accuracy, producer's accuracy, and the Kappa Coefficient (Lillesand et al., 2015; Mir et al., 2022). The Equations (4.2 to 4.5) were used to assess image accuracy.

Table 5.1. Landsat Information for the period under consideration, including the acquisition date, path/ row of images, image types, and image resolution

Reference data	Acquisition date Year/Month /Day	Path/row	Image	Resolution
2001	2001/12/10	166/54	Landsat 7	30 x 30 m
2020	2020/12/22	166/54	Landsat 8	30 x 30 m

$$\text{Overall accuracy} = \frac{\text{Total correctly classified pixels}}{\text{Total of classified pixels}} \text{X100} \qquad \text{Equation (4.2)}$$

Where, total correctly classified pixels are the sum of major diagonal and total of classified sample points are the total number of reference samples points.

$$\text{Producer accuracy} = \frac{\text{Number of correctly classified pixels per class}}{\text{Number of reference totals per class}} \text{X100} \qquad \text{Equation (4.3)}$$

Where, the producer’s accuracy indicates how well test set samples of the given cover type are classified.

$$\text{User accuracy} = \frac{\text{Number of correctly classified pixels per class}}{\text{Number of classified totals per class}} \text{X100} \qquad \text{Equation (4.4)}$$

Where, the user’s accuracy is a measure of commission error that indicates the probability that a pixel classified into a given category actually represents that category on the ground.

$$\text{Kstat} = \frac{\mathrm{N} \sum_{i=1}^{n} \mathrm{Sij} - \sum_{i=1}^{n} (\mathrm{S_{Rtot}} \text{ X } \mathrm{S_{Ctot}})}{\mathrm{N}^2 - \sum_{i=1}^{n} (\mathrm{S_{Rtot}} \text{ X } \mathrm{S_{Ctot}})} \text{X100} \qquad \text{Equation (4.5)}$$

where Kstat is Kappa statistic coefficient, N is total number of samples, Sij is the product of total number of sample and total diagonal values, S_{Rtot} is row total, S_{Ctot} is the column total and n, is the number of categories. The coefficient evaluates the difference between the actual agreement of classified map and chance agreement of random classifier compared with reference data (Lillesand et al., 2015).

In this study, two approaches were followed for the model analysis between the periods; firstly, the LULC changes were analyzed and secondly, the anlysis of the LULC change effects on the hydrological components were evaluated. Figure 5.2 shows the detail process for the study.

4.2.4. Calibration and validation

The SWAT model has been calibrated and validated using stream flow (Her et al., 2015) that used to simulate the hydrologic components. The SWAT model prediction under observed flow were evaluated and well performed (Welde et al., 2017; Daba, 2020; Galata et al., 2020; Kuma et al., 2021; Leta et al., 2021). In addition to the automatic calibration, manual calibration has been adopted in different watersheds (Santhi et al., 2001; Neitsch et al., 2011). Manual calibration of SWAT is tough in numerous large-scale applications. Nevertheless, manual calibration procedure inspires the user to well understand the model and their sensitivity of parameters (Arnold et al., 2012). In this research to strengths the model and facilitate the calibration process both manual and autocalibration approaches were used (Van et al., 2005).

More data were required for a reliable model calibration at the watershed scale (Koycegiz et al., 2019; Egigu, 2020). After the ARCSWAT model simulation is completed, the calibration was performed both automatically and manually (Arnold et al., 2012; Nobert et al., 2012). Monthly streamflow flow data at the outlet of the upper Erer subbasin is showed in (Figure 5.1) for the periods (1984-1990) and (1993-1996) were provided by the Ministry of Water and Energy of Ethiopia (MWEE). Model calibration and validation were performed using recorded daily stream flow data at Upper Erer River outlet of hydrological stations provided by the Ministry of Water and Energy of Ethiopia (MWEE). Hence, the daily flow data were changed to monthly flow data and arranged according to the SWAT-CUP input data format requirement for model calibration and validation. To execute calibration and validation processes, SUFI-2 (sequential uncertainty fitting) algorithm in SWAT-CUP2012 were used to identify sensitive parameters form selected parameters. SWAT-CUP is an auto-calibration and uncertainty analysis tool with four built-in analysis algorithms (Abbaspour et al., 2017).

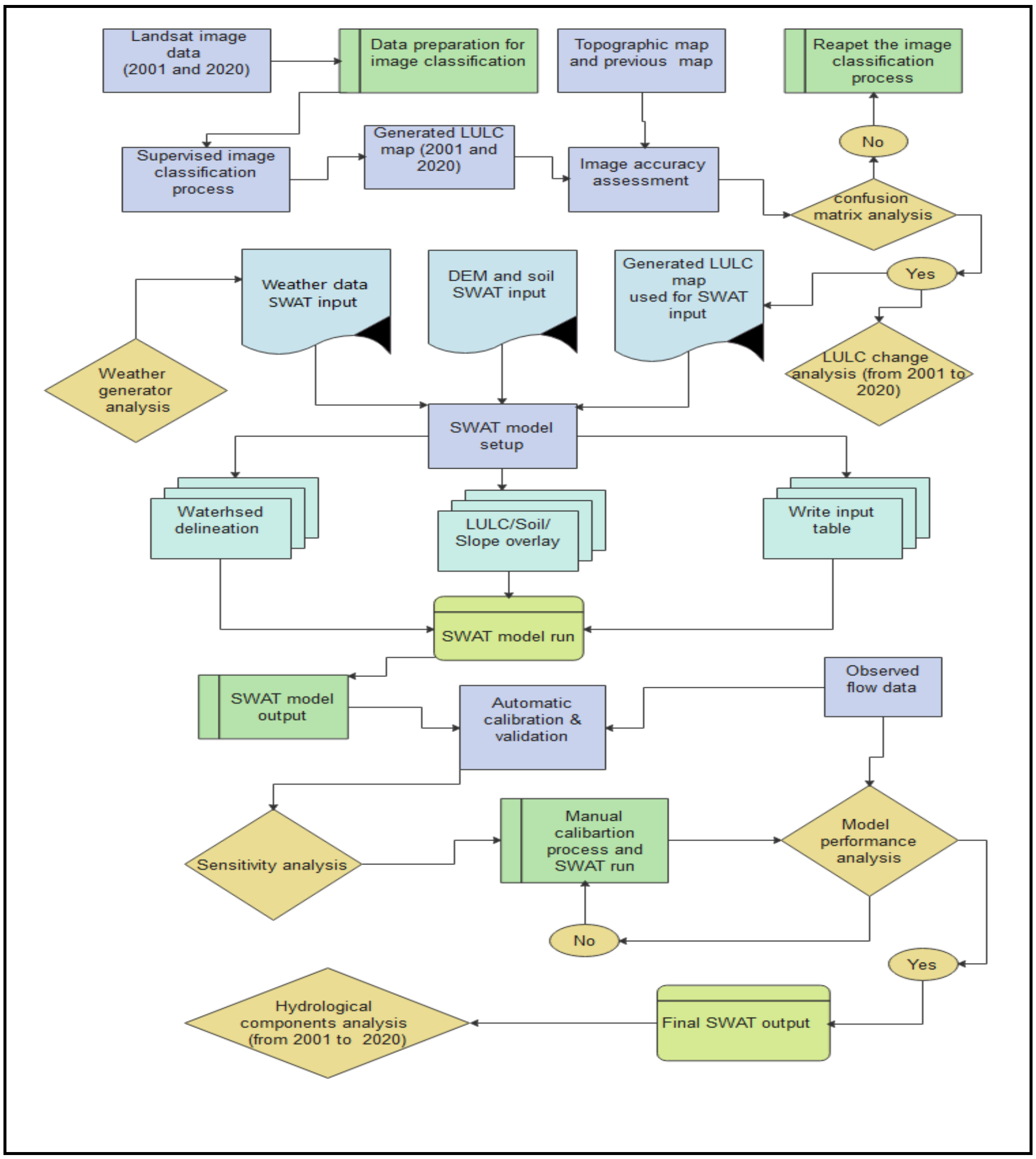

Figure 5.2. Conceptual frame work

The SWAT model simulation is run for period (1979-2014) as a monthly basis and the SWATCUP model is used to identify their sensitivity of parameters. Auto-calibration method was used to evaluate the sensitivity of parameters and used to determine parameter values ranges. The manual calibration/ validation involves varying the input parameter values within the recommended ranges to produce simulated flow data that were analyzed with the observed flow data (Balascio et al., 1998).

4.2.5. Sensitivity analysis and SWAT model performance evaluation

The sensitivity of parameter examination serves to distinguish the utmost influential flow parameters that during model calibration and validation (Abbaspour et al., 2017). The sensitivity analysis was performed using the SWAT-Calibration and Uncertainty Procedure (SWAT-CUP) (Abbaspour et al., 2015). SUFI-2 is an iterative aspect procedure to achieve a rational consequence (Roth et al., 20016; Abbaspour et al., 2017). The model was run under the best parameter output values and measure the model performance using the simulated and observed streamflow data using performance measures such as Nash-Sutcliffe coefficient (NS), coefficient of determination (R^2), and percent bias (PBIAS). The performance measures of NSE, R^2 and PBIAS were calculated using Equations (4.6, 4.7 and 4.8), respectively.

$$NSE = 1 - \left[\frac{\sum_{i=1}^{n}(Q_{oi} - Q_{si})^2}{\sum_{i=1}^{n}(Q_{oi} - \mathrm{Qoav})^2}\right] \qquad \text{Equation (4.6)}$$

$$R^2 = 1 - \left[\frac{\sum_{i=1}^{n}(Q_{oi} - Q_{sav})(Q_{oi} - Q_{oav})}{\sum_{i=1}^{n}(Q_{si} - Q_{sav})^2 \sum_{i=1}^{n}(Q_{oi} - Q_{oav})^2}\right] \qquad \text{Equation (4.7)}$$

$$PBIAS = 1 - \left[\frac{\sum_{i=1}^{n}(Q_{oi} - Q_{si})}{\sum_{i=1}^{n}(Q_{oi})}\right] \qquad \text{Equation (4.8)}$$

Where; Q_{oi} and Q_{si}: the observed and simulated streamflow data, Q_{oav} and Q_{sav} the average of the observed and simulated stream flow data. The model evaluation performance rankings were established for each recommended statistical value.

4.2.6. Land use change and their effects on hydrological response analysis

The land use change probably affects the water balance components as confirmed by varios studies such as (Koch et al., 2012; Marhaento et al., 2018). In this research the LCLC change analysis and their effects were examined. The LULC maps for the period of 2001 and 2020 were used to detect the LULC change. The changes in hydrological component results were assessed from the effects of the LULC change on the hydrologic response in the watershed.

5.3. Results and discussion

5.3.1. Image classification accuracy analysis

Using supervised/maximum likelihood classification land cover classes were generated applying training samples established from ground-truth reference sample data by employing Google Earth, previously generated map of the region, and topographic maps. The random reference sample points for the years 2001 and 2020 were 129 and 143, respectively were used. A matrix was generated using the reference samples along the rows and classified images along the columns that were compared to recognize the relativities. About six LULC classes were generated for the study area such as agricultural land, bare land, forest land, settlements, shrub lands, and water bodies.

After land cover classes were generated and the LULC maps of 2001 and 2020 were prepared a comparison were made using the sample LULC classes of the classified layer and the reference layer. Then, the classification accuracy of the resulting LULC maps, overall, producer's accuracy, user's accuracy and Kappa coefficient were computed using Equation (4.2, 4.3, 4.4 and 4.5), respectively. Table 5.2 and Table 5.3 shows the overall accuracy, producer's accuracy, user's accuracy, and kappa coefficient standards for the reference years. The overall accuracy for the years 2001 and 2020 was greater than the minimum value (85 %) recommended by (Anderson, 1976). The kappa coefficient for the years 2001 and 2020, was 0.84 and 0.89, respectively. The Kappa coefficient was greater than 0.81 as suggested by (Anderson, 1976), which implies the agreements are strong agreement.

The producer's accuracy for the years 2001 and 2020 for the settlement (URBN) land cover is 78.6 and 85.7 %, respectively. This imply the producer's accuracy assessment for settlement land cover is less than the others land cover. Similarly, the producer's accuracy for water body land cover for the year 2001 is 80 %. The user's accuracy for water bodies (WATR) for the year 2001 is 80%. The user's accuracy for shrub lands (RNGB) cover class for the year 2020 is 66.7% which is the smallest value.

Table 5.2. Image classification accuracy assessment for year 2001 (Overall accuracy= 87.6%, Kappa Coefficient=0.84)

Matrix	AGRL	BARR	FRST	URBN	RNGB	WATR	**Sum References**	**User's Accuracy**
AGRL	35	2	0	1	2	0	**40**	87.5
BARR	0	12	0	1	0	0	**13**	92.3
FRST	5	0	22	0	0	2	**29**	75.9
URBN	0	0	0	11	0	0	**11**	100.0
RNGB	0	0	0	1	25	0	**26**	96.2
WATR	0	0	2	0	0	8	**10**	80.0
Sum Classified	**40**	**14**	**24**	**14**	**27**	**10**	**129**	
Producer's Accuracy	87.5	85.7	91.7	78.6	92.6	80.0		

Table 5.3. Image classification accuracy assessment for year 2020 (Overall accuracy= 90.91%, Kappa Coefficient=0.89)

Matrix	AGRL	BARR	FRST	URBN	RNGB	WATR	**Sum References**	**User's Accuracy**
AGRL	40	2	0	0	1	0	**43**	93.0
BARR	1	15	0	1	0	0	**17**	88.2
FRST	0	0	26	0	0	0	**26**	100.0
URBN	0	0	0	18	0	0	**18**	100.0
RNGB	4	0	0	2	16	2	**24**	66.7
WATR	0	0	0	0	0	15	**15**	100.0
Sum Classified	**45**	**17**	**26**	**21**	**17**	**17**	**143**	
Producer's Accuracy	88.9	88.2	100.0	85.7	94.1	88.2		

5.3.2. Changes in Land use land cover analysis

Based on the image classification processing, six land cover classes were generated in the study area. The areal coverage and land cover change for the years 2001 and 2020 are showed on Table 5.4. Appendix 11 and 12 shows the spatial distribution LULC for the years 2001 and 2020, respectively. The result indicated that forest lands were significantly decreased from 2001 to 2020 by about 18.6 km2, followed by agricultural land (18.5 km2) and water bodies

(2.8 km2). But bare land, shrub land, and settlements were increased histrionically by 14.9, 14.3, and 10.8 km2, respectively from years 2001 to 2020. The forest land was decreased and the urban land was increased. This was confirmed by similar studies (Getachew & Assefa, 2012). From (Appendix 11 and 12) the bare lands were intensified at the southern part and at the periphery of the watershed outlet. The shrublands were increased at the expense of agricultural and forest lands. The new shrub lands were produced from years 2001 to 2020. This was probably due to high plantation of chat crop in the region, which is considered as shrub land. About 17.12 % of the total LULU type were transformed during the years from 2001 to 2020.

Shrub land, bare land, and settlements had increased from years 2001 to 2020. In contrast, forest land was decreased, perhaps as a result of growth in population and urbanization, this agrees with the study on the upper Genale River Basin (Shigute et al., 2022) nd other studies on other parts of the world (Mir et al., 2022). The LULC map demonstrated the agricultural land was the major LULC class, shrublands and bare lands were the second and third dominant coverage in the study area, respectively in Table 5.4. The forest land and water body showed a reduction and bare land and urban areas have increased, this agreed with the study done on Erer sub watershed (Weldu & Edo, 2020). But this output was disagreed with other study conducted on the Koga Watershed that indicated croplands were intensified (Ayele et al., 2023).

Table 5.5 shows the comparison matrix for the LULC changes. The comparison matrix revealed that the maximum changes in the LULC change were under forest and water body comparison and the minimum changes were detected under settlement and shrub land comparison. The change in LULC under agricultural and forest land comparison was nearly 1, this implies the change is comparable.

5.3.3. Watershed Delineation and HRU analysis

The watershed delineation was generated using the raster mask of the study area of DEM map using upper Erer subbasin outlet. At this position there was an re-installed hydrometric gauging instrument. The delineation process generates around 23 subbasins and 146 Hydraulic Response Units (HRUs) as showed in Appendix 8.

Appendix 10 shown the soil and slope classification map. This indicated that the Dystric Cambisols were mostly found at the higher elevation of the watershed. The Eutric Nitosols were found at the lower elevation of the watershed with most of the slope class range 8 to 15 %.

Table 5.4. LULC change analysis from years 2001 to 2020 (km2 denotes the area in square kilometers)

Land use Type	**2001 LULC**		**2020 LULC**		**LULC changes**	
	Area coverage		**Area coverage**		**Area coverage changes**	
	km2	%	km2	%	km2	%
AGRL	327.0	70.04	308.4	66.07	-18.5	-3.97
BARR	53.0	11.34	67.9	14.53	14.9	3.19
FRST	36.0	7.71	17.3	3.71	-18.6	-3.99
URBN	6.9	1.47	17.6	3.78	10.8	2.30
RNGB	40.4	8.66	54.8	11.73	14.3	3.07
WATR	3.6	0.78	0.8	0.18	-2.8	-0.60
TOTAL	466.8	100	466.8	100		

The soil data in the Upper Erer sub catchment were shown in Table 5.6. The major soil types in the region, namely: Dystric Cambisol, Eutric Nitosols, and Humic Cambisols. In the region, the land use land cover was classified in to six classes, namely: bare land, cropland, forestland, settlements, shrublands, and water body. In the region, the cropland covers the highest areas and the water body covers the minimum area (Weldu & Edo, 2020).

Table 5.5. Land use land cover change analysis matrix for the years 2001 to 2020

Matrix	AGRL	BARR	FRST	URBN	RNGB	WATR
AGRL	1	1.24	0.99	1.72	1.72	6.62
BARR		1	0.80	1.38	1.04	5.32
FRST			1	1.73	1.73	6.66
URBN				1	0.75	3.84
RNGB					1	5.12
WATR						1

In the classification processes, six major LULC classes were generated (Weldu & Edo, 2020). The LULC class description was taken from Arnold et al., 2011). Table 5.7 shows the SWAT code used to link the LULC map to the SWAT land use database. The prepared LULC, soil and slope maps have been systematically overlayed to get the HRU analysis results for the watershed. The maximum soil groups in the watershed were the Dystric Cambisol covering around 54.53 %, the Eutric Nitosols with an area coverage for 25.09 % and Humic Cambisol covering around 20.38% of the watershed.

Table 5.6. description of soil class and soil-code for SWAT model input for the region

Soil features	**Description soil map of the world (1974)**	**SWAT Soil Codes**
Soil features	Dystric Cambisols	Bd30-2-3c-9
	Humic Cambisols	Bh12-3c-31
	Eutric Nitosols	Ne15-3c-159

The maximum coverage slope class of 15 to 30% covers around 34.21 % of the watershed area, and the smallest coverage is 1.09 % with the slope class of less than 2 % slope. From the results, more than 70 % of the slope coverages were concentrated within the range of 2 to 30 % slope class and more than 62.6 % slope coverage were > 15 % slope class. This result was confirmed by (Wudineh et al., 2022).

Table 5.7. Description of LULC classification and LULC code for SWAT model

Value/ class	Original/ Map LULC Name	SWAT Description CROP NAME	SWAT CODE CPNM
1	Agricultural Lands	Agricultural land -generic	AGRL
2	Barren Lands	Barren	BARR
3	Forest Lands	Forest Mixed	FRST
4	Settlements	Residential	URBN
5	Shrub Lands	Range Brush	RNGB
6	Water Bodies	Water Body	WATR

5.3.4. Sensitivity analysis and model performance evaluation

Studies done globally (Gebre et al., 2022) rank the sensitive parameters such as CN2 (Initial soil conservation service (SCS) curve number), ALPHA_BF (Baseflow alpha factor), GW_DELAY (Groundwater delay), and GWQMN.gw (Threshold depth of water in the shallow aquifer for return flow to occur) have high sensitivity values. Other study reveals those parameters like: CN, ALPHA_BF, and GW_DELAY was more sensitive (Belihu et al., 2019). While, research conducted on tropical watershed indicated that CN2, GW_REVAP (Groundwater "revap" coefficient) and SOL AWC (Soil water available capacity) were more sensitive (Roth et al., 20016). Other research output indicated three sensitive parameters such as CN2, GW_DELAY, and SOL_K (1) (Saturated hydraulic conductivity of first soil layer) (Santhi et al., 2001; Winchell et al., 2013) were identified. Other scholar (Arnold et al., 2012) identified the influential parameters includes, surface runoff (CN2) and total flow parameters (SOL_AWC, ESCO (Soil evaporation compensation factor)).

Table 5.8. Literature survey of the most sensitive parameters in some related studies in Ethiopia

Sensitive parameters	**References**
ESCO, CN2, ALPHA_BF, REVAPMN, SOL_AWC, GW_REVAP, CH_K2, and GWQMN	(Setegn et al., 2008)
CN2, ESCO, SOL_AWC, SOL_Z, ALPHA_BF, ALPHA_BF, CH_K2, CH_K2, REVAPMN, and GWQMIN	(Assfaw, 2019)
CN2, SOL_AWC, SOL_Z and REVAPMN	(Mekonnen et al., 2009)
CN2, GW_REVAP.gw, RCHRG_DP.gw, SOL_AWC (1).sol, GW_DELAY.gw, ESCO.hru, SURLAG.bsn, REVAPMN.gs and GWQMN.gw	(Winchell et al., 2013)
CN2.mgt, _SOL_AWC (...).sol, RCHRG_DP.gw, CH_K2.rte, GW_DELAY.gw ALPHA_BF.gw, SLSUBBSN.hru, GW_REVAP.gw, EPCO.bsn, SOL_K (...).sol and HRU_SLP.hru	(Shigute et al., 2022)
Alpha_Bf, Cn2, Esco, Gw_Delay, Gwqmn, Revapmin, Rchrg_DP, Sol_Awc, Sol_K, and Surlag	(Shawul et al., 2013)
RCHRG_DP, SOL_K, CN2, GWQMN, ESCO, SLSUBBSN, GW_REVAP, SOL_AWC and ALPHA_BF	(Desta et al., 2017)

Meanwhile, other study output indicates that CN2, SURLAG (Surface runoff lag time), and CANMX (Maximum canopy storage) were the most three sensitive parameters (Galata et al., 2020). Table 5.8 were produced to summarize the influential parameters for similar studies in Ethiopia using the literature survey.

Among the sensitive parameters identified in various studies above CN2 parameter implied rapid changes in land use classes (Mekonnen et a., 2009; Singh & Saravanan, 2020). Understanding this sensitive parameter help to reduce the calibration iteration process (Ankita & Kazuo, 2014). The ranges of parameter value were adapted from the SWAT manual document (Arnold et al., 2011). Identification of the most influential parameters from various literatures were used to easily understand the mostly used parameters (Table 5.8). Under the literature survey identification about 17 parameters were identified and feed to the autocalibration process. The autocalibration process employed sensitivity analysis of sufi2 algorithm in the SWATCUP model for 17 selected parameters. The most influential 10 parameters in the region were identified from the auto-calibration output. Appendix 13 shows the sensitive parameters values of the autocalibration output of the SWAT-cup of sufi2 algorithms.

The identifier in Appendix 13 indicates (R_) state of the relative change in the parameter to the value from the SWAT database was multiplied by (1 + a given value), (V_) refers the parameter value from the SWAT database was changed by the given value and (A_) refers the value was added to the current parameter value. In this model, for spatial parameters (eg. CN2, hydraulic conductivity, bulk density, and others), we use (r_) or (a_) before the parameters of the model to modify the existing values (SWAT output) with new values (fitted values) by modification. But, for non -spatial parameters, we use (v_) to modify the existing values to the new values by replacement.

The smaller absolute p-value and the larger absolute t-value were considered and ten sensitive parameters were identified from seventeen parameters selected from the literature survey (Appendix 13). From the result, the most sensitive parameters were CN2, SOL_AWC, ESCO, GWQMN, and others. This agreed with most studies in Ethiopia (Setegn et al., 2008; Abbaspour et al., 2015; Gebre et al., 2022). The model performance is checked with manual calibration procedures using the SWAT model manual helper; repetitive simulation (twenty-eight) was carried out during the process by adjusting flow sensitive parameters. The final influential parameters and their fitted values were shown in Appendix 14. The four parameters; CN2, SOL_K, GWQMN, and REVAPMN were identified as the most influential parameters out of 10 parameters selected from autocalibration process.

5.3.5. Model simulation

The manual procedures suggested by (Arnold et al., 2011) were used to modify the SWAT model parameters. The manual calibration and validation were done by adjusting the sensitive parameters that were identified from autocalibration for groundwater parameters and surface runoff parameters and generally flow parameters. The flow calibration procedures suggested by (Neitsch et al., 2011) were implemented and the model simulation was performed for period (1979- 2014) under three years warmup period (1979-1981). The calibration and validation process taken place using observed monthly streamflow data for calibration period (1984–1990) and validation period (1993–1996). In the initial SWAT model simulation, the base flow was too low and the evaporation was too high, adjustments were made on the groundwater flow evaporation parameters; by decreasing GWQMN and GW-REVAP and increasing REVAPMN parameters repetitively until the model performance measures such as coefficient of determination (R^2), Nash–Sutcliffe efficiency (NSE), and percent of bias (PBIAS). Then, the baseflow became too high, and the peak flows were too low, adjustments were made to the surface runoff and baseflow parameters by increasing CN2 and decreasing the other flow parameters like; SURLAG, ESCO, EPCO. Finally, the same adjustments were made to the soil parameters (SOL_K (1), SOL_AWC (1)) until the statistical measures reaching acceptable values (Van et al., 2005; Abbaspour et al., 2015). The final SWAT model simulation output was found to be checked and performance parameters for calibration period were R^2 (0.84), NSE (0.65) and PBIAS (-23.04). Similar procedures were followed using the flow data for validation period found that the performance measures were R^2 (0.83), NSE (0.53) and PBIAS (-14.16). The result indicated that the model performance measures were in acceptable range (Moriasi et al., 2007; Moriasi et al., 2015) for NSE > 0.50 and R^2 > 0.70, and if PBIAS ± 25%.

During the manual calibration process has in the order of sensitivity and influence on the flow parameters for flow. First, the CN2 was calibrated and then the GW_REVAP, REVAPMN, and RCHRG_DP in the order of sensitivity of the parameters need adjustment (Van et al., 2005). The calibration and validation include all kinds of climate circumstances; like dry years, wet years, and moderate occur in both periods (Gan et al., 1997; Faramarzi et al., 2015). SWAT output values were checked as per the SWAT developers' suggestions and all output values for model performance were within the satisfactory range of PBIAS ≤ (±25%), R^2 > 0.7 and NSE > 0.5 suggested by (Moriasi et al., 2007; Neitsch et al., 201). This agreed with a similar study on Gilgel Gibe watershed (Warburton et al., 2012). Similarly, the results agreed with the study on Angreb watershed (Getachew & Assefa, 2012).

From the result, model performance values, R^2 values higher than 0.83 for both the calibration and validation periods as suggested by (Kenea et al., 2021), this indicates that there is a strong agreement between the simulation and measured data. This study result of the performance measure; PBIAS was difference with the study on hangar catchment of PBAIS which is less than 10% (Winchell et al., 2013). For this study, R^2 value was higher and NSE value was smaller than a similar study on Bilate catchment (Leta et al., 2021). In general, the performance indicator values found for the model simulation showed a very good performance rate in simulating the SWAT models as suggested by (Winchell et al., 2013). The simulated and measured monthly flow correlation diagram indicating the coefficients of determination (R^2) for calibration was 0.84 and for validation was 0.83 as shown in Appendix 15. The monthly steam flow hydrographs for the model simulation were shown in Appendix 16. The results showed that the model has overestimated the flow for July 1986 and September 1986 and under estimated flows for August 1989, September 1989, and August 1994.

5.3.6. Effects of land use land cover change on hydrological response

The hydrological response effect due to land use land cover change for the years 2001 and 2020 were accessible in Table 5.9. The groundwater flow increases by 10.39%, water yields by 8.22 %, surface runoff by 6.03% and lateral flow by 1.85% only. Whereas, evapotranspiration shows decrease by 3.34 % from 2001 to 2020. This was confirmed by a study on tropical catchments (Naha et al., 2021). The result indicated there was high evapotranspiration with low runoff in the region. Hydrological responses were varied due to the effects of the LULC changes in the region (Nobert et al., 2012). In this research the decrease in forested land led to a reduced in infiltration rate, this was probably due to the reduction in surface roughness and reduction in average annual evapotranspiration, and this agreed with the study on East African watershed (Baker & Miller, 2013). In the study region there was an increase in settlement lands and a decrease in natural forest, this contributed high surface runoff as confirmed by similar studies in other parts of Ethiopia (Weldu & Edo, 2020; Shigute et al., 2022). The results indicates that the evapotranspiration was decreased due to a shortage of soil moisture as a result of the decrease in natural vegetation cover (Berihun et al., 2019). Other study supporting the findings of this study revealed that the conversion of forest land to shrubs and settlements leads to a reduction in evapotranspiration and an increase in surface runoff (Gan et al., 1997). The surface runoff increased by 6.03 %, this finding was supported by other study conducted on Tekeze dam (Welde et al., 2017).

Table 5.9. Hydrological response of mean annual land use, land cover change

Hydrological response	LULC changes		Parameter increase/ decrease	
	LULC 2001	LULC 2020	Amount	%
Surface runoff (mm)	75.82	80.39	4.57	6.03
Groundwater flow (mm)	129.68	143.16	13.48	10.39
Evapotranspiration (mm)	574.2	555	-19.20	-3.34
Lateral flow (mm)	63.85	65.03	1.18	1.85
Water yields (mm)	230.25	249.18	18.93	8.22
Precipitation (mm)	844.4	844.4	-	-

The water yield was also increased in this study and this agreed with the similar study such as (Bessah et al., 2020). The surface runoff was increased due the expansion of settlement lands and the expense of other land covers (Getu et al., 2021). Other study supporting this study findings indicated that an increase in water yields and decrease in evapotranspiration due to the reduction and forest lands and tends to soil moisture decrease (Lu, Z. et al., 2015). Generally, the changes in surface runoff result from the conversion of natural vegetation to other lands as suggested in similar study (eg. Ankita & Kazuo, 2014; Singh & Saravanan, 2020). Overall, the results showed that about 68 and 65.2 % of the precipitation were lost to evapotranspiration for the years 2001 and 2020, respectively. Whereas, about 27.2 and 29.5 % of the total precipitation were only changed to water yields in 2001 and 2020, respectively.

These results indicates that the reduction in evapotranspiration was possibly related to the decrease in forest coverage. The groundwater consumption from precipitation were 15.3 % for the year 2001 and 16.95 % for the year 2020. This was probably due the natural vegetation land was reduced and the shrub lands were increased. Figure 5.3 shown the temporal distribution of water balance components in the study area. The results revels that the main rainy seasons from April to May and June to September were the maximum mean monthly surface runoff and water yields. However, October, November, December, and January were dry months with low surface runoff and water yields in the region (Shanko & Camberlin, 1998; Cook et al., 2013).

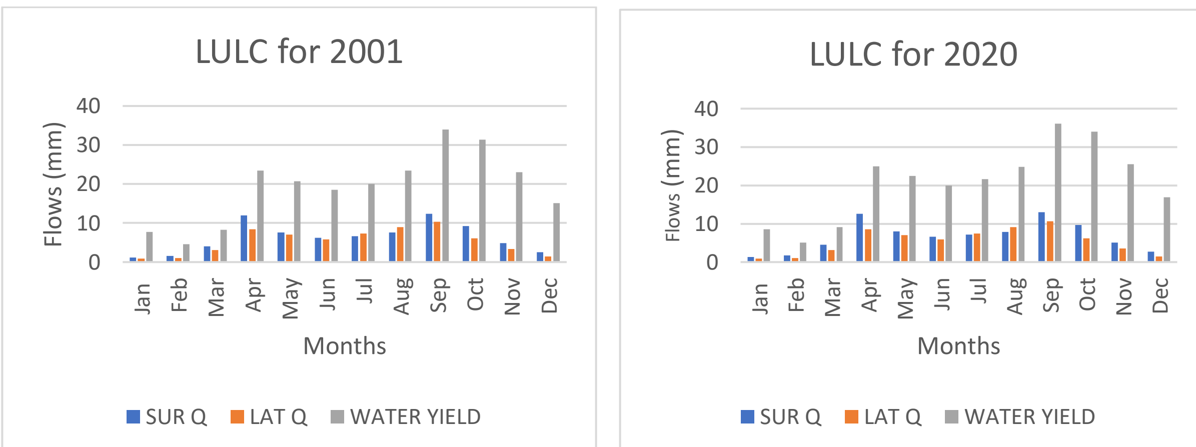

Figure 5.3. Average monthly distribution of hydrological response

5.4. Conclusions

This study was focused to assess the LULC change and their effects to the hydrological response from the years 2001 to 2020. In the watershed delineation process, around 23 subbasins and 146 HRUs were generated in the study sub basin. The HRUs were generated from the overlay analysis of HRUs analysis using the Arc SWAT interface of LULC, soil and slope maps of the watershed. Three soil types, namely: Dystric Cambisol, Eutric Nitosols, and Humic Cambisol and five slope categories were generated from the analysis.

The CN2, ESCO, SOL_AWC, and REVAPMN identified as the most influential parameters in the sub-basin that affect the flow. The LULC change assessment for the years 2001 to 2020 revealed the agricultural lands were reduced by 18.5 km2, water bodies by 2.8 km2, and forest lands by 18.6. However, shrub lands were increased by 14.3 km2. The bare lands and settlements were increased by 14.9 km2 and 10.8 km2, respectively. These were probably agricultural and forest lands were changed to shrub land and/ or settlements and/or bare land. The shrub lands were the maximum coverage increment next to bare land. This is due to the intensification of the Chat crop in the region were most of the agricultural and other lands were changed to this crop.

Under the LULC changes, the hydraulic responses effects for the sub-basin were evaluated from the years 2001 to 2020. The output showed that the surface runoff, ground water flow, and water yields were increased by 6.03, 10.39, and 8.22 % from 2001 to 2020, respectively. The evapotranspiration was decreased by 3.34 %, these were due to the decrease of the natural vegetation. The SWAT model simulation showed that the model well performed for the assessments of LULC changes in the upper Erer subbasin. Nevertheless, the hydro-meteorological data inadequacy and quality in the region indicated the satellite data involvement in the future to better understand the local conditions under changing situations. Even if the study of LULC change on the hydrological components are insufficient in the subbasin level but, slightly serves policy makers and stake holders for better utilization of natural resources and proposed management practices for future analysis.

Moreover, the manual calibration approach for the SWAT model assistances the user for improved knowledge and understanding the hydrological parameters. Future studies may need the integration of manual and automatic calibration approaches for the upper Erer subbasin by using refined hydrometeorological data for the improved output. Though, the LULC on hydrological process shows a considerable change in streamflow and overall hydrological responses, the study has not covered the sediment yield analysis that possibly affected by the LULC types. Future studies may consider the sediment yield in the subbasin including other parameters (such as; climate change) that affect the hydrological response in the region.

6. THE IMPLICATION OF SPATIOTEMPORAL RAINFALL DISTRIBUTION ON THE ESTIMATION OF AREAL RAINFALL CHARACTERISTICS IN UPPER ERER SUBBASIN, ETHIOPIA.

Abstract

The distribution of rainfall is not uniform in various regions of the world. Rainfall study is used to recognize the characteristics, duration, variability of temporal and spatial rainfall distribution. In Ethiopia, the annual and seasonal rainfall distribution are variable in space and time. This study is focused on the implication of spatiotemporal rainfall distribution on the areal rainfall estimation characteristics evaluation under the upper Erer subbasin, located in Eastern Ethiopia. In the study area average annual rainfall amount for Dire Dawa, Harar and Haramaya, Girawa, and Gursum stations are found to be 647, 816, 801, 958, and 840 mm with coefficients of variation of 23, 20, 20, 19 and 31%, respectively. In the study area, the rain gauges are sparsely distributed. The rainfall occurrence and distribution at various gauging stations have been found that vary significantly both temporally and spatially. The spatiotemporal rainfall distribution found in the stations was assessed using joint probability of rain days approach. The result indicated joint probability of rain days estimation approach under monthly time step has better performance than daily, decadal and seasonal. The joint probability approach is used along with rainfall amount under monthly rainfall for areal rainfall estimation assessment in rainfall-runoff modelling.

Keywords: areal rainfall, daily rainfall, decadal rainfall, Joint probability of rain days, monthly rainfall, seasonal rainfall

6.1. Introduction

Rainfall has significant role in the hydrologic cycle that used to manage the water supplies. Determination of areal rainfall of the catchment is the prerequisite for various water resource and watershed modeling studies (Bayraktar et al., 2005; Cheng et al., 2012). Average rainfall is usually used to calculate the spatial rainfall status of a region and its input into various rainfall-runoff models (Ayoad, 1983; Belay, A.S et al., 2019). So, rainfall analysis is considered as an imperative role in hydrology and in climatological studies that used to recognize its characteristics, duration, variability of temporal and spatial rainfall distribution (Gummadi et al., 2018). The distribution of rainfall is not uniform due regional orographic effects and sources of rains. Thus, Ethiopia receives rainfall in three main seasons. The main rainy season known as Summer (June–September) the long rainy season, the second short rainy season Spring (February–May) and the third rainy season, Winter (October–January) (Aldabagh et al., 1982; Seleshi and Zanke, 2004; NMSA, 1996; Cheung, W.H. et al., 2008). Rainfall variability is an important feature of semi-arid climates. Generally, in the region climate change is likely to increase rainfall variability with Summer seasonal rainfall comprises the largest share (Megersa et al., 2019; Al-Houri, 2014).

Inter-seasonal rainfall variation and intra-annual rainfall availability, as well as reliability, significantly affect agricultural activities, hydrologic conditions, and livelihoods (Misrak et al., 2019; Ramos & Martínez, et al., 2006). There is high intra-annual variability of rainfall in most parts of the country, Ethiopia (Seleshi and Zanke, 2004; Mengistu et al., 2014). The variability of monthly and seasonal rainfall is higher than that of annual rainfall (Aldabagh et al., 1982; Seleshi and Zanke, 2004; Ngongondo et al., 2011). Rainfall fluctuation was also occurred both in annual variability and interannual variability (Girma Eshetu et al., 20016). This is due rainfall occurrence in the regions at various gauging stations have been found to be vary significantly contingent to source of rain and regional landscape (Singh, V.P., 1992). The point rainfall data are recorded using gauging stations re-installed (Sen et al., 2000). This point rainfall data is converted to areal rainfall that represent the quantities of rainfall that fall on the region. Hence, areal rainfall estimations are very sensitive to the number and locations of rain gauges (Ngongondo et al., 2011; Wilson, E.M., 1970; Al-Timimi et al., 2020; Cho, W., et al., 2017; Bell and Moore, 2000).

Moreover, the average annual rainfalls depend on the elevation and tend to increase with increasing elevation (Misrak et al., 2019; Faures et al., 1995). The other biophysical factors also affect rainfall and resulted in marked spatiotemporal variability at small distances (Terink et al., 2018; Oettli and Camberlin, 2005). This relative difference in between rain gauges were determined as one more feature related to their biophysical factors (Ngongondo et al., 2011; Taesombat et al., 2009; J. Nyssen et al., 2005; Nandargi, and Mulye 2012; Zhang, T., Li et al., 2016; Bewket and Conway, 2014). The above studies indicate the spatiotemporal rainfall variability affect the rainfall occurrence and distribution in various regions.

In reply to increasing worry about rainfall studies, investigators have started to improve techniques of evaluating the rainfall distribution and intensities. Researchers calculate the amount of rain that falls on the station, by converting it from point rainfall data to represent the quantities that fall on the region as a whole and not on the station itself (Yuan et al., 2014). This is represented as the areal rainfall of the region. So far, several kinds of areal rainfall estimation methods are emerging (Cheng et al., 2012; Al-Timimi et al., 2020; Cho et al., 2017; Eruola et al., 2015) such as: Arithmetic Mean, Statistical, Isoheytes, and Thiessen methods, but no method accurately represents its distribution (Sen et al., 2000).

In this study area, we are faced with the problem of an inadequate network of rainfall measuring stations, and also ununiformly distributed. The scattered distribution of gauging stations affects the rainfall distribution and intensities in the gauging stations. Most of the above studies are limited to the rainfall amount, and a comprehensive method that involves the spatiotemporal rainfall distribution of mutual rainfall occurrence for the stations is missing.

The rainfall occurrences at similar time situation for the stations were evaluated using the probability of all or some of the stations to get rain jointly (mutually) would be the main concern. The joint probability of amount of rainfall occurrences at the stations used to assess the areal rainfall estimation characteristics in the region. This study aims to fill this gap by conducting a more comprehensive approach that consider the mutual rainfall occurrence including its amount of rainfall for the stations.

6.2. Materials and methods

6.2.1. Description of the study area

The study area is located in Upper parts of the Erer Sub-Basin, which is located 9°13’26.4” N to 9°31’26.4” N latitude and 42°4’40.8” E 42°20’38.4” E longitude in the eastern highlands of Ethiopia.

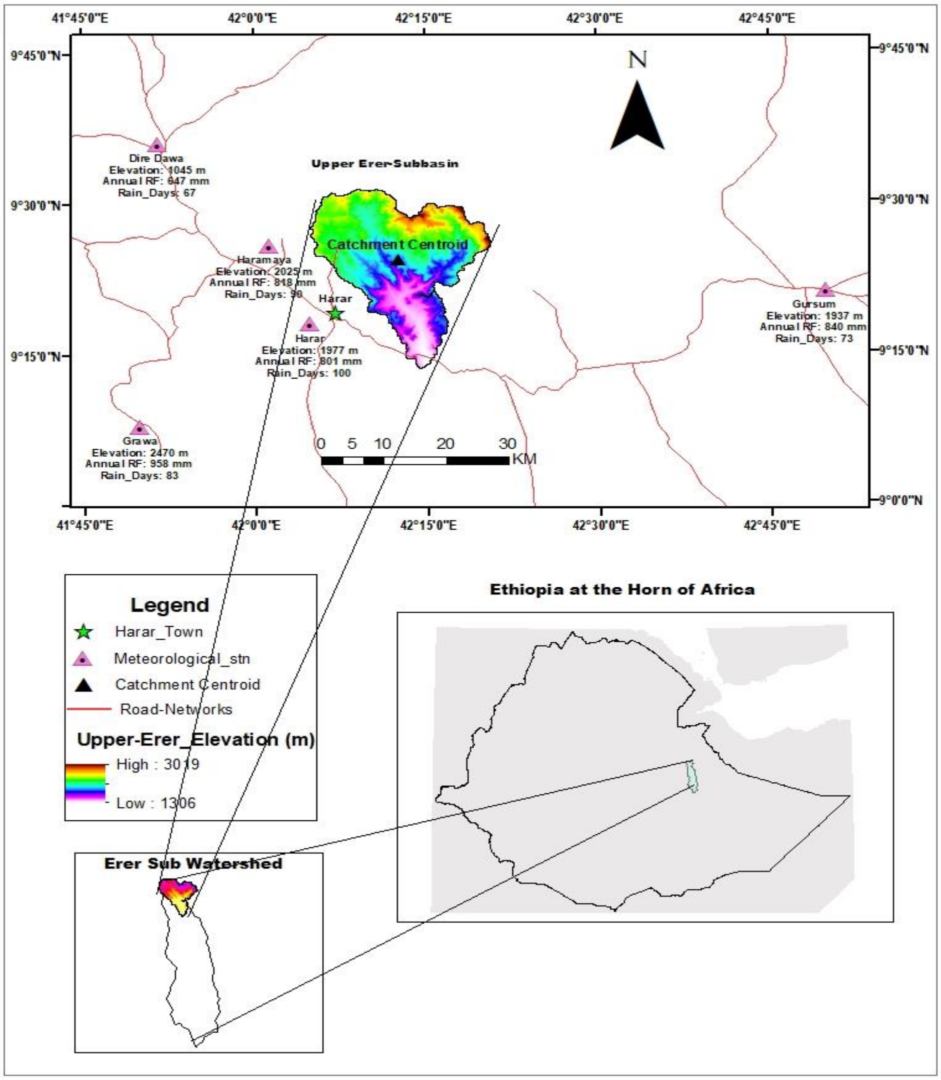

Figure 6.1. Location of the study area and the meteorological stations for spatiotemporal rainfall distribution analysis

The subbasin is categorized by high topographic relief with a topographic location fluctuating from of 1306 to 3019 meters above the mean sea level. Figure 6.1 shows the meteorological gauging stations and contour map for the study area. The Upper Erer River Alluvial Valley Plain segregates the two major water basins in Ethiopia (Awash and Wabishble) found about 10 to 20 km east and south east of Harar Town.

6.2.2. Datasets and methodology

Daily rainfall data for 5 stations (Dire Dawa, Haramya, Harar, Gursum and Grawa) that have relatively good quality and long records (>30 years) were collected from National Meteorological Institute of Ethiopia (NMIE). The observed rainfall data available duration for the study are 38 years (1983-2020) for Dire Dawa and Haramaya, 36 years (1985-2020) for Harar, and 35 years (1983-2017) for Grawa and Gursum. The missing values for all five stations are checked and all values are less than 20%. Normal ratio method is recommended for filling in missing values for missing values more than 10%, and the simple arithmetic mean method was used for missing values less than 10%. In this study Normal ratio method is used for filling in missing values. The detail description of the gauging station is shown in Appendix 7. Rain gauges accurately measure rainfall, they are rarely found in mountainous regions, and satellite rainfall data can be used as an alternative source over these regions (NMSA, 1996). This data is used to check the applicability of the ground rainfall data in the region.

Modern-Era Retrospective Analysis for Research and Applications, version 2 (Merraa-2) daily precipitation data from January 1983 to December, 2020 were adapted for this study. The daily data were converted to monthly data that helps for the analysis. This dataset was acquired from National Aeronautics and Space Administration Prediction of Worldwide Energy Resources (NASA POWER) website (https://power.larc.nasa.gov/). It has a spatial resolution of 0.5 x 0.625-degree latitude/longitude region (Yoo et al., 2008). Spatially, MERRA-2 data tended to closely predict rainfall amounts in high elevation to rugged mountainous zones (e.g., Mt. Kenya) (R^2 = 0.97) as outlined by (Randles et al., 2017). These demonstrate the promising potential of satellite remote sensing data (Merra-2) in complementing the existing meteorological observed data which are often marred by inconsistency and scarcity, and hence unreliable in the existing agricultural advisory and other climate-based applications in Kenya, and sub-Saharan Africa at large (Peterson and Easterling, 1994). MERRA-2 shows more observable areas with an elevation of more than 1500 m. MERRA-2 shows a variability ratio closer to one for monthly time step (Joseph et al., 2020). The satellite-based data products are particularly relevant to support rainfall measurements in Africa, which is challenged by low-density rain gauge networks and incomplete observations (Hafizi and Sorman, 2022). Similar study shows that the evaluation of MERRA-2 precipitation datasets is especially important for understanding the spatiotemporal distribution of precipitation (Ayehu et al., 2021).

The areal rainfall estimation was highly affected by the number of existing stations within the subbasin. The continues record of gauging stations data has been sustained attention in understanding the rainfall distribution by assessing its variation in amount and rainy days (Hamal et al., 2020; Mugalavai et al., 2008). In this study, the Merra-2 datasets were used as the first estimation that is to check their suitability using the linear regression method.

Homogeneity test and correlation analysis were also performed in the study to check the homogeneity and consistency of the ground gauged rainfall data, respectively. Double-mass curve techniques were used for the homogeneity test. The process indicates that the data are homogeneous showing the graph plots fitted a straight line. The observed rainfall data and the elevation relationship were also assessed to guess the rainfall distribution dependency on the topography (Taesombat & Sriwongsitanon, 2009). The spatial correlation coefficients of at least 0.7 between the test series and reference series are required (Randles et al., 2017). But the study (Ngetich et al., 2014) determined that the correlation (r) between the reference series and the candidate station had to be 0.80 or higher to be reliable enough to use for filling missing data.

The rainfall variability and distribution were evaluated using statistical method. Seasonal variation and contribution of rainfall amount and rain days were assessed. The rainfall amount and rain days variation was calculated using equation (5.1):

$$\mathrm{CV}\ (\%) = \frac{\sigma}{\mu} \mathrm{x} 100 \qquad \text{Equation (5.1)}$$

Where, CV is coefficient of variation; σ is the standarad diviation and μ is the mean. The degree of variability of rainfall events as low are classified (CV < 20 %), moderate (20 % < CV < 30 %), and high (CV > 30 %) (8, Peterson et al., 1998). The contribution of seasonal rainfall to the total annual rainfall in percent (CT) for each station is also computed.

In this study, the implication of spatiotemporal rainfall variation on the estimation areal rainfall characteristics was evaluated using the new comprehensive approach that consider the rainfall and mutual occurrence for the stations. To address the spatiotemporal distribution of the rain the joint probability of rain days was evaluated using Daily, Decadal, Monthly and Seasonals rainfall data from ground stations. During the process the Daily rainfall data starting from January 1, 1983 to December 31, 2020 are arranged in the array continuously in ascending order and estimate the mutual rain days (rainfall amount ≥ 1mm) for each observation days using various rain gauge station combination such (five, four, three and two). Then, sum up the mutual rain days for the stations and divide to the total numbers of observation and finally multiply the value with 100% to estimate the joint probability of rain days for the station combination. Similar procedures were followed to estimate for Decadal, Monthly and Seasonals time series. The general formula shown in equation (5.2) were used to estimate mutual rain days probability of the stations.

$$\mathrm{P(rain\ days)} = \frac{\mathrm{n}}{\mathrm{N}} * 100\% \qquad \text{Equation (5.2)}$$

Where P (joint rain days) is the joint probability of rain days, n is the joint rain days calculated by counting all mutual rain days for the stations combinations and N is the total number of days in the period under consideration. The rain gauging station combinations for different stations such as; five-stations, four-stations, three-stations, and two-stations are used for the analysis.

The performance of the model was checked using the correlation coefficient between the joint probability of rain days estimation and the observed joint arithmetic average areal rainfall. The linear regression was plotted for simulated values of probability of joint areal rainfall and observed joint arithmetic areal mean for the given time scale. The joint arithmetic average rainfall was calculated by equation (5.3)

$$P_{Joint} = \sum_i^n (\frac{p_{avg}}{N}) \qquad \text{Equation (5.3)}$$

P_{Joint} is the joint arithmetic rainfall amount in millimeters (mm), N is the number of observations and p_{avg} is calculated by the equation (5.4)

$$p_{avg} = \sum_i^n (\frac{p_n}{n}) \qquad \text{Equation (5.4)}$$

p_{avg} is average rainfall for the combined stations in mm, p_n is observed rainfall of each station under consideration and n is the number of stations under considerations. The maximum joint probability of rain days for the combined station are the determinant areal rainfall estimation for the region. This used to develop methods for estimating the areal rainfall characteristics distribution under inadequate data using the rainfall probability approach. The final analysis results are used to identify the times series with the maximum joint probability of rain days in the region.

6.3. Results and discussion

6.3.1. Correlation assessment for MERRA-2 and observed rainfall records

Linear regression for the total monthly records for the Merra-2 and ground rain gauge observation is shown (Figure 6.2). The results for the coefficient of determination ($R^2 > 0.5$), this indicate that the good correlation between the ground observation and Merra-2 reanalysis data for the region.

Table 6.1. Linear regression of monthly rainfall analysis for Merra-2 (Y) and measured rainfall (X) for 1983-2020 in the region

Station	**Regression equation**	**coefficient of determination (R^2)**
Dire Dawa	Y = 1.1222x	$R^2 = 0.752$
Haramaya	Y= 0.9353x	$R^2 = 0.799$
Gursum	Y = 0.5634x	$R^2 = 0.549$
Harar	Y = 0.9x	$R^2 = 0.689$
Grawa	Y = 0.784x	$R^2 = 0.750$

Spatially, MERRA version 2 (MERRA-2) data tended to closely predict rainfall amounts in the high elevation to rugged mountainous zones as suggested by (Senbeta and Olsson, 2009). Table 6.1 shows the linear regression of ground rain gauge observation and observed Merra-2 for specific station indicated with all coefficients of determination (R^2> 0.5). The first guessing of the correlation analysis of the ground rain gauge observation with Merra-2 observed data indicates that mutually correlated. It is probably fit with the global data and the gauged data probably used for the rainfall distribution analysis in the subbasin. The ground rainfall data has consistency with satellite observed data in the region. This suggested that the ground rainfall data are the representative of the stations in the study area and it may be used for analysis to estimate the areal rainfall characteristics.

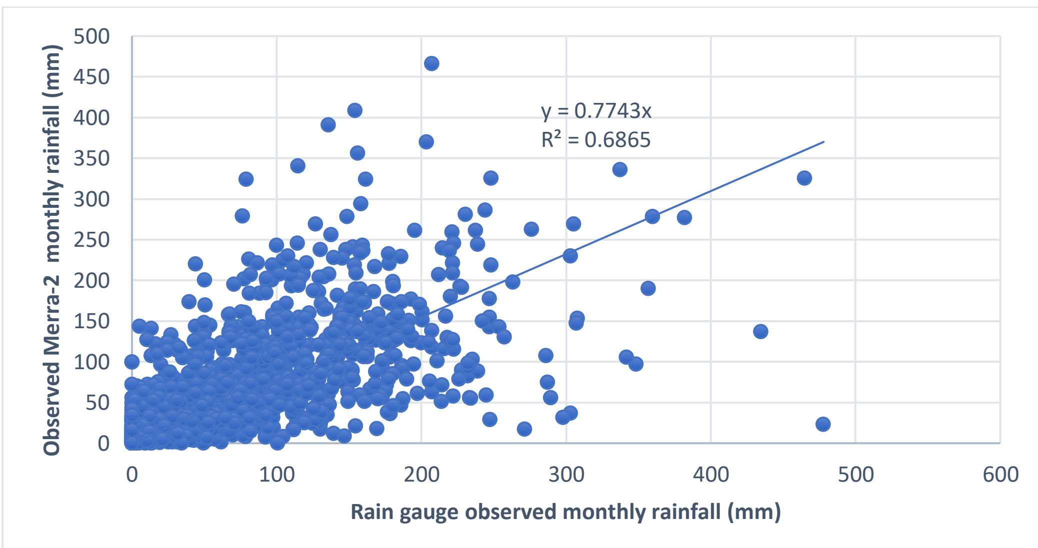

Figure 6.2. Linear regression of total monthly rainfall of all station ground rain gauges and for Merra-2 reanalysis (1983- 2020).

6.3.2. Rainfall distribution and elevation of gauging stations

Figure 6.3 shown the effect of elevation on rainfall is represented by the elevation regression method with the coefficient of determination (R^2= 0.9844). The rainfall stations located in neighboring areas have the same pattern among rainfall amount and their station positions (Taesombat & Sriwongsitanon, 2009). This agreed with similar studies suggested high elevation has got more precipitation compared to lower elevation (Gelaro et al., 2017; Al-Ozeer et al., 2020). The graph (Figure 6.3) shown the annual rainfall distribution has good agreement with increasing elevation in the region. This determines the annual rainfall amount will have positively correlated with the elevation. The rainfall amount may also depend on the elevation and high elevation receive high rainfall and vice versa in the region.

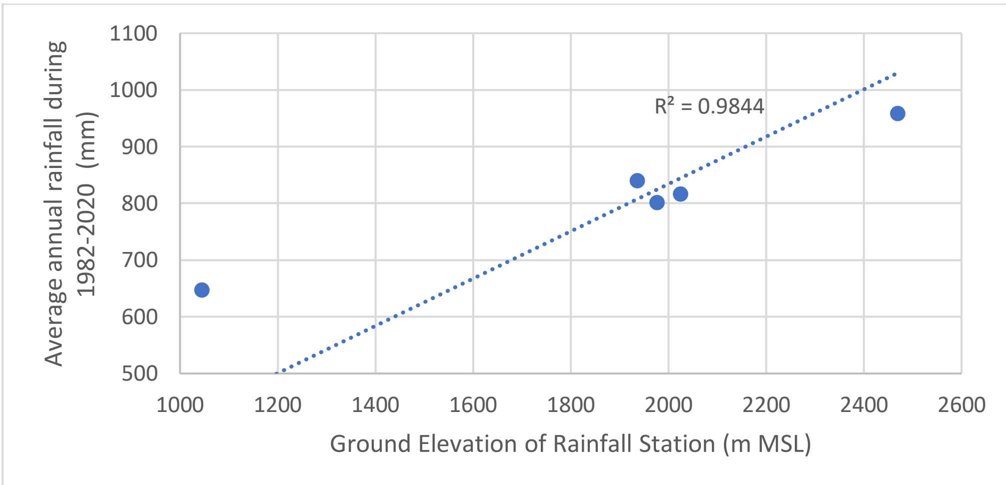

Figure 6.3. Linear regression of yearly average rainfall and elevation in the Upper Erer subbasin

6.3.3. Rainfall variability and seasonal contribution

The average annual rainfall for Dire Dawa, Harar,Haramaya, Girawa, and Gursum are found to be 647, 816, 801, 958, and 840 mm with coefficients of variation of 23, 20, 20, 19 and 31%, respectively (Table 6.2). The results showed that seasonal rainfall distributions are more variable than annual rainfall (Megersa et al., 2019). Spring season was more variable than Summer and less variable than Winter. The mean coefficient of variation for the stations shows that 27, 41 and 81% for Summer, Spring and Winter season, respectively. This also indicates that Summer and Spring seasons have a maximum annual contribution of 53 and 36%, respectively. This agrees with the study (Lebel et al., 1987), Spring contributes up to 40 % of the annual rainfall over northeastern, central, and southwestern Ethiopia.

The Winter season is characterized by significant inter-annual and intra-seasonal variability. The inter-annual and intra-seasonal variability makes the Winter season rainfall highly variable. Large scale rainfall variability with the highest rainfall amount (Hamal et al., 2020).

In addition, similar study confirmed also there is high rainfall amount and variability in most Ethiopia regions (Bewket and Conway, 2007).

Table 6.2. Statistical description and seasonal contribution of rainfall over the period (1983–2020) for Dire Dawa and Haramaya (1985-2020), for Harar (1983-2017) for Grawa and Gursum. Where, μ, stands for mean values of rainfall (mm), σ, stands standard deviation and CV, stands for coefficient of variation (%) and CT, stands for seasonal rainfall contribution (%).

Station name	**Summer Rainfall**				**Spring Rainfall**				**Winter Rainfall**				**Annual Rainfall**		
	μ	***σ***	**CV (%)**	**CT (%)**	***μ***	***σ***	**CV (%)**	**CT (%)**	***μ***	***σ***	**CV (%)**	**CT (%)**	***μ***	***σ***	**CV (%)**
Dire Dawa	309	96	31	48	260	118	45	40	78	69	88	12	647	150	23
Haramaya	447	98	22	55	283	95	33	35	86	71	83	11	816	162	20
Harar	408	106	26	51	306	132	43	38	87	60	69	11	801	157	20
Grawa	500	101	20	52	361	149	41	38	97	74	75	10	958	183	19
Gursum	424	148	35	50	331	145	44	39	85	76	88	10	840	262	31
Mean	**418**		**27**	**51**	**308**		**41**	**38**	**89**		**81**	**11**	**816**		**23**

From the result, mean monthly rainfall amount from November to January is less than 20 millimeters for all stations.

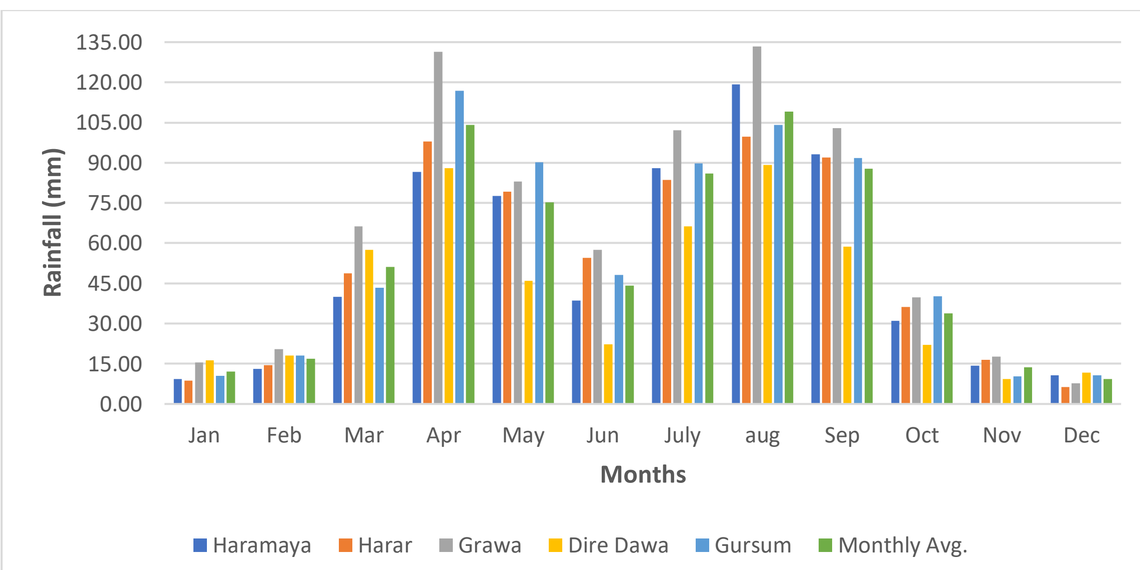

Figure 6.4. Monthly average rainfall distribution (mm)

The monthly peak rainfall occurs in August (monthly station average > 100 mm) for Summer season and April (monthly station average > 100mm) for the Spring season. Figure 6.4 shows monthly average rainfall distribution for the gauging stations from 1983 to 2020 at Dire Dawa and Haramaya, from 1985 to 2020 at Harar, and from 1983 to 2017 at Grawa and Gursum stations.

6.3.4. Seasonal distribution of rain days and rainfall amounts

As showed in Table 6.3, mean annual rain days ranged from 67 to 100 and the mean annual rainfall amount was in between 647 to 958 mm for all stations.

Table 6.3. The mean annual and mean seasonal mean rainy days and rainfall amounts over the period (1983–2020) for Dire Dawa and Haramaya (1985-2020) for Harar and (1983-2017) for Grawa and Gursum

Seasons		**Sations**				
		Dire Dawa	**Haramaya**	**Harar**	**Grawa**	**Gursum**
Annual	Rainy days	67	90	100	83	73
	Rainfall amounts (mm)	647	816	801	958	840
Summer	Rainy days	36	50	52	44	39
	Rainfall amounts (mm)	309	447	408	500	424
Spring	Rainy days	24	30	37	29	26
	Rainfall amounts (mm)	260	283	306	361	331
Winter	Rainy days	8	10	12	9	7
	Rainfall amounts (mm)	78	86	87	97	85

Dire Dawa station with relatively minimum mean annual rain days and rainfall amount. Summer season rain days distribution ranges more than half of the annual rain days contribution. But the seasonal contribution of Spring covers more than 1/3 of the annual rain days for all stations. This study agreed with (Megersa et al., 2019) considerable variations in annual and seasonal rainfall amounts. As discussed by (Bekele-Biratu et al., 2018), the number of rain days with rainfall amounting ≥ 0.1 mm ranged from 101 to 116 from June to October months of the monsoon season, which is the summer rainy season in India.

6.3.5. Annual, Summer, Spring, Winter rain days variability and distribution

The rainy days are the actual number of days for rain occurrence is 1mm or more (Seleshi and Zanke, 2004). The results in Table 6.4 showed, mean summer rainy days variability is less than 20% for Haramaya and Dire Dawa stations and for the rest the variability is all less than 30%. The mean annual rainy days were also the lowest for Haramaya and Dire Dawa stations, having a variability of 16 and 18%, respectively. Harar is the station with 39% variability for Spring season and Haramaya is the lowest, having 26% variability. For Dire Data station, the variability is high (coefficient of variation = 74%) and for the rest of all stations the variability is more than 50%.

Table 6.4. Seasonal mean rainy days, standard deviation, and coefficient of variation over the period (1983–2020) for Dire Dawa and Haramaya (1985-2020) for Harar (1983-2017) for Grawa and Gursum

Stations	**Mean rainy days for Summer season**			**Mean rainy days for Spring season**			**Mean rainy days for Winter season**			**Mean rainy days for Annual season**		
	μ	σ	**CV**	μ	σ	**CV**	μ	σ	**CV**	μ	σ	**CV**
Dire Dawa	36	7	19	24	9	37	8	6	74	67	12	18
Haramaya	50	7	15	30	8	26	10	6	59	90	14	16
Harar	52	13	25	37	14	39	12	6	54	100	25	25
Grawa	44	11	25	29	10	33	9	6	62	83	19	23
Gursum	39	9	24	27	9	34	8	5	67	73	17	23
Mean	**44**		**22**	**29**		**34**	**9**		**63**	**83**		**21**

As shown in Table 6.4, the maximum and minimum Summer daily coefficient of variation are 25 and 19%, respectively. The Spring seasonal rain days variability ranges from 26 to 37% and for Winter seasonal variability is all greater than 50% with a maximum value of 74%. But the annual rain days variability of 16% minimum value and 25% of the maximum variability. The annual rain days variability is less than seasonal; the minimum rain days variability is in summer season. But the maximum variability is occurred in Winter season with a mean variability of 63% for the stations (Bewket and Conway, 2014, Bekele-Biratu et al., 2018) that suggested that the stations receive variable rainfall in its amount and distribution.

6.3.6. Annual rain days and amount relationship with distance and elevation variance

The stations considered for the analysis were found at ~70 km radius from the centroid of the subbasin (Figure 6.1). The elevation of the gauging stations ranges from 2470-meters (Grawa) to 1045-meters (Dire Dawa) stations (Appendix 7). In Table 6.5, the relative distance from the centroid of the subbasin shows that Haramaya and Harar stations are the shortest distance of 18 and 21 km, respectively. Gursum station is the longest distance with 69 km from the centroid. In Table 6.5, the relative distance from the centroid of the subbasin shows that Haramaya and Harar stations has the shortest distance of 18 and 21 km, respectively. Gursum station is the longest distance with 69 km from the centroid. So, Haramaya and Harar which have the shortest distance between each may have highly probability to determines the occurrence and amount of rainfall in with in the stations.

Table 6.5. Correlation coefficients of mean annual rainy days, distance and elevation variance description. The values are described as correlation coefficients, distance between stations in kilometers, and the elevation difference in meters in the order from left to right. Bold values are the maximum

	Harar	**Haramaya**	**Grawa**	**Dire Dawa**	**Gursum**
Harar	1.00 (0) (0)				
Haramaya	**0.95 (16) (48)**	1.00 (0) (0)			
Grawa	0.81 (33) (493)	0.85 (39) (445)	1.00 (0) (0)		
Dire Dawa	0.71 (41) (932)	0.75 (25) (980)	0.88 (52) (1425)	1.00 (0) (0)	
Gursum	0.71 (82) (40)	0.75 (89) (88)	0.88 (112) (533)	**0.99 (110) (892)**	1.00 (0) (0)

High correlation coefficient value of 0.99 for Dire Dawa-Gursum with relative distance and elevation difference is 110 kilometers and 892 meters, respectively. This is due to the annual rain day at Dire Dawa and Gursum stations are relatively similar. At Haramaya-Harar, rainy days have extremely high correlation coefficient values of 0.95 and the relative distance is 16 kilometers and the elevation variation is 48 meters. From the result, he smallest coefficient of correlation value is 0.71, which is the correlation coefficient of Harar-Dire Dawa and Harar-

Gursum, and the relative distance and elevation difference is 41 kilometers and 932 meters and 82 kilometers and 40 meters respectively.

The rain days coefficient of correlation for Haramaya-Dire Dawa and Haramaya-Gursum is both 0.75 and with the relative distance of 25, 89 kilometers and elevation difference of 980, 88 meters respectively. This shows that the elevation-rainfall relationship is negative and the relative distance between the stations of Haramaya-Gursum is 89 kilometers, which is greater than 80 kilometers. The rain days coefficient of correlation not only depends on elevation, rather the relative distance but also has an impact. Generally, for all stations (rainy-days elevation) and (rainy-days- distance) correlation coefficients ($r > 0.50$) as suggested by (Kendall and Gibbons, 1990), implied there were high correlations. The rain days not only depends on elevation, but also the relative distance, this was also confirmed by a similar study (Ayoade, 1983). Although, the correlation coefficient was significant on the elevation-rainfall agreement as suggested (Oettli and Camberlin, 2005).

Table 6.6. Correlation coefficients of mean annual rainfall amount, distance, and elevation variance description. The values are described as correlation coefficients, distance between stations in kilometers, and the elevation difference in meters in the order from left to right. Bold values are the maximum

	Grawa	**Gursum**	**Haramaya**	**Harar**	**Dire Dawa**
Grawa	1.00 (0) (0)				
Gursum	0.88 (112) (533)	1.00 (0) (0)			
Haramaya	0.85 (39) (445)	**0.97** (89) (88)	1.00 (0) (0)		
Harar	0.84 (33) (493)	**0.95** (82) (40)	**0.98 (16) (48)**	1.00(0) (0)	
Dire Dawa	0.68 (110) (1425)	0.77 (110) (892)	0.79 (25) (980)	0.81 (41) (932)	1.0 (0) (0)

As shown in Table 6.6, the of correlation coefficient for mean annual rainfall amount for Haramaya-Harar is 0.98 having relative distance and elevation of 16 kilometers and 48 meters, respectively. So, Haramaya-Harar have good correlation and the relative distance and elevation gap is small. Haramaya-Gursum have an extremely high correlation coefficient (0.97) and Harar-Gursum also have an extremely high correlation (0.95), but the relative distance and elevation difference are 89 kilometers and 88 meters and 82 kilometers and 40 meters respectively. The correlation coefficients (r > 0.50) show the correlation are good agreement for all stations (Kendall and Gibbons, 1990).

For Haramaya-Harar, the correlation is extremely high and the relative distance and elevation difference is also minimum, and the correlation coefficient depends on the relative distance and elevation difference between the two stations. The smallest correlation coefficient value is 0.68, which is the correlation coefficient value for Grawa-Dire Dawa, where the distance between the stations is 110 kilometers, and the elevation difference is 1425 meters. This implies that the correlation coefficient depends on the relative distance and elevation between the stations. As the relative distance between the station and the elevation difference were high, the correlation coefficient was relatively small for Grawa-Dire Dawa station. For Gursum-Harar, (coefficient of correlation = 0.95) and the relative distance and elevation difference are 82 kilometers and 40 meters. This shows that even if the elevation difference is minimal and the distance between the two stations is more, the correlation for mean annual rainfall is extremely high.

The coefficient of correlation for Gursum Haramaya is extremely high with value of 0.97, and the distance and elevation difference are 89 kilometers and 88 meters. From the result, the relative distance between the two is more (89 kilometers), the elevation difference is minimal, the correlation coefficient for the mean annual rainfall amount is extremely high and has extremely high correlation. For Gursum-Haramaya and Gursum-Harar, the coefficient of correlation is 0.97 and 0.95, but the elevation difference is not a positive relation to the mean annual rainfall.

Haramaya-Dire Dawa and Harar-Dire Dawa correlation coefficient values are 0.79 and 0.81 with the relative distance of 25 and 41 meters and elevation difference of 980 and 932 meters. The result shows that the correlation coefficient of Haramaya-Dire Dawa is the smallest compared to Harar-Dire Dawa, the elevation difference is also maximum for Haramaya-Dire Dawa compared to Harar-Dire Dawa. For Grawa-Gursum and Grawa-Haramaya, the correlation coefficient of 0.88, 0.85, and the relative distance and elevation is 112, 39 kilometers and 533, 445 meters, the relative distance of Grawa to Gursum is high (= 112 kilometers) and the elevation difference only have no impact on the mean annual rainfall amount correlation coefficient and the relative distance also has an impact. But as discussed by Mishra (Mishra, 2013), significant variations were detected for stations found within 15 km distance.

6.3.7. Joint probability of rain days estimation with daily, decadal, monthly, and seasonal variations

The joint probability of rainfall incident for different combinations of gauging stations at a given period is calculated by counting the joint rainfall events in the whole period under consideration (in Appendix 17) and divide to the number of observation records, and then multiply by 100%. To identify the implication of spatiotemporal areal rainfall distribution of the gauging stations in the subbasin, requires designating the joint probability method considering continuous observed rainfall data for times series. The joint probability of rain days occurrence of the station indicated that the frequencies of all or parts of the gauging stations have rain simultaneously for the period under consideration.

The joint combination of the gauging station considers the rainfall incidence at a period that will estimate the areal rainfall characteristics using the probability approach method. The probability of daily rainfall for station combination receiving rain mutually are all less than 15 % except for Haramaya-Harar station combination which is greater than 15 %. The joint probability of all stations receiving rain mutually are 25.37 and 39.47 % for decadal and monthly periods, respectively. The joint probability of rain days for monthly of all combinations receiving rain mutually are greater than 39 % with the maximum joint probability of 62.50 %. The minimum joint probability for Summer and Spring seasons to receive rain mutually for the stations are 68.42 and 67. 42 %, with the maximum value of 89.47 and 89.47 %, respectively as showed in Appendix 17. The analysis result indicated that summer season has high probability of joint rainfall occurrence and daily time series with the smallest probability of joint rainfall for the stations in the region.

6.3.8. Joint arithmetic average rainfall estimation with daily, decadal, monthly and seasonal variations

The arithmetic average areal rainfall estimates as suggested by (Eruola et al., 2015). At least five temporal scales were analyzed. Such as; daily, decadal, monthly, Spring season, and Summer season. The different time scale rain gauge combinations were compared to get the best combinations out of 2, 3, 4, and 5. The areal rainfall estimation of joint arithmetic mean rainfall for different time scales is assessed. The arithmetic average of rainfall estimation for the stations under daily, decadal, monthly, and seasonal observed rainfall were calculated by averaging the rainfall amounts from January 1984 to December 2020 for different periods (in Appendix 18).

The joint average combination of the gauging station considers the rainfall amount at a period that will bring the arithmetic average rainfall for the region. Different rainfall station combinations like; five-station, four-station, three-station, two-station. About 23 gauging station combination is developed to identify the areal average rainfall in different periods such as daily decadal, monthly, Summer season, Spring season.

The result on Appendix 18 indicates that daily arithmetic average areal rainfall for station combination is all less than 3 % and for decadal arithmetic average areal rainfall of all stations is greater than 17 %. While, arithmetic average areal rainfall of all combinations for monthly (> 52 %), Summer (>79 %) and Spring (>59 %). The maximum arithmetic average areal rainfall of all combinations was 64.02 %, 100 % and 76.30 % for monthly, Summer and Spring, respectively. The result showed that summer season has high arithmetic average areal rainfall and daily time series has the smallest arithmetic average areal rainfall for the stations in the region.

6.3.9. The effects of joint rain gauge combination change on the joint probability of rain days estimation approach

The rain days probability for daily time step for the Upper Erer river basin is less than 20% probability and for decadal and monthly joint probability estimates were a minimum value of 25.37 and 39.47% respectively. The probability of joint rain days for daily time step is less than ≈ 15 %. The maximum joint probability estimation for rain days is ≈ 89 %, that is, for two-station combinations. The decadal joint probability estimation for the two station combinations is all > 40% and for three and four stations the values are > 35 and 25 %, respectively. And the joint probability estimation for five stations is > 25%.

The maximum and minimum monthly joint probability values of 62. 50 % and 39.47 % for two-and five-station combination, respectively. The seasonal joint probability estimation is with a maximum value of 89.47 and a minimum value of 67.42 % for two-and five-station combinations, respectively. As confirmed by Jackson (Jackson and Joseph, 1977; Jackson 1981) a better relationship occurs among monthly rainfall and number of rain days than among monthly rainfall and mean daily rainfall amount.

6.3.10. Relationship between joint probability of rain days and joint arithmetic mean method

Figure 6.5, Figure 6.6, Figure 6.7, Figure 6.8, and Figure 6.9 shown below define the scatter diagram of the probability of joint rainfall and joint arithmetic mean rainfall from January 1984 to 2020. This correlation was demonstrated for different time series. The linear regressions shown in the figures below has a better agreement between the probability of joint rainfall and joint arithmetic areal mean rainfall observations.

For the 23 stations combinations, the linear regression of the joint arithmetic mean and the probability of joint rain days for the different periods under consideration shows that the maximum correlation value is for monthly, R^2 is 0.9784. This shows that the linear regression of joint arithmetic monthly areal indicated high accuracy with respect to the probability of joint monthly rain observations. The seasonal linear regression for the Summer and Spring shows a good relationship for the joint areal seasonal mean rainfall with the probability of joint seasonal rain observation.

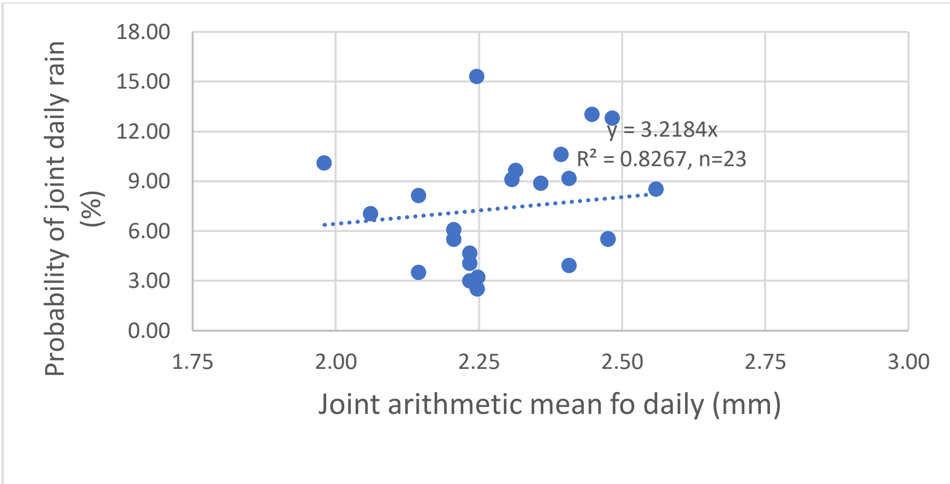

Figure 6.5. Linear regression of joint arithmetic mean and probability of joint daily rain.

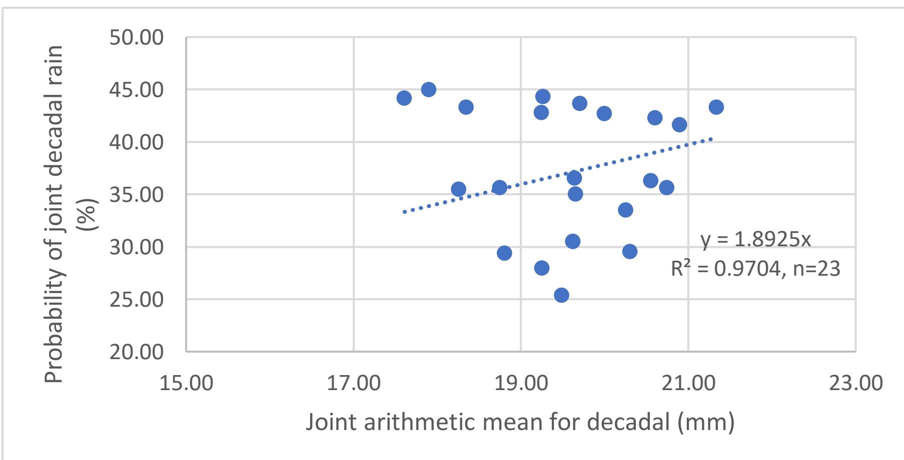

Figure 6.6. Linear regression of joint arithmetic mean and probability of joint decadal rain.

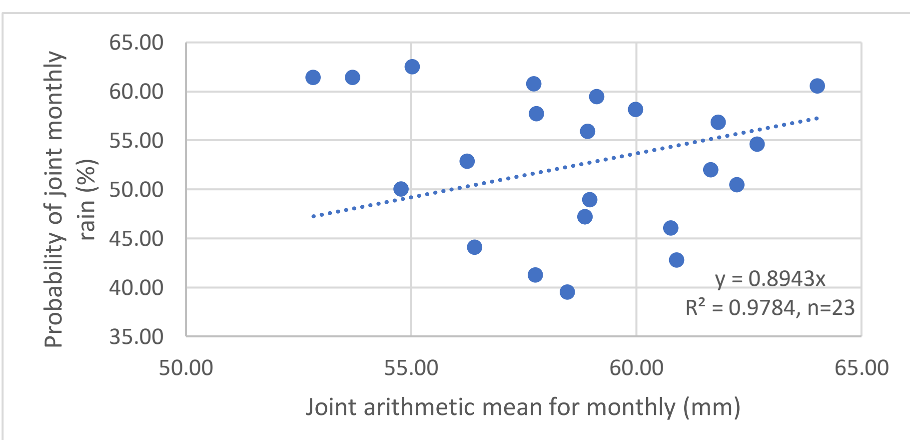

Figure 6.7. Linear regression of joint arithmetic mean and joint probability of rain days for monthly.

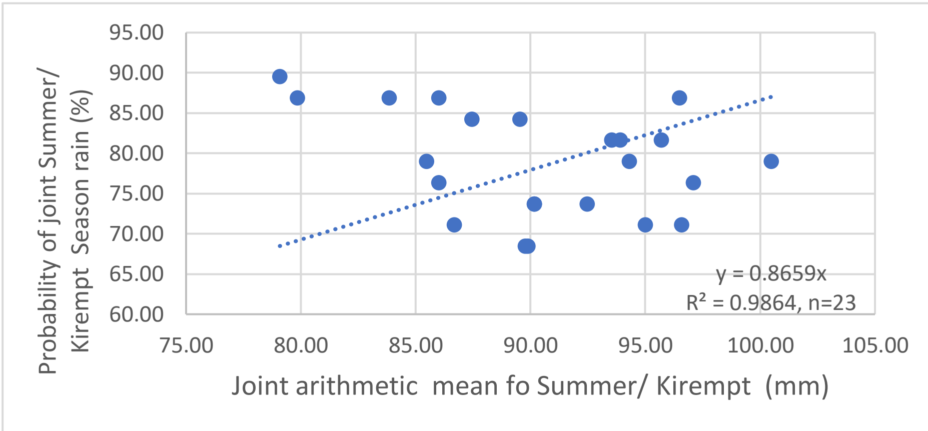

Figure 6.8. Linear regression of joint arithmetic mean and joint probability of rain days for Summer season.

And also, this study revealed that areal rainfall estimations are very sensitive to the position and number of rains gauging stations, that was also found by other scholars (Bell and Moore, 2000; Terink et al., 2018). Similarly, as confirmed (Nandargi, and Mulye 2012) the accuracies of the areal rainfall estimation tend to increase when the number of stations increases.

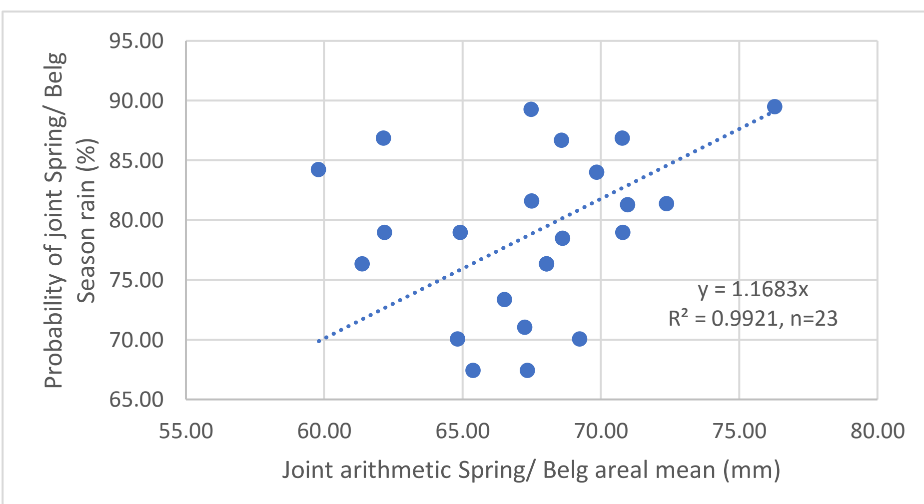

Figure 6.9. Linear regression of joint arithmetic mean and joint probability of rain days for Spring season rain.

6.3.11. Assessing the joint probability of rain days approaches

As shown in Table 6.7, the correlations between the joint probability rain days estimation using five different time scales and the observed joint arithmetic areal rainfall were assessed using the scatter diagram. From the result, the joint probability approach for monthly time scale is better estimating the areal rainfall of the region than the daily and decadal periods. But, the seasonal (Summer and Spring) is slightly more than the monthly time scale. During the Spring season the coefficient of determination is higher than the others time series (Table 6.7). The slope of the graph is approaching to 1 for monthly times scale than the others. These show that the relation is good agreement in monthly than others.

Table 6.7. Values of statistical indicators for different joint probability methods: The letter A and R^2 denotes the equation of the line and the coefficient of determination drawn using the Joint arithmetic (horizontal) and joint probability (vertical) respectively.

Indicators	**Joint probability of rain days estimation for different periods**				
	Daily	**Decadal**	**Monthly**	**Summer**	**Spring**
A	3.2184	1.8925	0.8943	0.8659	1.1683
R^2	0.8267	0.9704	0.9784	0.9864	0.9921

6.4. Conclusions

The study showed that up-to-date areal rainfall estimation characteristics of spatial and temporal behavior of the Upper Erer subbasin were identified. Moreover, analyzed the implication of daily, decadal, monthly and seasonal rainfall distribution characteristics using efficient approach over the upper Erer subbasin. The correlation of Haramaya-Harar is high and relative distance and elevation difference is also minimum. The correlation coefficient depends on the relative distance and elevation difference between the two stations. The smallest correlation coefficient value is 0.68, which is the correlation coefficient value for Grawa-Dire Dawa, where the distance between the stations is 110 kilometers, and the elevation difference is 1425 meters. The mean annual rainy days and mean annual rainfall amount of correlation coefficients ($r > 0.50$) for all gauging stations.

Linear regression for the total monthly records for the Merra-2 and ground rain gauge observation were analyzed. The results for the coefficient of determination ($R^2 > 0.5$), indicate that high correlation between the ground observation and Merra-2 reanalysis data for the region. The arithmetic average of areal rainfall estimation for daily, decadal, monthly, and seasonal observed rainfall by averaging the rainfall amounts from January 1984 to December 2020 for different time series. The probability of joint daily rain for the station combinations is all less than 20%. For decadal time series, the probability of rain days for all combinations are greater than 25 %. While, the probability of monthly time series for the station combinations are all greater than 50% except a few combinations. Out of 23 possibilities only eight of them are less than 50%.

The correlation between the probability of joint rainfall estimation using five different time scales and the observed joint arithmetic areal rainfall of the scatter diagram showed that the subbasin rainfall characteristics do not described well only by making direct averaging by any areal rainfall estimation known method, unless the probability of joint rainy days is determined. The result indicated, the joint probability of rain days estimate for daily and decadal timeseries were not determine the likely output. However, for monthly rain the joint probability determines the subbasin average areal rainfall characteristics reasonably well. So, the areal rainfall of the subbasin is recommended to be determined by the combination of the probability of joint monthly rainfall and the rainfall amount together for water resource assessment in rainfall-runoff modelling. The study analysis was conducted with a scattered and a few numbers of stations and future investigations should also consider additional gauging stations under different regions to further evaluate the present method. Especially more gauging stations sampling used for the integration of observations over time scales need to be discovered.

7. ESTIMATION OF DISCHARGE USING RATING CURVE UNDER DATA SCARCE REGION OF UPPER ERER RIVER, WABISHEBLE RIVER BASIN, ETHIOPIA

Abstract

For any hydrological researches the accessibility of flow discharge is significantly important. But direct measuring streamflow is costly and time consuming instead the stage – discharge relationship (rating curve) is developed to estimate the flow discharge. Precise estimation of the rating curve relationship across a river outlet is considered a key point for various water resource engineering application. This research explained to estimate the flow discharge using the rating curve in data scarce region of upper Erer river. A simple and quick Excel solver technique has been employed to develop the rating curve accurately. The performance of the rating curve model was evaluated using statistical measures such as root mean square error, coefficient of determination and Nash–Sutcliffe Efficiency. The results indicate a better performance of the modeling technique with coefficient of determination of (0.98), root mean square error (4.49) and Nash–Sutcliffe Efficiency (0.97). The output indicates that the rating curve was well performance for estimating the flow discharge in the study area. Hence, the estimated flow discharge using the developed rating curve model were applicable for hydrological model simulation in the region.

Keywords: Observed flow; Simulated flow; Water level; Rating curve

7.1. Introduction

Measurement of stream flow is a significant feature of hydrology associated project such as water quality monitoring, geomorphology, and flooding and others (Gore et al., 2017; Barbetta et al., 2017; Sikorska et al., 2017). Streamflow measurements are frequently done once in a day during normal periods and on an hourly basis during floods. Nevertheless, the collection of direct measurements of the stream flow discharge is costly and challenging (Patra, 2008; WMO, 2010; Othman et al., 2019). Hence, it has been known practice to simulate discharges from the water level record which is less expensive and easier approaches. Most of the time both stage and discharge of a stream vary on time. In order to obtain a continuous record of discharge, the stage is recorded and the discharge is computed from correlation of stage and discharge (Aytac and Azamathulla, 2012). For constructing stage-discharge relationship, the rating curve approach is commonly used technique and has been used on various gauging stations in the world (Guerrero J L. et.al., 2012). The rating curve is an crucial technique in flow discharge estimation (Asgeir, 2006; Mansanarez et al., 2018; Maghrebi and Ahmadi, 2017; Kiang et al., 2018). The availability and accurate rating curve are very essential for various hydrological applications including irrigation, water resources management, sediment controlling and hydrologic modeling (Sefe, 1996).

Rating curves construction is basically a trial-and-error task which requires a wide hypothetical background information in order to create a reliable tool for converting measured water level to discharge (Alfa, M. I., et al., 2018). In establishing the rating curve needs selecting appropriate gauging site and the gauging site would be permanent irrespective of erosion or deposition. The elevation of water surface corresponding to a given discharge (Sharma and Sharma, 2002) is similar. Gauging a stream flow level can be measured directly or indirectly. Water level gauges can be categorized as vertical staff gauge, inclined gauge, hook gauge, temporary gauge and crest stage gauge. Staff gauge is categorized under direct type, but self-recorder type and crest stage type are indirect gauge type (Subramanya, 2007; Adegbola and Olaniyan, 2012). Moreover, on site discharge measuring can be categorized as direct or indirect measurement. The velocity-area method is direct measurement by using current meter and floats. While, the indirect measurement includes slope-area method using flow measuring structures such as flumes, weir and gated structure. Typically, the velocity recorded by a current meter on the site and recorded staff gauge were used to estimate the discharge (Alfa, M. I., et al., 2018).

The accuracy of discharge estimated from the rating curve depends on the accuracy of stage measurement and developed rating curve technique (Muzzammil et al., 2018). Stage–discharge relationship has always continued to be an area of attention for hydrologists, and several efforts have been implemented to develop acceptable rating curves model by using different techniques. Muzzammil et al. (2018) used Excel solver technique for establishing the rating curve. Alfa et al. (2018) created a rating curve for Ofu River in Nigeria using linear regression analysis and analysis tool of Microsoft Excel. McGinn and Chubak, (2002) and

Braca (2008) suggested polynomial models for establishing stage–discharge relationships. Zhenquan et al. (2017) used Multiple Linear Regression Analysis (MLRA) for creating the Yellow river diversion model. Ghimire and Reddy (2010) used different algorithms approaches of multiple linear regression (MLR) methods for establishing a stage discharge relation in river. The use of appropriate rating curve approaches and extra measurements relative to different test sites were required (Di Baldassarre et al., 2011) to minimize the uncertainty of flood discharge data.

Most of the studies were concentrated on developed countries with sufficient data. In developing countries, the preservation of a watercourse gauge network is poor due to scarcity of funds (Hamilton et al., 2019) and the stage–discharge measurements are rare (Abate et al., 2017; Zimale et al., 2018) and rating curves are not updated after major storms (Negatu et al., 2022). Similarly, insufficiency of flow discharge data availability (Abebe et al. 2020) highly affected the water resource studies in various regions of Ethiopia (Goshime et al. 2021). In upper Wabisheble basin including the upper Erer subbasin finding recent river measured discharge data are difficult (Wudineh et al., 2021). So, this research explained to estimate flow discharge using the rating curve equation under own flow record for the period 2020-2021 at upper Erer sub basin outlet. In this recording process the number of records per day are more, despite usual methods of stream record in various parts of the country.

7.2. Materials and Methods

7.2.1. Study area description

The Upper Erer subbasin outlet that drains from the Harar highlands to the Wabisheble river basin were located about 15 km south east of Harar Town. The Harar town is located on geographic grid reference longitude 42°6'59.71"E, latitude 9°18'55.434"N. The upper Erer subbasin, is located physically in between 9^{o}13’26.4” N to 9^{o}31’26.4” N latitude and 42^{o}4’40.8” E 42^{o}20’38.4” E longitude. The catchment area of the upper Erer River is 466 km^2 with an elevation varying from 1306 to 3019 meters above sea level. The outlet of the upper Erer River is found at 9°14'10.339"N latitude and 42°15'2.301"E longitude. The upper Erer River is very useful to the inhabitants for domestic and agricultural purposes. The bridge (road crossing) at Erer-Jijiga road junction is found to be the outlet point for the study location where the staff gauge re-installed. Figure 7.1 shows the catchment area, stream flow and location of staff gauge.

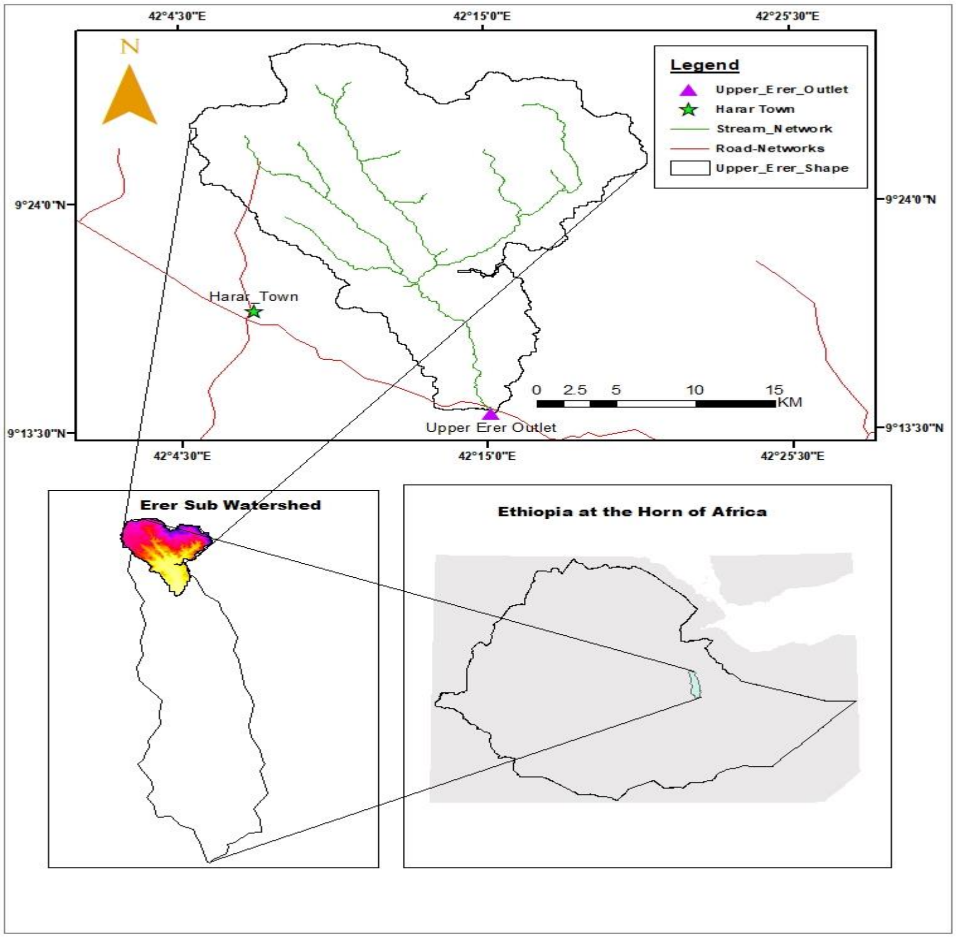

Figure 7.1. Upper Erer River subbasin showing location of staff gauge station for discharge estimation under data scarce area.

7.2.2. Data sources and collection

Stage–discharge data for upper Erer gauging station (specific location on Erer-Jijiga Road at Bridge) was collected from onsite records. In this research the stage reading was measured for the period of 18 months, starting from 13th May 2020 to 16th October 2021 using calibrated staff gauge. While, discharge measurement was observed using the ultrasonic current meter during base flow (delayed surface runoff or ground water flow), low flow and high flow periods for the months of May 2020, August 2020 and October 2021.

The selected staff gauging stations site was stable and satisfies all the standards for installing a gauging station as suggested by (Meals and Dressing, 2008; Sauer and Turnipseed 2010). The location of the gauging station is shown in Figure 7.1. The measuring of discharges was using current meter and the stage readings were recorded from the staff gauge (Figure 7.2). A stage time series data was collected once a day at 12:00 PM during base flow period and four times a day during low flow period at 06:00 AM, 10:00 AM, 02:00 PM and 06:00 PM. While, during high flow of summer season, to catch-up the peak flow, the staff gauge reading was recorded seven times a day; at 06:00 AM, 08:00 AM, 10:00 AM, 12:00 PM, 02:00, PM 04:00 PM and 06:00 PM.

Figure 7.2. Upper Erer River at Bridge: a) Staff gauge reading re-installed (2020), (b) Flow measuring process on site using crane movement for vertical current meter (2020) and c) Rivers at full stage during peak flow (August 2020).

7.2.3. Discharge estimation

The discharge estimation using indirect method can be implemented more accurately by employing the velocity-area method using the measured flow depth and velocity. The indirect measure of discharge includes two approaches; the mid-section and mean section methods (Subramanya, 2007). In this study, the mid-section approach was selected shown (Equation 6.1).

$$Q = \overline{V_1} D_1 \left[\frac{B_1 + B_2}{2}\right] + \overline{V_2} D_2 \left[\frac{B_2 + B_3}{2}\right] + \cdots \qquad \text{Equation (6.1)}$$

The method used to calculate the total discharge flowing in the section using the average discharge value calculated for each strip as shown (equation 6.2). And the discharge flows in the section at a given instant can be estimated by summing the discharge using (equation 6.3).

$$q = \overline{V_1} D_1 \left[\left(\frac{D_1 + D_2}{2} \right) \left(\frac{\overline{V_1} + \overline{V_2}}{2} \right) \right] + \cdots \qquad \text{Equation (6.2)}$$

$$Q = \sum q \qquad \text{Equation (6.3)}$$

Where, Q is the discharge (m3/s), $\overline{V_n}$ is the velocity (m/s), B_n = span length (m), D_n is the depth (m), n is the number of intervals along the section. The velocity of the flow increases from the bottom to the water surface across the channel section.

7.2.4. Determining stage – discharge relations

In this study discharge estimation involves two steps: the first step is measuring stage and the corresponding discharges in the river and establishing a relationship (rating curve), secondly measuring water level and estimating the discharge by using the established relationship. The stage-discharge relationship that does not change with time is permanent control and that change with time is shifting control. Shifting control occurs from erosion or deposition of sediment at the stage measurement station.

Practical relationship between stage and discharge can be developed by field measurement of stage and discharge and thereafter can be expressed as a rating curve. Although, literature presents a number of mathematical expressions for relating water levels to discharges in a given cross-section (Petersen, 2004; Franchini and Ravagnini, 2007). In this study the power-law (Equation 6.5), in light of its simplicity and various application (e.g. Petersen, 2004; Schmidt et al., 2008) was preferred. If H represents water level for flow discharge Q, then the relationship between H and Q can possibly be approximated using the equation (Equation 6.5) given by (Herschy, 1999 and Kennedy, 1984). The determination of datum correction (a) for Q = 0, (H + a) = 0, where a = -H.

$$Q = f(H) \qquad \text{Equation (6.4)}$$

Where, f(H) is an algebraic function of water level.

$$\mathrm{Q} = \mathrm{c}(\mathrm{H} + \mathrm{a})^{\mathrm{n}} \qquad \text{Equation (6.5)}$$

Where, Q is the flow in m3/s, H is the measured water level (m), c, a (stage for zero discharge (m)), and n are rating curve parameter and the main point is to calculate these parameters. Where "c" and "n" are rating curve constants, and "a" is a constant representing the gauge reading which corresponds to zero discharge.

Fundamentally rating curve equations are of nonlinear form., hence Microsoft Excel Solver of nonlinear solver is used to get the optimal values of rating curve constants. The programing of the Microsoft Excel Solver was demonstrated for specific applications by numerous scholars such as (Muzzammil et al., 2018).

7.2.5. Performance evaluation of rating curves

In this research the performance of rating curve model was verified using evaluation matrices shown (Equation 6.6 to 6.8). The performance measures include; Nash–Sutcliffe measure of efficiency (NSE), root-mean-square error (RMSE) and coefficient of determination (R^2). NSE shows how well the simulation coincides with the observation, and the values ranges between $-\infty$ and 1.0, with NSE=1 representing a perfect fit of the model. The higher the NSE value, the more reliable is the model. The coefficient of determination (R^2) is between 0 and 1, if the R^2 is 1 the performance of model is of higher fit. While the smallest values of RMSE means a good agreement of observed and simulated data (Nash and Sutcliffe, 1970; Hayden, Robert, 2009).

$$NSE = 1 - \left[\frac{\sum_{i=1}^{n}(Q_{oi} - Q_{si})^2}{\sum_{i=1}^{n}(Q_{oi} - \mathrm{Qoav})^2}\right] \qquad \text{Equation (4.6)}$$

$$R^2 = 1 - \left[\frac{\sum_{i=1}^{n}(Q_{oi} - Q_{sav})(Q_{oi} - Q_{oav})}{\sum_{i=1}^{n}(Q_{si} - Q_{sav})^2 \sum_{i=1}^{n}(Q_{oi} - Q_{oav})^2}\right] \qquad \text{Equation (6.7)}$$

$$\text{RMSE=} \quad \sqrt{\sum_{i=1}^{n}(Q_{oi} - Q_{si})/n} \qquad \text{Equation (6.8)}$$

Where, Q_{si} *is the observed discharge*, Q_{oi} is the estimated discharge, Qoav is the average of the observed data.

7.3. Results and discussion

7.3.1. The rating curve for the gaging station

The Excel solver available in Microsoft Excel was used in this study to estimate the value of a, c and n employing the regression analysis under the analysis tool park of Excel Solver as shown in Appendix 19. The abbreviations in the Appendix 19 denotes that H represent the height of the water level, Qo is the observed discharge and Qs is the simulated flow discharge.

The observed stage and respective discharge at a particular point of reading have used to develop rating curves following the least square method as per the general Equation given by (Equation 6.5).

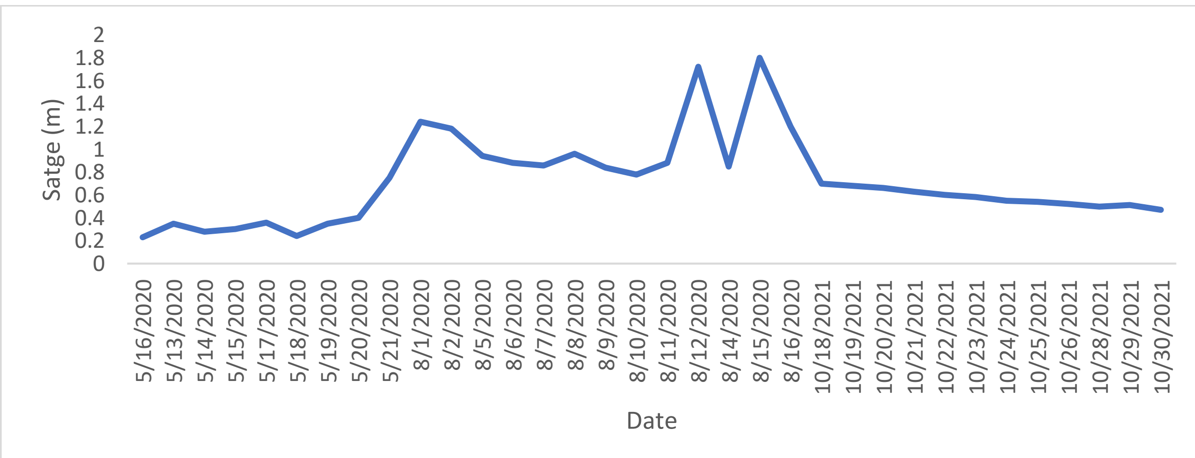

Figure 7.3. Average daily stage hydrograph of Upper Erer River at Erer Bridge Hydrometric Station.

In this research process the number of stage-discharge measurements was carried out within the period for the development of the rating curve (Appendix 19). The maximum water level observed was 1.8 m while the minimum of 0.23 m (Figure 7.3). The result shown in the graph indicates that the maximum stage levels were found during the months of August and May which exist on the rainy seasons of Summer and Spring in the region, respectively. While the minimum stage level was found in the months of May as shown in the graph. In the Month of

May in the region the starting period of rainy season and probably the local communities were using the river water as well as the soil surface was not saturated and the first drop of rain fall were not approaching the river outlet.

The graph shown in Figure 7.3 indicates that the water level reduced as of October and reaching zero, this is the beginning of Winter season in the region with dry season and local communities divert the river for local consumption and the river flow is becoming at zero stage. In this river gauging site, the zero-stage level is recorded for most of the year except for rainy seasons.

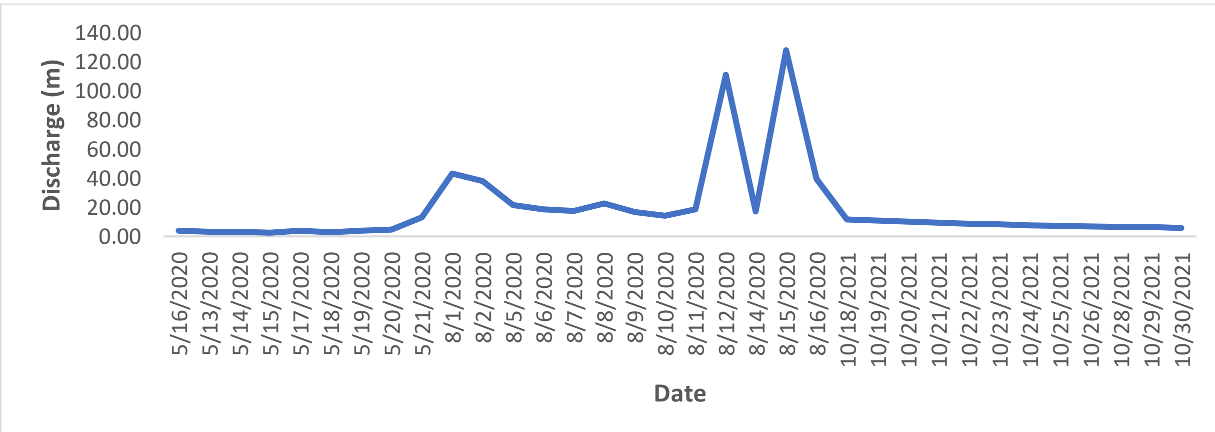

Figure 7.4. Discharge Hydrograph for Upper Erer River using fitted Rating Curve.

The observed event shown in Figure 7.4 noted some major flood event happening. The major flood occurred in 12^{th} August 2020 and 15^{th} August 2020 causing the probably shifting controls to happen. The discharge hydrograph shown in (Figure 7.4) with similar pattern to that of the stage hydrograph (Figure 7.3) for the study area. Figure 7.5 showed the observed, estimated discharge with developed rating curve for the whole 18 months records. Using the observed flood event data, power regression type was plotted as shown in Figure 7.5. The line representing the mean value of the two variables involved.

Taking the difference between the simulated and observed discharge and making the sum of square of errors by employing the Excel solver method. The minimum of square of errors for different iterations and the constant values are calculated and repeat the iteration of the solver computation process until the minimum sum of square of errors appear. Accordingly, the value of “a” is 1.1533 m, value “c” is 0.4769 and the value of “n” is 5.1656, thus will give the Equation of the rating curve equals to:

$$Q= 0.4769(h + 1.1533)^{5.1656} \qquad \text{Equation (6.9)}$$

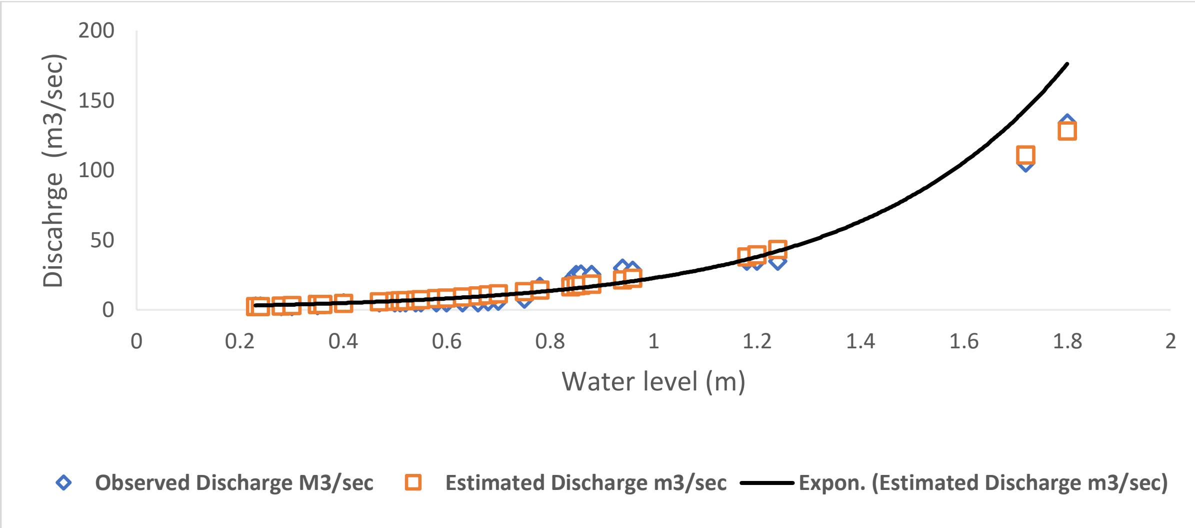

Figure 7.5. Predicted and observed stage discharge rating curve at Upper Erer River

The developed rating curve represents the actual discharge crossing the gauging station with the corresponding water level. In most developing countries, stage–discharge measurements are rare. Hence, usual approaches cannot be used to estimate the rating curves of rivers. In addition, the climate of these countries are monsoon climates (Ros et al., 2013), where all the rainfall concentrated to few months period. This brings storm in various rivers that can vary the bedding of the river channel in most regions.

7.3.2. The Goodness of Fit

The performance of the developed rating curve was evaluated using the performance measures. Table 7.1 indicates the statistical measures of root-mean-square error (RMSE), Nash–Sutcliffe Efficiency (NSE) and coefficient of determination (R^2) to evaluate the quality of the adjusted dataset on different time scales. The result indicates that the statistical performance evaluation gave a strong NSE (0.97), RMSE (4.49) and with R^2 (0.98). In addition, the result for the observed and simulated discharge in the Figure 7.6 shows the slope of the Equation (0.94).

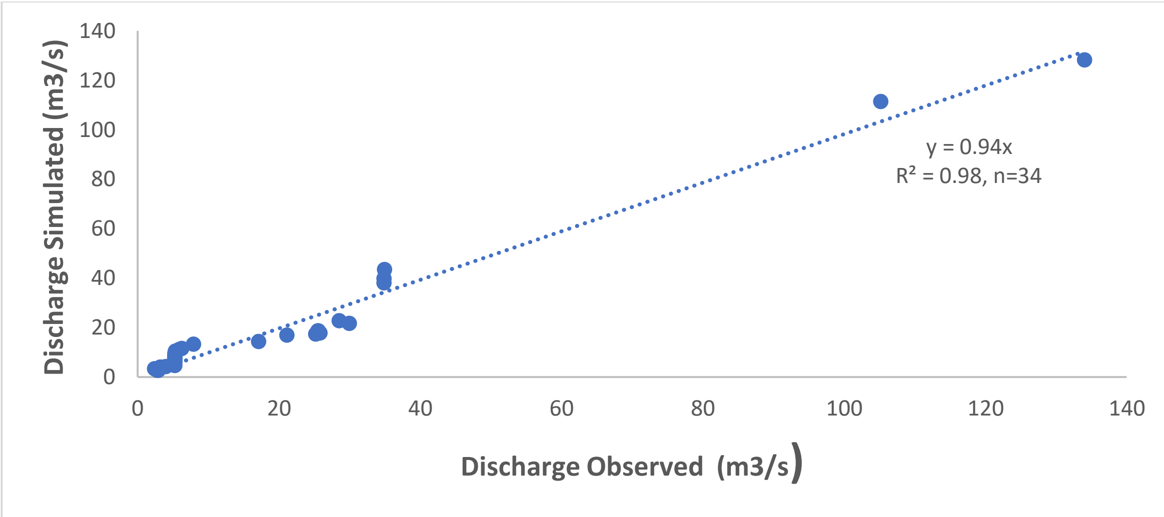

Figure 7.6. relationship of simulated and observed discharge for the rating curve constant estimation

The result from the Excel solver is a promising tool for estimating rating curve parameters. it has been found that Excel solver minimizes the time-consuming during trial and error for formulating stage–discharge relations. This result supports that the Equation represents the best fit.

Table 7.1. Parameters for validation of curve fitting process

Parameter	**Value**
RMSE	4.49
NSE	0.97
R^2	0.98
Slope	0.94

7.3.3. Estimating discharge using the developed rating curve

The rating curve is a very important tool in surface hydrology because the reliability of discharge data values is highly dependent on a satisfactory stage-discharge relationship at the gauging site. It can be used to obtain an estimate of the discharge of a large flood where only the stage data is available only by the extension of the rating curve (Patra, 2008).

Figure 7.7 shown the observed stage data during the period from 13th May 2020 to 16th October 2021. About 2020 stage reading were collected during the period of observations.

During the rainy season the stage level is maximum and after the rainy season passed the stage decrease and becomes zero-level. This is happening for the months of December, January, February and March.

At these months the stage reading were recorded once a day since this is the zero-discharge level. As shown in the graph some reading has stage levels more than 1.5 meters and most of the reading fall between 1 meter to 1.5 meters. While some observations surpass 2 meters. Generally, these indicate, the stage levels are above 0.5 meter, except at some observations that the river has significantly minimum flow.

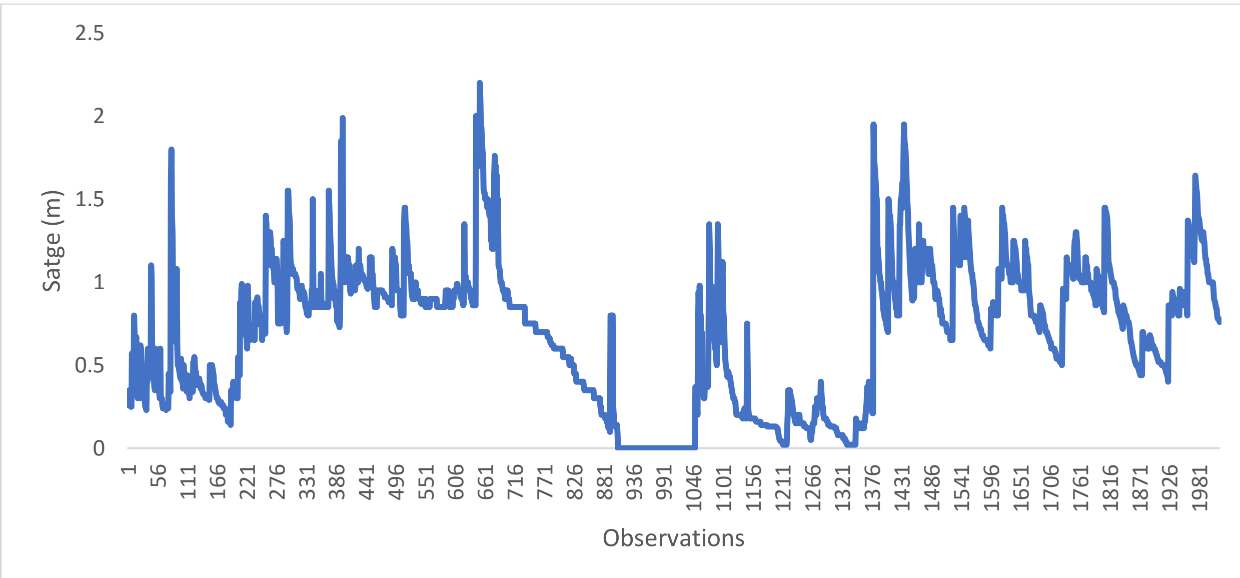

Figure 7.7. Observed stage (meter) during the data collection process

The rating curve Equation (6.9) is used to estimate the discharge estimation with a given stage and constant parameters identified by multiple regression analysis. Figure 7.8 shows the estimated flow discharge in the gauging stations from the observed stage. In this study the peak discharge was captured. This implies that the stage reading observation helps to catch-up the maximum discharge in the gauging station. The peak flow records were used to design hydraulic structures in the subbasin.

During the stage reading observation the stage with zero-level is also existing. The stage with zero-level were excluded from the data and stage vs. estimated discharge was plotted as shown in Figure 7.9 (a and b) using coefficient of determination of power and exponential trends in Excel. Around 1877 observations were considered at this stage.

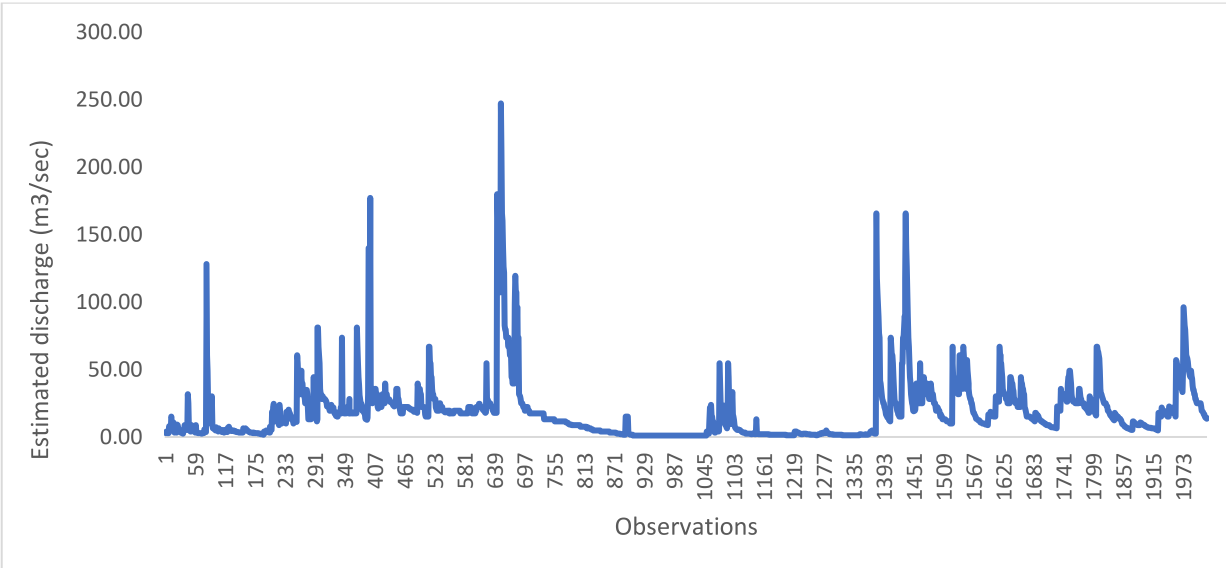

Figure 7.8. Estimated (m3/Sec) from observed stage reading using rating curve

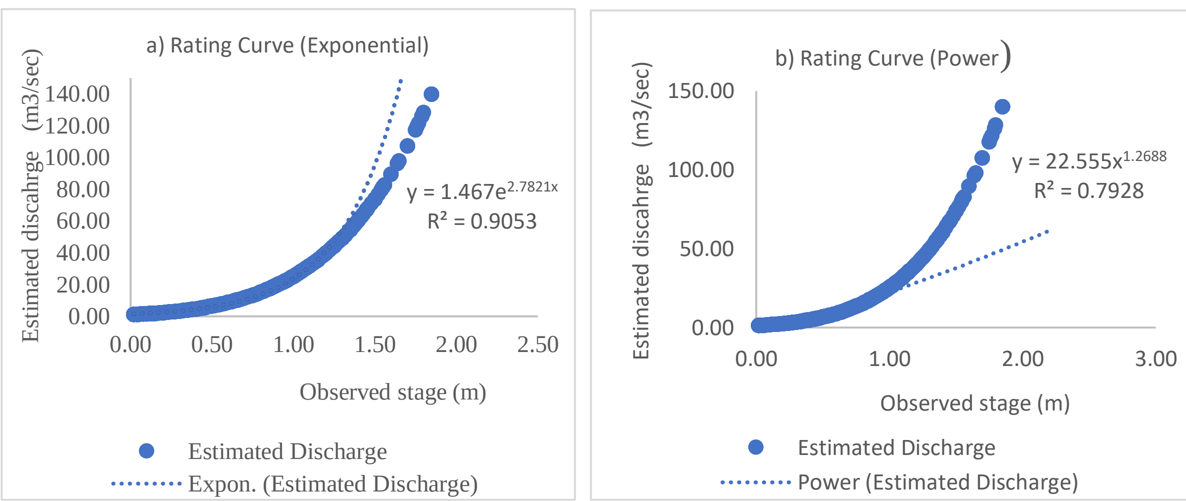

Figure 7.9. Stage-estimated discharge (Qs-h) relationship under a) Exponential trendlines, b) Power trendlines for gauging station

The result indicates that the coefficient of determination was ($R^2 = 0.9044$) for exponential and ($R^2 = 0.7928$) for power function which indicates that the exponential curve best fits the data. This indicates the developed rating curve was accurately used for estimating discharge in the study area.

7.4. Conclusions

The estimation of flow discharge in the upper Erer subbasin were performed using on site records of the stage and discharge and developing stage-discharge relation (rating curve). The streamflow data was calculated based on general rating curve Equation using the observed flow stage data and validated parameters. The rating curve Equation relating discharge Q in m3/s and stage H in meter was developed for upper Erer River at Erer-Jijiga Bridge of hydrometric station. This Equation can be used for the transformation of available stage in to discharge. Regression analysis of the observed flood data indicate good relationship with the simulated values. By solving the simultaneous Equations, the value of the constant c, a and n were obtained. In this study and for other studies in the upper Erer subbasin, this gauging station serves as a permanent control structure which makes the developed curve reliable until there is a change in this control.

In this research the estimated flow discharge can improve the unavailability of streamflow and will allow the local and regional water sector administrator used this discharge data in upper Erer river subbasin for any hydraulic structures. The estimated flow discharge in this research showed its potential for applicability of rating curve for stream flow estimation in the study area and other regions. The stage reading data are not frequent and continuous stage reading is required to improve model performance for estimation of flow discharge in the region. Future studies may also include additional information such as sediment transport modeling and geomorphologic characteristics in addition to streamflow to well determine the application of the developed model of rating curve of the river basin. The local water sector may develop water resource planning and river development works are important in the upper Erer River Basin for efficient use of limited water resources in the region.

8. CONCLUSIONS AND RECOMMENDATION FOR FURTHER RESEARCH

8.1. Conclusions

The water supply source sustainability of the town was investigated under various circumstances. In this study emphasis was given to the assessment of water supply sources sustainability, quantifying the factors affecting the water supply sources sustainability and the assessment of inadequacies of hydrometric and rain gauge stations distribution and data such as observed rainfall and stream flow data. To attain the objectives of this study various activities are conducted: a) assess the water supply sources sustainability by employing AHP approaches using the integrated multi criteria and evaluation criteria under alternative scenarios, b) to quantify the external driving factors that affects the accessibility of water resources such as climate change and LULC change impacts were evaluated by employing SWAT model, the LULC change anlysis for the past 20 years and climate change impacts analysis for the future (2024-2070) were examined, c) the spatiotemporal rainfall distribution on the rain gauge stations were evaluated using the new approach of joint probability methods that consider both the rain days and their mutual occurrences, d) the stream flow gap in the study area was filled by on site measurements of stream flow data by employing rating curve. The findings of the study work attained to the following key conclusions stated by point by point.

- The water supply sources sustainability result indicates that the most influential evaluation criteria that affect the water resources are capital cost, political availability, seasonality of the sources, and performance of the sources and policy.
- Using the most influential evaluation criteria as key indicators to analyses the alternative scenarios among the three alternative water sources the best alternative is advanced potable water supply sources scenario, followed by potable water supply and the least preference is business as usual scenario.
- This research evaluated the last 20-years (2001-2020) LULC change and their impacts on the water resources. The result indicates the main change were increase of agricultural lands and shrub lands and decrease of forest lands.

- The hydraulic responses were affected by the LULC change and the surface runoff, ground water flow, and water yields were increased. An increase in shrub lands and decrease of forest lands consequences to increase in surface runoff and decrease in evapotranspiration.
- The climate variables projections and their effects from historical period (1979-2014) to future period (2024-2070) were evaluated under RCP-4.5 and RCP-8.5. The result indicates that the mean monthly temperature is expected to be increasing under both scenarios of RCP-4.5 and RCP-8.5. While the mean monthly rainfall will be variable under RCP-4.5 and RCP-8.5.
- The SWAT model output shows the annual hydrological responses will decrease in both scenarios except the potential evapotranspiration. But the monthly hydrological responses indicates that the hydrological response is variable.
- The spatiotemporal rainfall distribution implication on areal rainfall estimation characteristics in the study area (Upper Erer subbasin) were evaluated. The correlation on two adjoining stations depends on the relative distance and topography.
- The joint probability rain for monthly time series indicates that high performance to examine the rainfall distribution among the stations.
- The subbasin areal rainfall characteristics do not define well by only straight averaging of areal rainfall estimation using identified method, unless and otherwise the probability of joint rainy days is determined.
- Estimation of discharge using onsite measurements of stream flow data by employing rating curve indicates that the model was potentially applicable in the study area.
- The estimated flow discharge serves the water sector community to fill the data gap on the stream flow measurements in the study area.
- The re-installed staff gauge is used as a reliable permanent control point for developing the rating curve unless there is a shift in this control.
- In the region the main alternative sources identified was the water harvesting that need the integrated water management strategies. Hence, urbanization either small scale as well as high scale industries in the watershed that affect the ecosystem were not recommended to be developed.

8.2. Recommendation for Further Research

The investigation of water supply sources sustainability requires additional indicators and experts' preferences. The prediction of the external driving factors that affects the water resources not only restricted to LULC change and climate change. The hydrological model used to quantify the impacts of the driving forces requires accurate rainfall and stream flow data that affects the uncertainty of the simulation. Mostly the gauging station distribution and stream flow data are inadequate that require further study.

- In this research a limited criteria weights and restricted experts' involvements suggests future studies accommodate additional indicators and a greater number of experts for getting improved result.
- To well understand the qualitative benefits of sustainability analysis further identification of water supply sources is highly important.
- The adaptation measures specially at the upstream of the watershed is important and awareness creation for communities within the watershed be recommended. The river periphery surrounding activities will be minimized. In the future water resource management policies that govern stakeholders will be developed by the involvement of all stakeholders.
- The water balance components from the SWAT model output suggests that they are decreasing under both scenarios. Hence, the watershed conservation lows implementation may promote the usage of the water resources in the region and sustainable water resource will be achieved.
- In this study the observed stream flow data and meteorological data used for model simulation were affect the calibration and validation process. Hence, future research may use refined hydrometric data to achieve best model performance.
- To fix the model uncertainties five RCMs from different GCMs datasets were used in the study. Future studies may use a greater number of RCMs from diversified GCMs for improved climate projection with minimal uncertainties.

- Although, at this stage the water resources sustainability in holistic approaches were assessed in the upper Erer subbasin. The adaptation strategies and watershed management are missing and future research uses the implementation of adaptation strategies and watershed management.
- The assessment of hydrological process effects under changing and climate and LULC demonstrates a significant change in hydrological response in the upper Erer subbasin. In this study hydrological response analysis has not considered the sediment yield analysis that is possibly affected. Hence, it should be assessed in future research.
- The joint probability approaches for estimation areal rainfall distribution characteristics in the upper Erer subbasin successfully performed with a scattered and a few numbers of stations. But future studies should be conducted with dense and greater numbers of stations under different regions.
- The rainfall distribution was affected by topography and distance of the gauging stations in the upper Erer subbasin. So, further study may be conducted in other regions to evaluate the present method was affected by the topographic and location of gauging sites.
- In this study the stage recording per day are more than usual methods. Still continuous long term measurement data are required. Therefore, future studies may adapt the continuous stage reading to develop updated stage-discharge rating curve in the region.
- Even though the climate and LULC change impacts on hydrological response was evaluated under the hydrological model. But the future study requires continuous stream flow for model calibration and validation. In this study the prediction was performed on few years (6 years for calibration and 4 years for validation) due to shortage of stream records in the region. Hence, more years of stream records is vital for appropriate model simulation output that represent the actual status of the subbasin. Also, continuous stage reading is recommended in the re-installed staff gauge in the upper Erer river subbasin.
- The estimated discharge using the rating curve suggested in this study showed its potential for applicability to analyze water resources assessment in the region.
- The estimated water supply sources generated from SWAT output is much less than the estimated demand for the end of the design period (2070) (Appendix 25). So, additional water sources would be investigated in the future, as the population increase in the town is

dramatic due to the emergence of new urban areas which are currently rural and inclusion of the population just outside the periphery of the existing towns into the urban limits.

- If water supply development work is implanted in the upper Erer river, the surface water flow in the upper Erer river is expected to satisfy the population increase up to the next 20 to 25 years for Harar town. But appropriate water resources management will be implemented and finding additional water resources in the near vicinity of the town is important in the future to satisfy the demand of the whole 50 years design period.

REFERENCES

Abate, M., Nyssen, J., Moges, M. M., Enku, T., Zimale, F. A., Tilahun, S. A., ... & Steenhuis, T. S. (2017). Long-term landscape changes in the Lake Tana Basin as evidenced by delta development and floodplain aggradation in Ethiopia. *Land Degradation & Development*, *28*(6), 1820-1830.

Abbaspour, K. C. (2015). SWAT calibration and uncertainty programs. *A user manual*, *103*, 17-66.

Abbaspour, K. C., Rouholahnejad, E., Vaghefi, S. R. I. N. I. V. A. S. A. N. B., Srinivasan, R., Yang, H., & Kløve, B. (2015). A continental-scale hydrology and water quality model for Europe: Calibration and uncertainty of a high-resolution large-scale SWAT model. *Journal of hydrology*, *524*, 733-752.

Abbaspour, K. C., Vaghefi, S. A., & Srinivasan, R. (2017). A guideline for successful calibration and uncertainty analysis for soil and water assessment: a review of papers from the 2016 international SWAT conference. *Water*, *10*(1), 6.

Abbaspour, K. C., Vejdani, M., Haghighat, S., & Yang, J. (2007, December). SWAT-CUP calibration and uncertainty programs for SWAT. In *MODSIM 2007 international congress on modelling and simulation, modelling and simulation society of Australia and New Zealand* (pp. 1596-1602). Dübendorf, Switzerland: Swiss Federal Institute of Aquatic Science and Technology.

Abbaspour, K. C., Yang, J., Maximov, I., Siber, R., Bogner, K., Mieleitner, J., ... & Srinivasan, R. (2007). Modelling hydrology and water quality in the pre-alpine/alpine Thur watershed using SWAT. *Journal of hydrology*, *333*(2-4), 413-430.

Abdulahi, S. D., Abate, B., Harka, A. E., & Husen, S. B. (2022). Response of climate change impact on streamflow: the case of the Upper Awash sub-basin, Ethiopia. *Journal of Water and Climate Change*, *13*(2), 607-628.

Abebe, G. (2017). Long-term climate data description in Ethiopia. *Data in brief*, *14*, 371-392.

Abed, M. H., Monavari, M., Karbasi, A., Farshchi, P., & Abedi, Z. (2011, July). Site selection using Analytical Hierarchy Process by geographical information system for sustainable coastal tourism. In Proceedings International Conference Environmental and Agriculture Engineering, Chengdu, China (Vol. 15, pp. 120-124).

Abrishamchi, A., Ebrahimian, A., Tajrishi, M., & Mariño, M. A. (2005). Case study: application of multicriteria decision making to urban water supply. *Journal of water resources planning and management*, *131*(4), 326-335.

Addis, H. K., Strohmeier, S., Ziadat, F., Melaku, N. D., & Klik, A. (2016). Modeling streamflow and sediment using SWAT in Ethiopian Highlands. *International Journal of Agricultural and Biological Engineering*, *9*(5), 51-66.

Adegbola, A. A and Olaniyan, O.S. (2012). Temporal Variation of Sediment Transport in River-Omi, South Western Nigeria. International Journal of Applied Engineering Research, 4(7), pp. 421-431.

Aldabagh, A. S., Rasheed, H., & Ramamoorthy, M. V. (1982). Dry days analysis for planning supplemental irrigation schemes. *Transactions of the ASAE*, *25*(1), 150-0153.

Alegre, H., Baptista, J. M., Cabrera Jr, E., Cubillo, F., Duarte, P., Hirner, W., ... & Parena, R. (2016). Performance indicators for water supply services. IWA publishing.

Alemu, Z. A., & Dioha, M. O. (2020). Modelling scenarios for sustainable water supply and demand in Addis Ababa city, Ethiopia. Environmental Systems Research, 9, 1-14.

Alfa, M. I., Adie, D. B., Ajibike, M. A., & Mudiare, O. J. (2018). Development of rating curve for Ofu River at Oforachi hydrometric station. *Nigerian Journal of Technological Development*, *15*(1), 14-19.

Al-Houri, Z. (2014). Detecting variability and trends in daily rainfall characteristics in Amman-Zarqa basin, Jordan. *International Journal of Applied*, *4*(6).

Al-Ozeer, A., Abdaki, M. A., Al-Iraqi, A., Al-Samman, S., & Al-Hammadi, N. (2020). Estimation of mean areal rainfall and missing data by using gis in nineveh, Northern Iraq. *The Iraqi Geological Journal*, 93-103.

Al-Timimi, Y. K., Al-Lami, A. M., & Al-Shamarti, H. K. (2020). Calculation of the mean annual rainfall in Iraq using several methods in GIS. *Plant Archives*, *20*(2), 1156-1160.

Anders, A. M., Roe, G. H., Hallet, B., Montgomery, D. R., Finnegan, N. J., & Putkonen, J. (2006). Spatial patterns of precipitation and topography in the Himalaya.

Anderson, J. R. (1976). *A land use and land cover classification system for use with remote sensor data* (Vol. 964). US Government Printing Office.

Andrade, C. W., Montenegro, S. M., Montenegro, A. A., Lima, J. R. D. S., Srinivasan, R., & Jones, C. A. (2021). Climate change impact assessment on water resources under RCP scenarios: A case study in Mundaú River Basin, Northeastern Brazil. *International Journal of Climatology*, *41*, E1045-E1061.

Ankita, D. P., & Kazuo, N. (2014). Modeling hydrological response to land use change in watersheds of viti levu island, FIJI. *Journal of Environmental Research and Development*, *8*(3), 492.

Anose, F. A., Beketie, K. T., Zeleke, T. T., Ayal, D. Y., & Feyisa, G. L. (2021). Spatio-temporal hydro-climate variability in Omo-Gibe River Basin, Ethiopia. *Climate Services*, *24*, 100277.

Aragaw, H. M., Goel, M. K., & Mishra, S. K. (2021). Hydrological responses to human-induced land use/land cover changes in the Gidabo River basin, Ethiopia. *Hydrological Sciences Journal*, *66*(4), 640-655.

Aredo, M. R., Hatiye, S. D., & Pingale, S. M. (2021). Impact of land use/land cover change on stream flow in the Shaya catchment of Ethiopia using the MIKE SHE model. *Arabian Journal of Geosciences*, *14*(2), 114.

Arnold, J. G., & Allen, P. M. (1999). Automated methods for estimating baseflow and ground water recharge from streamflow records 1. *JAWRA Journal of the American Water Resources Association*, *35*(2), 411-424.

Arnold, J. G., Kiniry, J. R., Srinivasan, R., Williams, J. R., Haney, E. B., & Neitsch, S. L. (2011). *Soil and water assessment tool input/output file documentation version 2009*. Texas Water Resources Institute.

Arnold, J. G., Moriasi, D. N., Gassman, P. W., Abbaspour, K. C., White, M. J., Srinivasan, R., ... & Jha, M. K. (2012). SWAT: Model use, calibration, and validation. *Transactions of the ASABE*, *55*(4), 1491-1508.

Arnold, J. G., Srinivasan, R., Muttiah, R. S., & Williams, J. R. (1998). Large area hydrologic modeling and assessment part I: model development 1. *JAWRA Journal of the American Water Resources Association*, *34*(1), 73-89.

Asgeir, P. O. (2006). Modelling of stage-discharge relationships affected by hysteresis using jones formula and nonlinear regression. *Hydrological Sciences-Journal des Sciences Hydrologiques*, *51*(3), 365-388.

Ashofteh, P. S., Haddad, O. B., & A. Mariño, M. (2013). Climate change impact on reservoir performance indexes in agricultural water supply. *Journal of Irrigation and Drainage Engineering*, *139*(2), 85-97.

Ashraf Vaghefi, S., Abbaspour, K. C., Faramarzi, M., Srinivasan, R., & Arnold, J. G. (2017). Modeling crop water productivity using a coupled SWAT–MODSIM model. *Water*, *9*(3), 157.

Assfaw, A. T. (2019). Calibration, validation and performance evaluation of SWAT model for sediment yield modelling in Megech reservoir catchment, Ethiopia. *Journal of Environmental Geography*, *12*(3-4), 21-31.

Atlas of Our Changing Environment (2008). Lake Haramaya, Ethiopia.

Awal, R., Fares, A., & Bayabil, H. (2018). Assessing potential climate change impacts on irrigation requirements of major crops in the brazos headwaters Basin, Texas. Water, 10(11), 1–15. https://doi.org/10.3390/w10111610.

Ayehu, G. T., Tadesse, T., & Gessesse, B. (2021). Spatial and temporal trends and variability of rainfall using long-term satellite product over the Upper Blue Nile Basin in Ethiopia. *Remote Sensing in Earth Systems Sciences*, *4*, 199-215.

Ayele, H. A., Aga, A. O., Belayneh, L., & Wanjala, T. W. (2023). Hydrological Responses to Land Use/Land Cover Changes in Koga Watershed, Upper Blue Nile, Ethiopia. *Geographies*, *3*(1), 60-81.

Ayoade, J. (1983). Introduction to Climatology for the Tropics. Wiley, Hoboken, 258 p.

Ayugi, B., Ngoma, H., Babaousmail, H., Karim, R., Iyakaremye, V., Sian, K. T. L. K., & Ongoma, V. (2021). Evaluation and projection of mean surface temperature using CMIP6 models over East Africa. *Journal of African Earth Sciences*, *181*, 104226.

Azadi, F., Ashofteh, P. S., & Chu, X. (2021). Evaluation of the effects of climate change on thermal stratification of reservoirs. *Sustainable Cities and Society*, *66*, 102531.

Baker, T. J., & Miller, S. N. (2013). Using the Soil and Water Assessment Tool (SWAT) to assess land use impact on water resources in an East African watershed. *Journal of hydrology*, *486*, 100-111.

Balascio, C. C., Palmeri, D. J., & Gao, H. (1998). Use of a genetic algorithm and multi-objective programming for calibration of a hydrologic model. *Transactions of the ASAE*, *41*(3), 615-619.

Balyani, H. H., Sohani, A., Sayyaadi, H., & Karami, R. (2015). Acquiring the best cooling strategy based on thermal comfort and 3E analyses for small scale residential buildings at diverse climatic conditions. International Journal of Refrigeration, 57, 112-137.

Barbetta, S., Moramarco, T., & Perumal, M. (2017). A Muskingum-based methodology for river discharge estimation and rating curve development under significant lateral inflow conditions. *Journal of Hydrology*, *554*, 216-232.

Bates, B., Kundzewicz, Z., & Wu, S. (2008). *Climate change and water*. Intergovernmental Panel on Climate Change Secretariat.

Bayraktar, H., Turalioglu, F. S., & Şen, Z. (2005). The estimation of average areal rainfall by percentage weighting polygon method in Southeastern Anatolia Region, Turkey. *Atmospheric research*, *73*(1-2), 149-160.

Bekele-Biratu, E., Thiaw, W. M., & Korecha, D. (2018). Sub-seasonal variability of the Belg rains in Ethiopia. *International Journal of Climatology*, *38*(7), 2940-2953.

Belay, A. S., Fenta, A. A., Yenehun, A., Nigate, F., Tilahun, S. A., Moges, M. M., ... & Walraevens, K. (2019). Evaluation and application of multi-source satellite rainfall product CHIRPS to assess spatio-temporal rainfall variability on data-sparse western margins of Ethiopian highlands. *Remote Sensing*, *11*(22), 2688.

Belihu, M., Tekleab, S., Abate, B., & Bewket, W. (2020). Hydrologic response to land use land cover change in the Upper Gidabo Watershed, Rift Valley Lakes Basin, Ethiopia. *HydroResearch*, *3*, 85-94.

Bell, V. A., & Moore, R. J. (2000). The sensitivity of catchment runoff models to rainfall data at different spatial scales. *Hydrology and Earth System Sciences*, *4*(4), 653-667.

Berihun, M. L., Tsunekawa, A., Haregeweyn, N., Meshesha, D. T., Adgo, E., Tsubo, M., ... & Ebabu, K. (2019). Hydrological responses to land use/land cover change and climate variability in contrasting agro-ecological environments of the Upper Blue Nile basin, Ethiopia. *Science of the Total Environment*, *689*, 347-365.

Bessah, E., Raji, A. O., Taiwo, O. J., Agodzo, S. K., Ololade, O. O., & Strapasson, A. (2020). Hydrological responses to climate and land use changes: The paradox of regional and local climate effect in the Pra River Basin of Ghana. *Journal of Hydrology: Regional Studies*, *27*, 100654.

Bewket, W., & Conway, D. (2007). A note on the temporal and spatial variability of rainfall in the drought-prone Amhara region of Ethiopia. *International Journal of Climatology: A Journal of the Royal Meteorological Society*, *27*(11), 1467-1477.

Boukhari, S., Djebbar, Y., Amarchi, H., & Sohani, A. (2018). Application of the analytic hierarchy process to sustainability of water supply and sanitation services: the case of Algeria. Water Science and Technology: Water Supply, 18(4), 1282-1293.

Braca, G. (2008). *Stage-discharge relationships in open channels: Practices and problems*. London, UK: Univ. degli Studi di Trento, Dipartimento di Ingegneria Civile e Ambientale.

Buytaert, W., Celleri, R., Willems, P., De Bievre, B., & Wyseure, G. (2006). Spatial and temporal rainfall variability in mountainous areas: A case study from the south Ecuadorian Andes. *Journal of hydrology*, *329*(3-4), 413-421.

Canadell, J. G., Monteiro, P. M., Costa, M. H., Cotrim da Cunha, L., Cox, P. M., Eliseev, A. V., ... & Zickfeld, K. (2023). Intergovernmental Panel on Climate Change (IPCC, 2023). Global carbon and other biogeochemical cycles and feedback. In *Climate change 2021: The physical science basis. Contribution of working group I to the sixth assessment report of the intergovernmental panel on climate change* (pp. 673-816). Cambridge University Press.

Chemura, A., Rwasoka, D., Mutanga, O., Dube, T., & Mushore, T. (2020). The impact of land-use/land cover changes on water balance of the heterogeneous Buzi sub-catchment, Zimbabwe. *Remote Sensing Applications: Society and Environment*, *18*, 100292.

Chen, Y., Marek, G. W., Marek, T. H., Porter, D. O., Moorhead, J. E., Wang, Q., ... & Brauer, D. K. (2020). Spatio-Temporal Analysis of Historical and Future Climate Data in the Texas High Plains. *Sustainability*, *12*(15), 6036.

Cheng, C. S., Li, Q., Li, G., & Auld, H. (2012). Climate change and heavy rainfall-related water damage insurance claims and losses in Ontario, Canada. *Journal of Water Resource and Protection*, *4*(2), 49-62.

Cherie, G. G., & Fentaw, A. (2015). Climate change impact assessment of dire dam water supply. *AAUCED HES, Ethiopia*.

Cheung, W. H., Senay, G. B., & Singh, A. (2008). Trends and spatial distribution of annual and seasonal rainfall in Ethiopia. *International Journal of Climatology: A Journal of the Royal Meteorological Society*, *28*(13), 1723-1734.

Chiew, F. H. S., & Vaze, J. (2015). Hydrologic non-stationarity and extrapolating models to predict the future: Overview of session and proceeding. *Proceedings of the International Association of Hydrological Sciences*, *371*(371), 17-21.

Cho, W., Lee, J., Park, J., & Kim, D. (2017). Radar polygon method: an areal rainfall estimation based on radar rainfall imageries. *Stochastic Environmental Research and Risk Assessment*, *31*, 275-289.

Cook, K. H., & Vizy, E. K. (2013). Projected changes in East African rainy seasons. *Journal of Climate*, *26*(16), 5931-5948.

CSA (1991). The 1984 Population and Housing Census of Ethiopia: Analytical Report at National Level.

CSA, 1994. The 1994 Population and housing Census of Ethiopia results for Harar town administration, Volume I- Statistical report, Ethiopia.

CSA, 2007. The 2007 Population and Housing Census of Ethiopia: Statistical Report for Harar town Administration, third Population and Housing Census, Ethiopia.

CSA, 2012. Inter-Censal Population Survey [ICPS], Population Projections for Ethiopia 2007-2037.

Daba, M. H. (2010). Sensitivity of SWAT Simulated Runoff to Temperature and Rainfall in the Upper Awash Sab-Basin, Ethiopia. Hydrol Current Res 9: 293. doi: 10.4172/2157-7587.1000293 Page 2 of 7 Volume 9• Issue 1• 1000293 Hydrol Current Res, an open access journal ISSN: 2157-7587 The daily weather data required to run the SWAT hydrological model were acquired from the National Meteorology Agency (NMA). The daily data for maximum and minimum temperature, rainfall, relative humidity, and wind speed were obtained (Doctoral dissertation, these data cover a period of 30 years from 1980 to).

Daba, M. H., & You, S. (2020). Assessment of climate change impacts on river flow regimes in the upstream of Awash, Basin, Ethiopia: based on IPCC fifth assessment report (AR5) climate change scenarios. *Hydrology*, *7*(4), 98.

Dariane, A. B., & Pouryafar, E. (2021). Quantifying and projection of the relative impacts of climate change and direct human activities on streamflow fluctuations. *Climatic Change*, *165*(1), 34.

De Carvalho, J. W. L. T., Iensen, I. R. R., & dos Santos, I. (2021). Resilience of hydrologic similarity areas to extreme climate change scenarios in an urban watershed. *Urban Water Journal*, *18*(10), 817-828.

De Oliveira Serrao, E. A., Silva, M. T., Ferreira, T. R., de Ataide, L. C. P., dos Santos, C. A., de Lima, A. M. M., ... & Gomes, D. J. C. (2022). Impacts of land use and land cover changes on hydrological processes and sediment yield determined using the SWAT model. *International Journal of Sediment Research*, *37*(1), 54-69.

Demissie, T. A., & Sime, C. H. (2021). Assessment of the performance of CORDEX regional climate models in simulating rainfall and air temperature over southwest Ethiopia. *Heliyon*, *7*(8).

Desta, H., & Lemma, B. (2017). SWAT based hydrological assessment and characterization of Lake Ziway sub-watersheds, Ethiopia. *Journal of Hydrology: Regional Studies*, *13*, 122-137.

Di Baldassarre, G., & Claps, P. (2011). A hydraulic study on the applicability of flood rating curves. *Hydrology Research*, *42*(1), 10-19.

Dibaba, W. T., Demissie, T. A., & Miegel, K. (2020). Watershed hydrological response to combined land use/land cover and climate change in highland Ethiopia: Finchaa catchment. Water, 12(6), 1801.

Dibaba, W. T., Miegel, K., & Demissie, T. A. (2019). Evaluation of the CORDEX regional climate models performance in simulating climate conditions of two catchments in Upper Blue Nile Basin. *Dynamics of Atmospheres and Oceans*, *87*, 101104.

Dile, Y. T., & Srinivasan, R. (2014). Evaluation of CFSR climate data for hydrologic prediction in data‐scarce watersheds: an application in the Blue Nile River Basin. *JAWRA Journal of the American Water Resources Association*, *50*(5), 1226-1241.

Dile, Y. T., Berndtsson, R., & Setegn, S. G. (2013). Hydrological response to climate change for gilgel abay river, in the lake tana basin-upper Blue Nile basin of Ethiopia. *PloS one*, *8*(10), e79296.

Ding, Y., Feng, H., & Zou, B. (2022). Remote Sensing-Based Estimation on Hydrological Response to Land Use and Cover Change. *Forests*, *13*(11), 1749.

Dioha, M. O., & Kumar, A. (2020). Exploring greenhouse gas mitigation strategies for agriculture in Africa: The case of Nigeria. *Ambio*, *49*(9), 1549-1566.

Domene, E., & Saurí, D. (2006). Urbanisation and water consumption: Influencing factors in the metropolitan region of Barcelona. Urban studies, 43(9), 1605-1623.

Eggimann, S., Mutzner, L., Wani, O., Schneider, M. Y., Spuhler, D., Moy de Vitry, M., ... & Maurer, M. (2017). The potential of knowing more: A review of data-driven urban water management. Environmental science & technology, 51(5), 2538-2553.

Egigu, M. (2020). Techniques of filling missing values of daily and monthly rain fall data: a review. *SF J. Environ. Earth Sci*, *3*(1).

Endris, H. S., Lennard, C., Hewitson, B., Dosio, A., Nikulin, G., & Panitz, H. J. (2016). Teleconnection responses in multi-GCM driven CORDEX RCMs over Eastern Africa. *Climate Dynamics*, *46*, 2821-2846.

Eruola A. O., Ufoegbune G. C., Awomeso J. A., and Abhulimen, S. A (2015). Determination of areal rainfall using estimation methods in a tropical wet and dry climate: Merit Research Journal of Environmental Science and Toxicology (ISSN: 2350-2266), Vol. 3(7), pp. 079-082.

Eshetu, G., Johansson, T., & Garedew, W. (2016). Rainfall trend and variability analysis in Setema-Gatira area of Jimma, Southwestern Ethiopia. *African Journal of Agricultural Research*, *11*(32), 3037-3045.

Faramarzi, M., Abbaspour, K. C., Vaghefi, S. A., Farzaneh, M. R., Zehnder, A. J., Srinivasan, R., & Yang, H. (2013). Modeling impacts of climate change on freshwater availability in Africa. *Journal of Hydrology*, *480*, 85-101.

Faramarzi, M., Srinivasan, R., Iravani, M., Bladon, K. D., Abbaspour, K. C., Zehnder, A. J., & Goss, G. G. (2015). Setting up a hydrological model of Alberta: Data discrimination analyses prior to calibration. *Environmental Modelling & Software*, *74*, 48-65.

Faures, J. M., Goodrich, D. C., Woolhiser, D. A., & Sorooshian, S. (1995). Impact of small-scale spatial rainfall variability on runoff modeling. *Journal of hydrology*, *173*(1-4), 309-326.

Ficklin, D. L., Luo, Y., Luedeling, E., & Zhang, M. (2009). Climate change sensitivity assessment of a highly agricultural watershed using SWAT. *Journal of hydrology*, *374*(1-2), 16-29.

Franchini, M., & Ravagnani, F. (2007). Costruzione della scala di deflusso in una sezione con sole misure di livello utilizzando le portate registrate a monte ed un modello diffusivo-convettivo. *L'acqua*, *5*, 9-19.

Frederick, K. D., Major, D. C., & Stakhiv, E. Z. (Eds.). (2013). *Climate change and water resources planning criteria*. Springer Science & Business Media.

Fuka, D. R., Walter, M. T., MacAlister, C., Degaetano, A. T., Steenhuis, T. S., & Easton, Z. M. (2014). Using the Climate Forecast System Reanalysis as weather input data for watershed models. *Hydrological Processes*, *28*(22), 5613-5623.

Gadissa, T., Nyadawa, M., Behulu, F., & Mutua, B. (2018). The effect of climate change on loss of lake volume: case of sedimentation in central rift valley basin, Ethiopia. Hydrology, 5(4), 67.

Galata, A. W., Demissei, T. A., & Leta, M. K. (2020). Watershed hydrological responses to changes in land use and land cover at Hangar Watershed, Ethiopia. *Iranica Journal of Energy & Environment*, *11*(1), 1-7.

Gan, T. Y., Dlamini, E. M., & Biftu, G. F. (1997). Effects of model complexity and structure, data quality, and objective functions on hydrologic modeling. *Journal of hydrology*, *192*(1-4), 81-103.

Gebere, S. B., Alamirew, T., Merkel, B. J., & Melesse, A. M. (2015). Performance of high-resolution satellite rainfall products over data scarce parts of Eastern Ethiopia. *Remote Sensing*, *7*(9), 11639-11663.

Gebre, S. L., Getahun, D., Fufa, F., Diriba, O. H., & Alemayehu, E. (2022). Hydrological responses of land use land cover change on the Hangar catchment, Blue Nile Basin. *Ethiopian Journal of Applied Science and Technology*, *13*(1), 33-44.

Gebremicael, T. G., Mohamed, Y. A., & Van der Zaag, P. (2019). Attributing the hydrological impact of different land use types and their long-term dynamics through combining parsimonious hydrological modelling, alteration analysis and PLSR analysis. *Science of the Total Environment*, *660*, 1155-1167.

Gelaro, R., McCarty, W., Suárez, M. J., Todling, R., Molod, A., Takacs, L., ... & Zhao, B. (2017). The modern-era retrospective analysis for research and applications, version 2 (MERRA-2). *Journal of climate*, *30*(14), 5419-5454.

Geleta, T. D., Dadi, D. K., Funk, C., Garedew, W., Eyelade, D., & Worku, A. (2022). Downscaled climate change projections in urban centers of Southwest Ethiopia using CORDEX Africa simulations. *Climate*, *10*(10), 158.

Getachew, H. E., & Melesse, A. M. (2012). The impact of land use change on the hydrology of the Angereb Watershed, Ethiopia. *International Journal of Water Sciences*, *1*(6).

Getu Engida, T., Nigussie, T. A., Aneseyee, A. B., & Barnabas, J. (2021). Land use/land cover change impact on hydrological process in the Upper Baro Basin, Ethiopia. *Applied and Environmental Soil Science*, *2021*, 1-15.

Ghimire, B. N., & Reddy, M. J. (2010, May). Development of stage-discharge rating curve in river using genetic algorithms and model tree. In *International workshop advanced in statistical hydrology, Italy*.

Giorgi, F., Jones, C., & Asrar, G. R. (2009). Addressing climate information needs at the regional level: the CORDEX framework. *World Meteorological Organization (WMO) Bulletin*, *58*(3), 175.

Girma, M., Tesfaye, K., Getnet, M., Tana, T., Jaletab, M., & Lakew, B. (2019). Rainfall variability and its implications for wheat and barley production in central Ethiopia. *Ethiopian Journal of Crop Science*, *7*(2), 89-111.Gummadi, S., Rao, K. P. C., Seid, J., Legesse, G., Kadiyala, M. D. M., Takele, R., ... & Whitbread, A. 2018. Spatio-temporal variability and trends of precipitation and extreme rainfall events in Ethiopia in 1980–2010. *Theoretical and Applied Climatology*, *134*, 1315-1328.

Golfam, P., & Ashofteh, P. S. (2022). Performance indexes analysis of the reservoir-hydropower plant system affected by climate change. *Water Resources Management*, *36*(13), 5127-5162.

Golfam, P., Ashofteh, P. S., & Loáiciga, H. A. (2021). Modeling adaptation policies to increase the synergies of the water-climate-agriculture nexus under climate change. *Environmental Development*, *37*, 100612.

Gore, J. A., & Banning, J. (2017). Discharge measurements and streamflow analysis. In *Methods in Stream Ecology, Volume 1* (pp. 49-70). Academic Press.

Graham, L. P., Andréasson, J., & Carlsson, B. (2007). Assessing climate change impacts on hydrology from an ensemble of regional climate models, model scales and linking methods–a case study on the Lule River basin. *Climatic Change*, *81*(Suppl 1), 293-307.

Gregrio, A., & Jansen, J. (2000). Land cover classification system (LCCS); Classification concepts and user manual for software version 2.

Guerrero, J. L., Westerberg, I. K., Halldin, S., Xu, C. Y., & Lundin, L. C. (2012). Temporal variability in stage–discharge relationships. *Journal of Hydrology*, *446*, 90-102.

Gummadi, S., Rao, K. P. C., Seid, J., Legesse, G., Kadiyala, M. D. M., Takele, R., ... & Whitbread, A. (2018). Spatio-temporal variability and trends of precipitation and extreme rainfall events in Ethiopia in 1980–2010. *Theoretical and Applied Climatology*, *134*, 1315-1328.

Gutowski Jr, W. J., Giorgi, F., Timbal, B., Frigon, A., Jacob, D., Kang, H. S., ... & Tangang, F. (2016). WCRP coordinated regional downscaling experiment (CORDEX): a diagnostic MIP for CMIP6.

Gyamfi, C., Ndambuki, J. M., & Salim, R. W. (2016). Application of SWAT model to the Olifants Basin: calibration, validation and uncertainty analysis. *Journal of Water Resource and Protection*, *8*(03), 397.

Gyamfi, C., Ndambuki, J. M., & Salim, R. W. (2016). Hydrological responses to land use/cover changes in the Olifants Basin, South Africa. *Water*, *8*(12), 588.

Hafizi, H., & Sorman, A. A. (2022). Performance assessment of CHIRPSv2. 0 and MERRA-2 gridded precipitation datasets over complex topography of Turkey. *Environmental Sciences Proceedings*, *19*(1), 21.

Haile, A. T., Geremew, Y., Wassie, S., Fekadu, A. G., & Taye, M. T. (2023). Filling streamflow data gaps through the construction of rating curves in the Lake Tana sub-basin, Nile basin. *Journal of Water and Climate Change*, *14*(4), 1162-1175.

Hajkowicz, S. (2007). A comparison of multiple criteria analysis and unaided approaches to environmental decision making. Environmental Science & Policy, 10(3), 177-184.

Hajkowicz, S., & Collins, K. (2007). A review of multiple criteria analysis for water resource planning and management. *Water resources management*, *21*, 1553-1566.

Hamal, K., Sharma, S., Khadka, N., Baniya, B., Ali, M., Shrestha, M. S., ... & Dawadi, B. (2020). Evaluation of MERRA-2 precipitation products using gauge observation in Nepal. *Hydrology*, *7*(3), 40.

Hamilton, S., Watson, M., & Pike, R. (2019). The role of the hydrographer in rating curve development. *Confluence: Journal of Watershed Science and Management*, *3*(1).

Harar Water Supply and Sewerage Authority (HWSSA), (2014). Evaluation of Groundwater Resource Potential of Upper Errer Valley by Geo-Engineering Service.

Hayden, R. W. (2009). A Review of:"Common Errors in Statistics (and How to Avoid Them), by PI Good and JW Hardin" New York: Wiley, 2009, ISBN 978-0-470-45798-6, xiii+ 273 pp., $59.95.

Hendrik, R., Katrin, B., Raghavan, S., & Indrajeet Ch, J. G. (2016). Documentation for preparing simulated climate change data for hydrologic impact studies. *CMhyd User Manual*.

Henry, et al., (2019). A new multi-Criteria decision analysis methodology for the selection of new water supply infrastructure. Water, 11(4), 805.

Her, Y., Frankenberger, J., Chaubey, I., & Srinivasan, R. (2015). Threshold effects in HRU definition ofthe soil and water assessment tool. *Transactions of the ASABE*, *58*(2), 367-378.

Homdee, T., Pongput, K., & Kanae, S. (2011). Impacts of Land Cover Changes on Hydrologic Responses: A Case Study of Chi River Basin, Thailand. Annual Journal of Hydraulic Engineering, 55, 31-36

Huimin, Li, Xia, Wen, Q., Wang, S., L., & Lv, L. (2019). Identifying factors affecting the sustainability of water environment treatment public-private partnership projects. *Advances in civil Engineering*, *2019*.

Hurni, H., 1998. Agroecological belts of Ethiopia. *Explanatory notes on three maps at a scale of*, *1*(1,000,000).

IPCC, Intergovernmental Panel on Climate Change. Climate Change 2013: The Physical Science Basis. Contribution of Working Group I to the Fifth Assessment Report of the Intergovernmental Panel on Climate Change; Cambridge University Press.

Jaber, Jamal O., and Mousa S. Mohsen (2001). "Evaluation of non-conventional water resources supply in Jordan." Desalination 136.1-3: 83-92.

Jackson, I. J. (1977). *Climate, water and agriculture in the tropics*. New York (USA) Longman Scientific. Food and Agriculture Organization of the United

Jackson, I.J. Dependence of wet and dry days in the tropics. *Arch. Met. Geoph. Biocl., Ser. B* **29**, 167–179 (1981). https://doi.org/10.1007/BF02278199.

Kang, M. G., & Lee, G. M. (2011). Multicriteria Evaluation of Water Resources Sustainability in the Context of Watershed Management 1. JAWRA Journal of the American Water Resources Association, 47(4), 813-827.

Kassa, M. (2017). Evaluation of water supply and demand: the case of Shambu town, Western Oromia, Ethiopia. International Journal of Water Resources and Environmental Engineering, 9(5), 96-101.

Kassie, B. T., Rötter, R. P., Hengsdijk, H., Asseng, S., Van Ittersum, M. K., Kahiluoto, H., & Van Keulen, H. (2014). Climate variability and change in the Central Rift Valley of Ethiopia: challenges for rainfed crop production. *The Journal of Agricultural Science*, *152*(1), 58-74.

Kebede, A., Diekkrüger, B., & Moges, S. A. (2013). An assessment of temperature and precipitation change projections using a regional and a global climate model for the Baro-Akobo Basin, Nile Basin, Ethiopia. *J. Earth Sci. Clim. Change*, *4*, 133.

Kendall, M.G. and Gibbons, J.D. (1990) Rank Correlation Methods. Oxford University Press, New York

Kenea, U., Adeba, D., Regasa, M. S., & Nones, M. (2021). Hydrological responses to land use land cover changes in the Fincha'a Watershed, Ethiopia. *Land*, *10*(9), 916.

Kennedy, E. J. (1984). *Discharge ratings at gaging stations* (Vol. 3). US Government Printing Office.

Khan, S., Guan, Y., Khan, F., & Khan, Z. (2020). A comprehensive index for measuring water security in an urbanizing world: the case of Pakistan's capital. Water, 12(1), 166.

Kiang, J. E., Gazoorian, C., McMillan, H., Coxon, G., Le Coz, J., Westerberg, I. K., ... & Mason, R. (2018). A comparison of methods for streamflow uncertainty estimation. *Water Resources Research*, *54*(10), 7149-7176.

Kiker, G. A., Bridges, T. S., Varghese, A., Seager, T. P., & Linkov, I. (2005). Application of multicriteria decision analysis in environmental decision making. Integrated environmental assessment and management: An international journal, 1(2), 95-108.

Kim, J., Waliser, D. E., Mattmann, C. A., Goodale, C. E., Hart, A. F., Zimdars, P. A., ... & Favre, A. (2014). Evaluation of the CORDEX-Africa multi-RCM hindcast: systematic model errors. *Climate dynamics*, *42*, 1189-1202.

Koch, F. J., Van Griensven, A., Uhlenbrook, S., Tekleab, S., & Teferi, E. (2012). The Effects of land use change on hydrological responses in the choke mountain range (Ethiopia)-a new approach addressing land use dynamics in the model SWAT.

Koneti, S., Sunkara, S. L., & Roy, P. S. (2018). Hydrological modeling with respect to impact of land-use and land-cover change on the runoff dynamics in Godavari River Basin using the HEC-HMS model. *ISPRS International Journal of Geo-Information*, *7*(6), 206.

Kools, S., Van Loon, A., Sjerps, R., & Rosenthal, L. (2019). The quality of drinking water resources in the 592 Netherlands. Nieuwegein, the Netherlands.

Koycegiz, C., & Buyukyildiz, M. (2019). Calibration of SWAT and two data-driven models for a data-scarce mountainous headwater in semi-arid Konya closed basin. *Water*, *11*(1), 147.

Kuma, H. G., Feyessa, F. F., & Demissie, T. A. (2021). Hydrologic responses to climate and land-use/land-cover changes in the Bilate catchment, Southern Ethiopia. *Journal of Water and Climate Change*, *12*(8), 3750-3769.

Lade, O., Oloke, D., Chinyio, E., & Fullen, M. (2012). Use of multi-criteria decision analysis methods for water supply problems: A framework for improved rainwater harvesting. Journal of Environmental Science and Engineering. A, 1(7A), 909.

Lafon, T., Dadson, S., Buys, G., & Prudhomme, C. (2013). Bias correction of daily precipitation simulated by a regional climate model: a comparison of methods. *International journal of climatology*, *33*(6), 1367-1381.

Lai, E., Lundie, S., & Ashbolt, N. J. (2008). Review of multi-criteria decision aid for integrated sustainability assessment of urban water systems. *Urban water journal*, *5*(4), 315-327.

Langemeyer, J., Gómez-Baggethun, E., Haase, D., Scheuer, S., & Elmqvist, T. (2016). Bridging the gap between ecosystem service assessments and land-use planning through Multi-Criteria Decision Analysis (MCDA). *Environmental Science & Policy*, *62*, 45-56.

Lebel, T., Bastin, G., Obled, C., & Creutin, J. D. (1987). On the accuracy of areal rainfall estimation: a case study. *Water Resources Research*, *23*(11), 2123-2134.

Lenderink, G., Buishand, A., & Van Deursen, W. (2007). Estimates of future discharges of the river Rhine using two scenario methodologies: direct versus delta approach. *Hydrology and Earth System Sciences*, *11*(3), 1145-1159.

Leta, M. K., Demissie, T. A., & Tränckner, J. (2021). Modeling and prediction of land use land cover change dynamics based on land change modeler (Lcm) in nashe watershed, upper blue nile basin, Ethiopia. *Sustainability*, *13*(7), 3740.

Liersch, S., Rust, H., Dobler, A., Kruschke, T., & Fischer, M. (2018). Bias-corrected CORDEX precipitation, min/mean/max temperature for Ethiopia, RCP 4.5 and RCP 8.5.

Lillesand, T.M.; Kiefer, R.W.; Chipman, J.W. (2015). Remote Sensing and Image Interpretation, 7th ed.; Wiley: New York, NY, USA, 2015, ISBN 9781118343289.

Lu, Y. P., Yang, K., Che, Y., Shang, Z. Y., Zhu, H. F., & Jian, Y. (2013). Cost-effectiveness-based multi-criteria optimization for sustainable rainwater utilization: A case study in Shanghai. *Urban water journal*, *10*(2), 127-143.

Lu, Z., Zou, S., Qin, Z., Yang, Y., Xiao, H., Wei, Y., ... & Xie, J. (2015). Hydrologic responses to land use change in the loess plateau: case study in the Upper Fenhe River Watershed. *Advances in Meteorology*, *2015*.

Luck, M., Landis, M., & Gassert, F. (2015). Aqueduct water stress projections: decadal projections of water supply and demand using CMIP5 GCMs. Washington, DC.

Maghrebi, M. F., & Ahmadi, A. (2017). Stage-discharge prediction in natural rivers using an innovative approach. *Journal of hydrology*, *545*, 172-181.

Mango, L. M., Melesse, A. M., McClain, M. E., Gann, D., & Setegn, S. (2011). Land use and climate change impacts on the hydrology of the upper Mara River Basin, Kenya: results of a modeling study to support better resource management. *Hydrology and earth system sciences*, *15*(7), 2245-2258.

Mansanarez, V., Westerberg, I. K., Lyon, S. W., & Lam, N. (2018). Estimating uncertainties in hydraulicallymodelled rating curves for discharge time series assessment. In *E3S Web of Conferences* (Vol. 40, p. 06013). EDP Sciences.

Marhaento, H., Booij, M. J., & Hoekstra, A. Y. (2018). Hydrological response to future land-use changes and climate change in a tropical catchment. *Hydrological sciences journal*, *63*(9), 1368-1385.

Marques, R. C., da Cruz, N. F., & Pires, J. (2015). Measuring the sustainability of urban water services. Environmental Science & Policy, 54, 142-151.

Mascaro, G., White, D. D., Westerhoff, P., & Bliss, N. (2015). Performance of the CORDEX-Africa regional climate simulations in representing the hydrological cycle of the Niger River basin. *Journal of Geophysical Research: Atmospheres*, *120*(24), 12425-12444.

Masood, M. U., Haider, S., Rashid, M., Aldlemy, M. S., Pande, C. B., Đurin, B., ... & Elkhrachy, I. (2023). Quantifying the impacts of climate and land cover changes on the hydrological regime of a complex dam catchment area. *Sustainability*, *15*(21), 15223.

Mathewos, Y., Abate, B., & Dadi, M. (2022). Performance of the CORDEX-Africa Regional Climate Model in capturing precipitation and air temperature conditions in the Omo Gibe River Basin, Ethiopia.

McGinn, R., & Chubak, N. (2002). A rating curve based on lake levels: evaluating outlet flow for clear creek, riding mountain national park, Manitoba. *Prairie Perspect: Geogr Essays*, *5*, 17-29.

Meals, D. W., & Dressing, S. A. (2008). Surface water flow measurement for water quality monitoring projects, Tech Notes 3, March 2008. *Developed for US Environmental Protection Agency by Tetra Tech, Inc., Fairfax, VA*, *16*.

Megersa, G., Tesfaye, K., Getnet, M., Tana, T., Jaletab, M., & Lakew, B. (2019). Rainfall variability and its implications for wheat and barley production in central Ethiopia. *Ethiopian Journal of Crop Science*, *7*(2), 89-111.

Mekonnen, M. A., Wörman, A., Dargahi, B., & Gebeyehu, A. (2009). Hydrological modelling of Ethiopian catchments using limited data. *Hydrological Processes: An International Journal*, *23*(23), 3401-3408.

Mengistu, D., Bewket, W., & Lal, R. (2014). Recent spatiotemporal temperature and rainfall variability and trends over the Upper Blue Nile River Basin, Ethiopia. *International Journal of Climatology*, *34*(7), 2278-2292.

Mihertu, Y. F. (2019). Over View of Socio-Economic Data on Eastern Ethiopia Region (Harar Biodiversity Center Working Zone). *Acta Scientific Agriculture*, *3*, 196-206.

Mir, S. A., Mattoo, D., Bhat, M. S., & Maheen, M. M. (2022). Dynamics of land-use/land cover changes in upper Jhelum catchment of Kashmir Himalayas, India. *Indian Journal of Ecology*, *49*(5), 1634-1641.

Mirshahi, B., Onof, C., & Wheater, H. (2008, September). Spatialtemporal daily rainfall simulation for a semi-arid area in Iran: a preliminary evaluation of generalised linear models. In *Sustainable Hydrology for the 21st Century, Proceedings of the 10th BHS National Hydrology Symposium, Exeter, UK* (pp. 145-52).

Mishra, A. K. (2013). Effect of rain gauge density over the accuracy of rainfall: a case study over Bangalore, India. *SpringerPlus*, *2*, 1-7.

Moghadam, S. H., Ashofteh, P. S., & Loáiciga, H. A. (2019). Application of climate projections and Monte Carlo approach for assessment of future river flow: Khorramabad River Basin, Iran. *Journal of Hydrologic Engineering*, *24*(7), 05019014.

Moghadam, S. H., Ashofteh, P. S., & Loáiciga, H. A. (2023). Investigating the performance of data mining, lumped, and distributed models in runoff projected under climate change. *Journal of Hydrology*, *617*, 128992.

Mohammad, M. E., Al-Ansari, N., & Knutsson, S. (2016). Application of SWAT model to estimate the annual runoff and sediment of Duhok reservoir watershed. In *8th International Conference on Scour and Erosion-Oxford, Uk< 12-15 September 2016* (pp. 1129-1136). Taylor & Francis Group.

Moreira, L. L., Schwamback, D., & Rigo, D. (2018). Sensitivity analysis of the Soil and Water Assessment Tools (SWAT) model in streamflow modeling in a rural river basin. *Revista Ambiente & Água*, *13*, e2221.

Moriasi, D. N., Arnold, J. G., Van Liew, M. W., Bingner, R. L., Harmel, R. D., & Veith, T. L. (2007). Model evaluation guidelines for systematic quantification of accuracy in watershed simulations. *Transactions of the ASABE*, *50*(3), 885-900.

Moriasi, D. N., Arnold, J. G., Van Liew, M. W., Bingner, R. L., Harmel, R. D., & Veith, T. L. (2007). Model evaluation guidelines for systematic quantification of accuracy in watershed simulations. *Transactions of the ASABE*, *50*(3), 885-900.

Moss, R. H., Edmonds, J. A., Hibbard, K. A., Manning, M. R., Rose, S. K., van Vuuren, D. P., Carter, T. R., Emori, S., Kainuma, M., Kram, T., & Wilbanks, T. J. (2010). The next generation of scenarios for climate change research and assessment. Nature, 463(7282), 747 756. https://doi.org/10.1038/nature08823.

MoWR., 2004. Water Sector Development Program Report. Addis Ababa.

MoWIE., 2019. Water Supply & Sanitation Sector National ODF Campaign Framework.

Mugalavai, E. M., Kipkorir, E. C., Raes, D., & Rao, M. S. (2008). Analysis of rainfall onset, cessation and length of growing season for western Kenya. *Agricultural and forest meteorology*, *148*(6-7), 1123-1135.

Musie, M., Sen, S., & Chaubey, I. (2020). Hydrologic responses to climate variability and human activities in Lake Ziway Basin, Ethiopia. *Water*, *12*(1), 164.

Muzzammil, M., Alam, J., & Zakwan, M. (2018). A spreadsheet approach for prediction of rating curve parameters. In *Hydrologic Modeling: Select Proceedings of ICWEES-2016* (pp. 525-533). Springer Singapore.

Naha, S., Rico-Ramirez, M. A., & Rosolem, R. (2021). Quantifying the impacts of land cover change on hydrological responses in the Mahanadi River basin in India. *Hydrology and Earth System Sciences*, *25*(12), 6339-6357.

Nair, S., Srinivasan, G., & Nemani, R. (2009). Evaluation of multi-satellite TRMM derived rainfall estimates over a western state of India. *Journal of the Meteorological Society of Japan. Ser. II*, *87*(6), 927-939.

Nandargi, S., & Mulye, S. S. (2012). Relationships between rainy days, mean daily intensity, and seasonal rainfall over the Koyna catchment during 1961–2005. *The Scientific World Journal*, *2012*.

Napoli, M., Massetti, L., & Orlandini, S. (2017). Hydrological response to land use and climate changes in a rural hilly basin in Italy. *Catena*, *157*, 1-11.

Nash, J. E., & Sutcliffe, J. V. (1970). River flow forecasting through conceptual models' part I—A discussion of principles. *Journal of hydrology*, *10*(3), 282-290.

Nazli Aydin Y. (2014). Scenario-based sustainability assessment to provide interactive decision support for the Long-term transition of urban water supply systems (Doctoral dissertation, Technische Universität Kaiserslautern).

NCEI (2020). Climate Forecasting System (CRFS). National Centers for Environmental Information. Available from: https://www.ncdc.noaa.gov/data-access/model-data/model-datasets/climate-forecast systemversion2-cfsv2.

Negatu, T. A., Zimale, F. A., & Steenhuis, T. S. (2022). Establishing stage–discharge rating curves in developing countries: Lake Tana Basin, Ethiopia. *Hydrology*, *9*(1), 13.

Negese, A. (2021). Impacts of land use and land cover change on soil erosion and hydrological responses in Ethiopia. *Applied and Environmental Soil Science*, *2021*, 1-10.

Negewo, T. F., & Sarma, A. K. (2019). Evaluation of climate change-induced impact on streamflow and sediment yield of Genale watershed, Ethiopia. *The Nature, Causes, Effects and Mitigation of Climate Change on the Environment*.

Negreiros, J., Costa, A. C., & Painho, M. (2011). Evaluation of stochastic geographical matters: Morphologic geostatistics, conditional sequential simulation and geographical weighted regression. *Trends in Applied Sciences Research*, *6*(3), 237-255.

Neitsch, S. L., Arnold, J. G., Kiniry, J. R., & Williams, J. R. (2011). *Soil and water assessment tool theoretical documentation version 2009*. Texas Water Resources Institute.

Neupane, R. P., White, J. D., & Alexander, S. E. (2015). Projected hydrologic changes in monsoon-dominated Himalaya Mountain basins with changing climate and deforestation. *Journal of Hydrology*, *525*, 216-230.

Ngetich, K. F., Mucheru-Muna, M., Mugwe, J. N., Shisanya, C. A., Diels, J., & Mugendi, D. N. (2014). Length of growing season, rainfall temporal distribution, onset and cessation dates in the Kenyan highlands. *Agricultural and Forest Meteorology*, *188*, 24-32.

Ngondo, J., Mango, J., Nobert, J., Dubi, A., Li, X., & Cheng, H. (2022). Hydrological response of the Wami–Ruvu basin to land-use and land-cover changes and its impacts for the future. *Water*, *14*(2), 184.

Ngongondo, C., Xu, C. Y., Gottschalk, L., & Alemaw, B. (2011). Evaluation of spatial and temporal characteristics of rainfall in Malawi: a case of data scarce region. *Theoretical and applied climatology*, *106*, 79-93.

Nikulin, G., Jones, C., Giorgi, F., Asrar, G., Büchner, M., Cerezo-Mota, R., ... & Sushama, L. (2012). Precipitation climatology in an ensemble of CORDEX-Africa regional climate simulations. *Journal of Climate*, *25*(18), 6057-6078.

Nkiaka, E., Nawaz, N. R., & Lovett, J. C. (2017). Evaluating global reanalysis datasets as input for hydrological modelling in the Sudano-Sahel region. *Hydrology*, *4*(1), 13.

NMSA (1996). Climatic & agroclimatic resources of Ethiopia. Meteorological Research Report Series, vol. 1, No. 1, Addis Ababa.

Nnaji, C. C., & Banigo, A. (2018). Multi-criteria evaluation of sources for self-help domestic water supply. Applied water science, 8, 1-13.

Nobert, J., & Jeremiah, J. (2012). Hydrological response of watershed systems to land use/cover change. a case of Wami River Basin. *The Open Hydrology Journal*, *6*(1).

Nyembo, L. O., Mwabumba, M., Jahangeer, J., & Kumar, V. (2022). Historical and projected spatial and temporal rainfall status of Dar es Salaam, Tanzania, from 1982 to 2050. *Frontiers in Environmental Science*, *10*, 1025760.

Nyssen, J., Vandenreyken, H., Poesen, J., Moeyersons, J., Deckers, J., Haile, M., ... & Govers, G. (2005). Rainfall erosivity and variability in the Northern Ethiopian Highlands. *Journal of Hydrology*, *311*(1-4), 172-187.

Oettli, P., & Camberlin, P. (2005). Influence of topography on monthly rainfall distribution over East Africa. *Climate Research*, *28*(3), 199-212.

Okeola, O. G., & Sule, B. F. (2012). Evaluation of management alternatives for urban water supply system using Multicriteria Decision Analysis. Journal of King Saud University-Engineering Sciences, 24(1), 19-24.

Onyutha, C. (2016). Influence of hydrological model selection on simulation of moderate and extreme flow events: a case study of the Blue Nile basin. *Advances in Meteorology*, *2016*.

Osima, S., Indasi, V. S., Zaroug, M., Endris, H. S., Gudoshava, M., Misiani, H. O., ... & Dosio, A. (2018). Projected climate over the Greater Horn of Africa under 1.5 C and 2 C global warming. *Environmental Research Letters*, *13*(6), 065004.

Othman, N. Y., Abd Saleh, Z., & Omran, Z. A. (2019). Development of stage-distance-discharge relationship and rating curve using least square method. *Civil Eng J*, *5*(9), 1959-1969.

Ougahi, J. H., Karim, S., & Mahmood, S. A. (2022). Application of the SWAT model to assess climate and land use/cover change impacts on water balance components of the Kabul River Basin, Afghanistan. *Journal of Water and Climate Change*, *13*(11), 3977-3999.

Pachauri, R. K., Allen, M. R., Barros, V. R., Broome, J., Cramer, W., Christ, R., ... & van Ypserle, J. P. (2014). *Climate change 2014: synthesis report. Contribution of Working Groups I, II and III to the fifth assessment report of the Intergovernmental Panel on Climate Change* (p. 151). Ipcc.

Pandey, B. K., & Khare, D. (2018). Identification of trend in long term precipitation and reference evapotranspiration over Narmada River basin (India). *Global and planetary change*, *161*, 172-182.

Pandey, B. K., Khare, D., Kawasaki, A., & Meshesha, T. W. (2021). Integrated approach to simulate hydrological responses to land use dynamics and climate change scenarios employing scoring method in upper Narmada basin, India. *Journal of Hydrology*, *598*, 126429.

Pannu, J., McCarthy, A., Martin, A., Hamouda, T., Ciotti, S., Fothergill, A., & Sutcliffe, J. (2009). NB-002, a novel nanoemulsion with broad antifungal activity against dermatophytes, other filamentous fungi, and Candida albicans. *Antimicrobial agents and chemotherapy*, *53*(8), 3273-3279.

Patra, K. C. (2008). Hydrology and Water Resources Engineering, Second Edition. New Delhi. Narosa Publishing House.

Petersen - Øverleir, A. (2004). Accounting for heteroscedasticity in rating curve estimates. *Journal of Hydrology*, *292*(1-4), 173-181.

Peterson, T. C., & Easterling, D. R. (1994). Creation of homogeneous composite climatological reference series. *International journal of climatology*, *14*(6), 671-679.

Peterson, T. C., Easterling, D. R., Karl, T. R., Groisman, P., Nicholls, N., Plummer, N., ... & Parker, D. (1998). Homogeneity adjustments of in situ atmospheric climate data: a review. *International Journal of Climatology: A Journal of the Royal Meteorological Society*, *18*(13), 1493-1517.

Ramos, M. C., & Martínez-Casasnovas, J. A. (2006). Trends in precipitation concentration and extremes in the Mediterranean Penedes-Anoia region, NE Spain. *Climatic Change*, *74*, 457-474.

Randles, C. A., Da Silva, A. M., Buchard, V., Colarco, P. R., Darmenov, A., Govindaraju, R., ... & Flynn, C. J. (2017). The MERRA-2 aerosol reanalysis, 1980 onward. Part I: System description and data assimilation evaluation. *Journal of climate*, *30*(17), 6823-6850.

Raneesh, K. Y. (2014). Impact of climate change on water resources. *Journal of Earth Science & Climatic Change*, *5*(3), 1.

Rathjens, H., Bieger, K., Srinivasan, R., Chaubey, I., & Arnold, J. (2016). Documentation for preparing simulated climate change data for hydrologic impact studies. *URL: http://swat. tamu. edu/software/cmhyd*.

Ros, F. C., Tosaka, H., Sidek, L. M., Desa, M. N., & Arifin, K. (2013, June). Stage discharge curve for Guillemard Bridge streamflow sation based on rating curve method using historical flood event data. In *IOP Conference Series: Earth and Environmental Science* (Vol. 16, No. 1, p. 012130). IOP Publishing.

Roth, V., Nigussie, T. K., & Lemann, T. (2016). Model parameter transfer for streamflow and sediment loss prediction with SWAT in a tropical watershed. *Environmental Earth Sciences*, *75*(19), 1321.

Saaty, T. L. (1977). A scaling method for priorities in hierarchical structures. Journal of mathematical psychology, 15(3), 234-281.

Saaty, T. L. (2010). *Mathematical principles of decision making (Principia mathematica decernendi)*. RWS publications.

Saaty, T.L (2005). The analytic hierarchy and analytic network processes for the measurement of intangible criteria and for decision-making. In Multicriteria Decision Analysis: State of the Art Surveys; Figueira, J., Greco, S., Ehrgott, M., Eds.; Springer Science + Business Media, Inc.: Boston, MA, USA, pp. 363–419. ISBN 978-0-387-23081-8.

Sahely, H. R., Kennedy, C. A., & Adams, B. J. (2005). Developing sustainability criteria for urban infrastructure systems. *Canadian Journal of Civil Engineering*, *32*(1), 72-85.

Santhi, C., Arnold, J. G., Williams, J. R., Dugas, W. A., Srinivasan, R., & Hauck, L. M. (2001). Validation of the swat model on a large rwer basin with point and nonpoint sources 1. *JAWRA Journal of the American Water Resources Association*, *37*(5), 1169-1188.

Santos-Pereira, Cordery, I., & Iacovides, I. (2009). Coping with water scarcity: Addressing the challenges. Springer Science & Business Media.

Sauer, V. B., & Turnipseed, D. P. (2010). *Stage measurement at gaging stations* (No. 3-A7). US Geological Survey.

Schaefli, B. (2015). Projecting hydropower production under future climates: a guide for decision-makers and modelers to interpret and design climate change impact assessments. *Wiley Interdisciplinary Reviews: Water*, *2*(4), 271-289.

Schmidt, A. R., & Yen, B. C. (2008). Theoretical development of stage-discharge ratings for subcritical open-channel flows. *Journal of Hydraulic Engineering*, *134*(9), 1245-1256.

Schurz, C., Hollosi, B., Matulla, C., Pressl, A., Ertl, T., Schulz, K., & Mehdi, B. (2019). A comprehensive sensitivity and uncertainty analysis for discharge and nitrate-nitrogen loads involving multiple discrete model inputs under future changing conditions. *Hydrology and Earth System Sciences*, *23*(3), 1211-1244.

Sefe, F. T. K. (1996). A study of the stage-discharge relationship of the Okavaiigo River at Mohembo, Botswana. *Hydrological sciences journal*, *41*(1), 97-116.

Seleshi, Y., & Zanke, U. (2004). Recent changes in rainfall and rainy days in Ethiopia. *International Journal of Climatology: A Journal of the Royal Meteorological Society*, *24*(8), 973-983.

Sen, Z., & Habib, Z. (2000). Spatial precipitation assessment with elevation by using point cumulative semivariogram technique. *Water resources management*, *14*, 311-325.

Senbeta, A. F., & Olsson, J. A. (2009). Climate change impact on livelihood, vulnerability and coping mechanisms: A case study of West-Arsi Zone, Ethiopia. *Lund University, Lund*, *54*.

Serageldin, I. (1995). Water resources management: A new policy for a sustainable future. Water International, 20(1), 15-21.

Setegn, S. G., Srinivasan, R., & Dargahi, B. (2008). Hydrological modelling in the Lake Tana Basin, Ethiopia using SWAT model. *The Open Hydrology Journal*, *2*(1).

Shanko, D., & Camberlin, P. (1998). The effects of the Southwest Indian Ocean tropical cyclones on Ethiopian drought. *International Journal of Climatology: A Journal of the Royal Meteorological Society*, *18*(12), 1373-1388.

Shawul, A. A., Alamirew, T., & Dinka, M. O. (2013). Calibration and validation of SWAT model and estimation of water balance components of Shaya mountainous watershed, Southeastern Ethiopia. *Hydrology and Earth System Sciences Discussions*, *10*(11), 13955-13978.

Shigute, M., Alamirew, T., Abebe, A., Ndehedehe, C. E., & Kassahun, H. T. (2022). Understanding Hydrological Processes under Land Use Land Cover Change in the Upper Genale River Basin, Ethiopia. *Water, 14*(23), 3881.

Sikorska, A. E., & Renard, B. (2017). Calibrating a hydrological model in stage space to account for rating curve uncertainties: general framework and key challenges. *Advances in water resources*, *105*, 51-66.

Singh, L., & Saravanan, S. (2020). Simulation of monthly streamflow using the SWAT model of the Ib River watershed, India. *HydroResearch*, *3*, 95-105.

Singh, V. P. (1995). What is environmental hydrology? In *Environmental hydrology* (pp. 1-12). Dordrecht: Springer Netherlands.

Sohani, A., Naderi, S., & Torabi, F. (2019). Comprehensive comparative evaluation of different possible optimization scenarios for a polymer electrolyte membrane fuel cell. *Energy conversion and management*, *191*, 247-260.

Somorowska, U. (2017). Climate-driven changes to streamflow patterns in a groundwater-dominated catchment. *Acta Geophysica*, *65*(4), 789-798.

Subramanya, K., 2007. Engineering Hydrology. Second Edition. Tata McGraw-Hill Publishing Company Limited, New Delhi.

Szabo, Z. K., Szadoczki, Z., Bozoki, S., Stanciulescu, G. C., & Szabo, D. (2021). An analytic hierarchy process approach for prioritisation of strategic objectives of sustainable development. Sustainability, 13(4), 2254.

Taesombat, W., & Sriwongsitanon, N. (2009). Areal rainfall estimation using spatial interpolation techniques. *Science Asia*, *35*(3), 268-275.

Takala, W., Adugna, T., & Tamam, D. (2016). The effects of land use land cover change on hydrological process of Gilgel Gibe, Omo Gibe Basin, Ethiopia. *Int. J. Sci. Eng. Res*, *7*(8), 117-128.

Tan, M. L., Ficklin, D. L., Ibrahim, A. L., & Yusop, Z. (2014). Impacts and uncertainties of climate change on streamflow of the Johor River Basin, Malaysia using a CMIP5 General Circulation Model ensemble. *Journal of Water and Climate Change*, *5*(4), 676-695.

Taye, H. (2016). *Dynamics of land use land cover changes on stream flow in Fincha Amerti Neshe sub-basin* (Doctoral dissertation, School of Graduate Studies of Addis Abeba University).

Taye, M. T., Haile, A. T., Fekadu, A. G., & Nakawuka, P. (2021). Effect of irrigation water withdrawal on the hydrology of the Lake Tana sub-basin. *Journal of Hydrology: Regional Studies*, *38*, 100961.

Taye, M. T., Willems, P., & Block, P. (2015). Implications of climate change on hydrological extremes in the Blue Nile basin: a review. *Journal of Hydrology: Regional Studies*, *4*, 280-293.

Taylor, K. E. (2001). Summarizing multiple aspects of model performance in a single diagram. *Journal of geophysical research: atmospheres*, *106*(D7), 7183-7192.

Tekleab, S., Mohamed, Y., Uhlenbrook, S., & Wenninger, J. (2014). Hydrologic responsees to land cover change: the case of Jedeb mesoscale catchment, Abay/Upper Blue Nile basin, Ethiopia. Hydrological processes, 28, 5149–5162. https://doi.org/10.1002/hyp.9998.

Terink, W., Leijnse, H., van den Eertwegh, G., & Uijlenhoet, R. (2018). Spatial resolutions in areal rainfall estimation and their impact on hydrological simulations of a lowland catchment. *Journal of Hydrology*, *563*, 319-335.

Teutschbein, C., & Seibert, J. (2010). Regional climate models for hydrological impact studies at the catchment scale: a review of recent modeling strategies. *Geography Compass*, *4*(7), 834-860.

Teutschbein, C., & Seibert, J. (2012). Bias correction of regional climate model simulations for hydrological climate-change impact studies: Review and evaluation of different methods. *Journal of hydrology*, *456*, 12-29.

Torabi Haghighi, A., Darabi, H., Shahedi, K., Solaimani, K., & Kløve, B. (2020). A scenario-based approach for assessing the hydrological impacts of land use and climate change in the Marboreh Watershed, Iran. *Environmental Modeling & Assessment*, *25*(1), 41-57.

Tufa, D. F., Abbulu, Y. E. R. R. A. M. S. E. T. T. Y., & Srinivasarao, G. V. R. (2014). Watershed hydrological response to changes in land use/land covers patterns of river basin: A review. *International Journal of Civil, Structural, Environmental and Infrastructure Engineering Research and Development (IJCSEIERD)*, *4*(2), 157-170.

Tumsa, B. C. (2021). Statistical evaluation of RCM's performances in simulation of climate variables at Upper Awash Basin, case study of Akaki Catchment.

United Nations (UN) (2019). How certain are the United Nations global populations Projections? Population facts, department of Economic and social affairs, number 2019/6.

Valenti, W. C., Kimpara, J. M., Preto, B. D. L., & Moraes-Valenti, P. (2018). Indicators of sustainability to assess aquaculture systems. Ecological indicators, 88, 402-413.

Van Liew, M. W., Arnold, J. G., & Bosch, D. D. (2005). Problems and potential of auto-calibrating a hydrologic model. *Transactions of the ASAE*, *48*(3), 1025-1040.

Varum, C. A., & Melo, C. (2007). Strategic planning in an uncertain business environment: the diffusion of scenario planning. In Conference Factores de Competitividade, Competitiveness Factors: A Portuguese Perspective, Aveiro.

Villarini, G. (2010). Evaluation of the research-version TMPA rainfall estimate at its finest spatial and temporal scales over the Rome metropolitan area. *Journal of applied meteorology and climatology*, *49*(12), 2591-2602.

Wangpimool, W., Pongput, K., Supriyasilp, T., Sakolnakhon, K., & Vonnarart, O. (2013). Hydrological Evaluation with SWAT Model and Numerical Weather Prediction for Flash Flood Warning System in Thailand. Journal of Earth Science and Engineering, 6, 349-357.

Warburton, M. L., Schulze, R. E., & Jewitt, G. P. (2012). Hydrological impacts of land use change in three diverse South African catchments. *Journal of Hydrology*, *414*, 118-135.

Welde, K., & Gebremariam, B. (2017). Effect of land use land cover dynamics on hydrological response of watershed: Case study of Tekeze Dam watershed, northern Ethiopia. *International Soil and Water Conservation Research*, *5*(1), 1-16.

Weldu Woldemariam, G., & Edo Harka, A. (2020). Effect of land use and land cover change on soil erosion in Erer sub-basin, Northeast Wabi Shebelle Basin, Ethiopia. *Land*, *9*(4), 111.

WG, I. (2013). The physical science basis. *Contribution of working group I to the fifth assessment report of the intergovernmental panel on climate change*, *1535*.

WHO; UNICEF Joint Water Supply, & Sanitation Monitoring Programme. (2015). Progress on sanitation and drinking water: 2015 update and MDG assessment. World Health Organization.

Wilby, R. L., & Harris, I. (2006). A framework for assessing uncertainties in climate change impacts: low-flow scenarios for the River Thames, UK. Water Resources Research, 42. https://doi.org/10.1029/2005WR004065.

Wilby, R. L., & Wood, P. J. (2012). Introduction to adapting water management to climate change: putting our science into practice. *Area*, *44*(4), 394-399.

Wilson, E.M. (1970). Engineering hydrology, Macmillan and Co. Ltd. London.

Winchell, M., Srinivasan, R., Di Luzio, M., & Arnold, J. G. (2013). ArcSWAT Interface for 521 SWAT2012 User's Guide. *Blackland Research and Extension Center: Temple, TX, USA*, *522*, 439-464.

Worku, G., Teferi, E., Bantider, A., Dile, Y. T., & Taye, M. T. (2018). Evaluation of regional climate models performance in simulating rainfall climatology of Jemma sub-basin, Upper Blue Nile Basin, Ethiopia. *Dynamics of Atmospheres and Oceans*, *83*, 53-63.

WHO; UNICEF (2006). Meeting the MDG drinking water and sanitation target: the urban and rural challenge of the decade. World Health Organization.

WMO. World Meteorological Organization (2010). Manual on StreamGauging.wmo.int/pages/pro

Wu, F., Zhan, J., Su, H., Yan, H., & Ma, E. (2015). Scenario-based impact assessment of land use/cover and climate changes on watershed hydrology in Heihe River Basin of northwest China. *Advances in Meteorology*, *2015*, 1-11.

Wudineh, F. A., Moges, S. A., & Kidanewold, B. B. (2021). Flood change detection and attribution using simulation approach in data-scarce watersheds: A case of Wabi Shebele river basin, Ethiopia. *Journal of Water Resource and Protection*, *13*(5), 362-393.

Wudineh, F. A., Moges, S. A., & Kidanewold, B. B. (2022). Flood Generation Mechanisms and Potential Drivers of Flood in Wabi-Shebele River Basin, Ethiopia. *Natural Resources*, *13*(1), 38-51.

Yeboah, K. A., Akpoti, K., Kabo-bah, A. T., Ofosu, E. A., Siabi, E. K., Mortey, E. M., & Okyereh, S. A. (2022). Assessing climate change projections in the Volta Basin using the CORDEX-Africa climate simulations and statistical bias-correction. *Environmental Challenges*, *6*, 100439.

Yilmaz, M. T., Houser, P., Shrestha, R., & Anantharaj, V. G. (2010). Optimally merging precipitation to minimize land surface modeling errors. *Journal of applied meteorology and climatology*, *49*(3), 415-423.

Yoo, C., Kim, U., Kim, K., & Kim, K. (2008). Inter-station correlation and estimation errors of areal average rain rate. *Stochastic Environmental Research and Risk Assessment*, *22*, 143-157.

Yu, H., Yang, Z., & Li, B. (2020). Sustainability assessment of water resources in Beijing. Water, 12(7), 1999.

Yuan, W., Sun, W., Chen, H., & Yu, R. (2014). Topographic effects on spatiotemporal variations of short-duration rainfall events in warm season of central North China. *Journal of Geophysical Research: Atmospheres*, *119*(19), 11-223.

Zewdu, E., Hadgu, G., & Nigatu, L. (2020). Impacts of climate change on sorghum production in North Eastern Ethiopia. *African Journal of Environmental Science and Technology*, *14*(2), 49-63.

Zhang, B., Shrestha, N. K., Daggupati, P., Rudra, R., Shukla, R., Kaur, B., & Hou, J. (2018). Quantifying the impacts of climate change on streamflow dynamics of two major rivers of the Northern Lake Erie Basin in Canada. *Sustainability*, *10*(8), 2897.

Zhang, T., Li, B., Wang, J., Hu, M., & Xu, L. (2016). Estimation of areal mean rainfall in remote areas using B-SHADE Model. *Advances in Meteorology*, *2016*, 1-13.

Zhang, Y., You, Q., Chen, C., & Ge, J. (2016). Impacts of climate change on streamflows under RCP scenarios: A case study in Xin River Basin, China. *Atmospheric research*, *178*, 521-534.

Zhao, Q., Gao, Q., Zou, C. H., Yao, T., & Li, X. M. (2019). IMPACT OF CHANGES IN LAND USE AND CLIMATE ON THE RUNOFF BASED ON SWAT MODEL IN DAWEN RIVER BASIN, CHINA. *Applied Ecology & Environmental Research*, *17*(2).

Zhenquan Li, Qiaoyu Li, Haijun Qiu, Yimin Wang, and Zezhong Zhang (2017). Application Research of Multiple Linear Regression Analysis in Yellow River Water Diversion of the Lower Reachs. *Revista de la Facultad de Ingeniería UCV*, *32*, 925-930.

Zhou, J. L., Xu, Q. Q., & Zhang, X. Y. (2018). Water resources and sustainability assessment based on group AHP-PCA method: a case study in the Jinsha River Basin. Water, 10(12), 1880.

Zimale, F. A., Moges, M. A., Alemu, M. L., Ayana, E. K., Demissie, S. S., Tilahun, S. A., & Steenhuis, T. S. (2018). Budgeting suspended sediment fluxes in tropical monsoonal watersheds with limited data: The Lake Tana basin. *Journal of Hydrology and Hydromechanics*, *66*(1), 65-78.

Zyoud, S. H., Shaheen, H., Samhan, S., Rabi, A., Al-Wadi, F., & Fuchs-Hanusch, D. (2016). Utilizing analytic hierarchy process (AHP) for decision making in water loss management of intermittent water supply systems. Journal of Water, Sanitation and Hygiene for Development, 6(4), 534-546.

APPENDICES

Appendix 1. Questioners for survey
Date: ………………………………………
Profession: ……………….…………….……….
Education Status: ☐ Diploma (10+4 or 10+3) ☐ Degree ☐ Master degree ☐ PhD Degree ☐ others
Job Experience: ☐ < 5 year ☐ 5 -10 year ☐ 10-15 ☐ >15
Job Position: ☐ Executive ☐ Manger ☐ Team leader ☐ experts ☐ others

Rating scale	Definition	Explanation
1	Equal importance	Two criteria contribute equally to the objectives
2	Weak importance	Criterion contribution is between equal and moderate
3	Moderate importance	Experience and judgment slightly favor one criterion over another
4	Moderate plus importance	Criterion contribution is between moderate and strong
5	Strong importance	Experience and judgment strongly favor one criterion over another
6	Strong plus importance	Criterion contribution is between strong and very strong
7	Very strong importance	Experience and judgment very strongly favor one criterion over another
8	Very, very strong importance	Criterion contribution is between very strong and extreme
9	Extreme importance	Experience and judgment extremely favor one criterion over another

Example:

- ***The importance of criteria (a) over criteria (b) whatever the case is from extreme to equal; the left rating scale value from (9 -1) is the score;***

✓ **If criterion (a) has extreme importance over criterion (b) the *rating scale* value 9 is ticked as per table A.**

- ***The importance of criteria (b) over criteria (a) whatever the case is from equal to extreme; the left rating scale value from (1 -9) is the score.***

✓ **If criterion (b) has strong importance over criterion (a) the *rating scale* value 5 is ticked.**

Table A: Criterion (a) has from equal to extreme importance over criterion (b)

Criterion (a)										Criterion (b)					
9	8	7	6	5	4	2	1	2	3	4	5	6	7	8	9
☒	☐	☐	☐	☐	☐	☐	☐	☐	☐	☐	☐	☐	☐	☐	☐

Table B: Criterion (b) has from equal to extreme importance over criterion (a)

Criterion (a)										Criterion (b)					
9	8	7	6	5	4	2	1	2	3	4	5	6	7	8	9
☐	☐	☐	☐	☐	☐	☐	☐	☐	☐	☐	☒	☐	☐	☐	☐

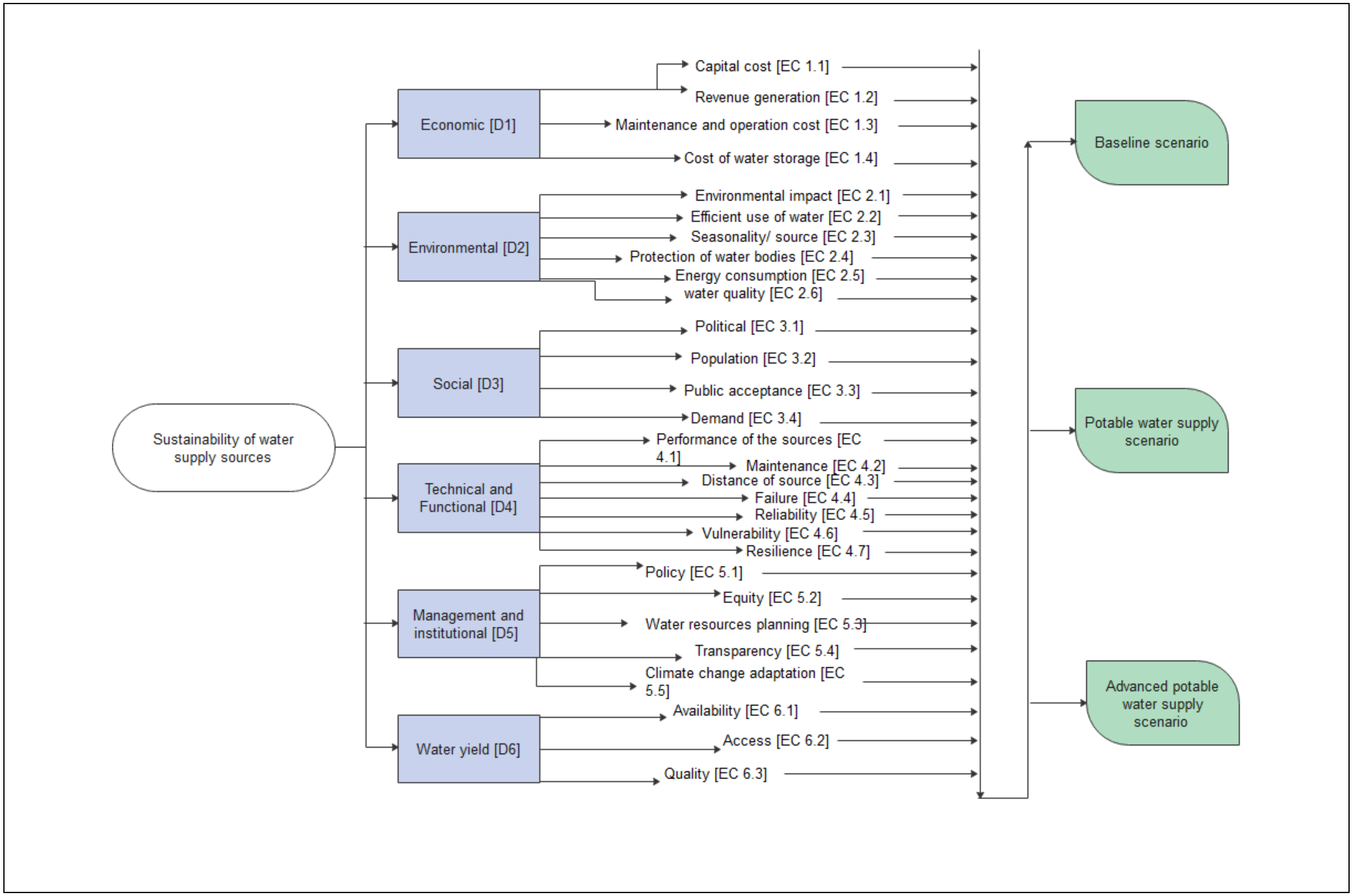

Appendix 2. Basic structure of analytical hierarchy matrix for the sustainability analysis of water supply sources

Appendix 3. Saaty numerical scale for pairwise comparisons in AHP; source (Saaty, 1980)

Intensity of importance	Definition	Explanations
1	Equal importance of two elements	Two activities contribute equally to the objective
3	Weak preference (element i over element j)	Slightly favor one activity over another
5	Strong preference (i over j)	Strongly favor one activity over another
7	Very strong preference (i over j)	An activity is favored very strongly over another; its dominance demonstrated in practice
9	Absolute preference (i over j)	The evidence favoring one activity over another is of the highest possible order of affirmation
2, 4, 6, 8	Intermediate values between two judgments (i over j)	
1/3	Weak preference (j over i)	
1/5	Strong preference (j over i)	
1/7	Very strong preference (j over i)	
1/9	Absolute preference (j over i)	
½, ¼, 1/6, 1/8	Intermediate values between two judgments (j over i)	

Appendix 4. random index (RI), source: from (Saaty, 2008**).**

N	1	2	3	4	5	6	7	8	9	10	11	12	13	14	15
RI	0	0	0.52	0.89	1.11	1.25	1.35	1.40	1.45	1.49	1.52	1.54	1.56	1.58	1.59

Appendix 5. Global and local weights for evaluation criteria

Goal	Criteria	Local weights (%)	Evaluation criteria	Local weights (%)	Global weights of EC (%)
Sustainabilit	Economic (C 1)	21.10	Capital cost (EC 1.1)	58.46	12.33
			Revenue generation (EC 1.2)	14.14	2.98
			Maintenance and operation cost (EC	19.01	4.01

Goal	Criteria	Local weights (%)	Evaluation criteria	Local weights (%)	Global weights of EC (%)
			1.3)		
			Cost of water storage (EC 1.4)	8.40	1.77
	Environmental (C 2)	17.01	Environmental impact (EC 2.1	4.68	0.80
			Efficient use of water (EC 2.2)	9.13	1.55
			Seasonality/ source (EC 2.3)	35.24	5.99
			Protection of water bodies (EC 2.4)	16.38	2.79
			Energy consumption (EC 2.5)	9.35	1.59
			water quality (EC 2.6)	25.21	4.29
	Social (C 3)	18.24	Political (EC 3.1)	41.01	7.48
			Population (EC 3.2)	18.72	3.42
			Public acceptance (EC 3.3)	19.64	3.58
			Demand (EC 3.4)	20.62	3.76
	Technical and Functional (C 4)	17.45	Performance of the sources (EC 4.1)	31.73	5.54
			Maintenance (EC 4.2)	20.78	3.63
			Distance of source (EC 4.3)	10.49	1.83
			Reliability (EC 4.4)	26.57	4.64
			Vulnerability (EC 4.5)	5.30	0.93
			Resilience (EC 4.6)	5.13	0.90
	Management and institutional (C 5)	14.84	Policy (EC 5.1)	37.08	5.50
			Equity (EC 5.2)	24.98	3.71
			Water resources planning (EC 5.3)	16.71	2.48
			Transparency (EC 5.4)	11.41	1.69
			climate change adaptation (EC 5.5)	9.82	1.46
	Water yields (C 6)	11.34	Availability (EC 6.1)	54.16	6.16
			Access (EC 6.2)	25.41	2.89
			Quality (EC 6.3)	20.42	2.32

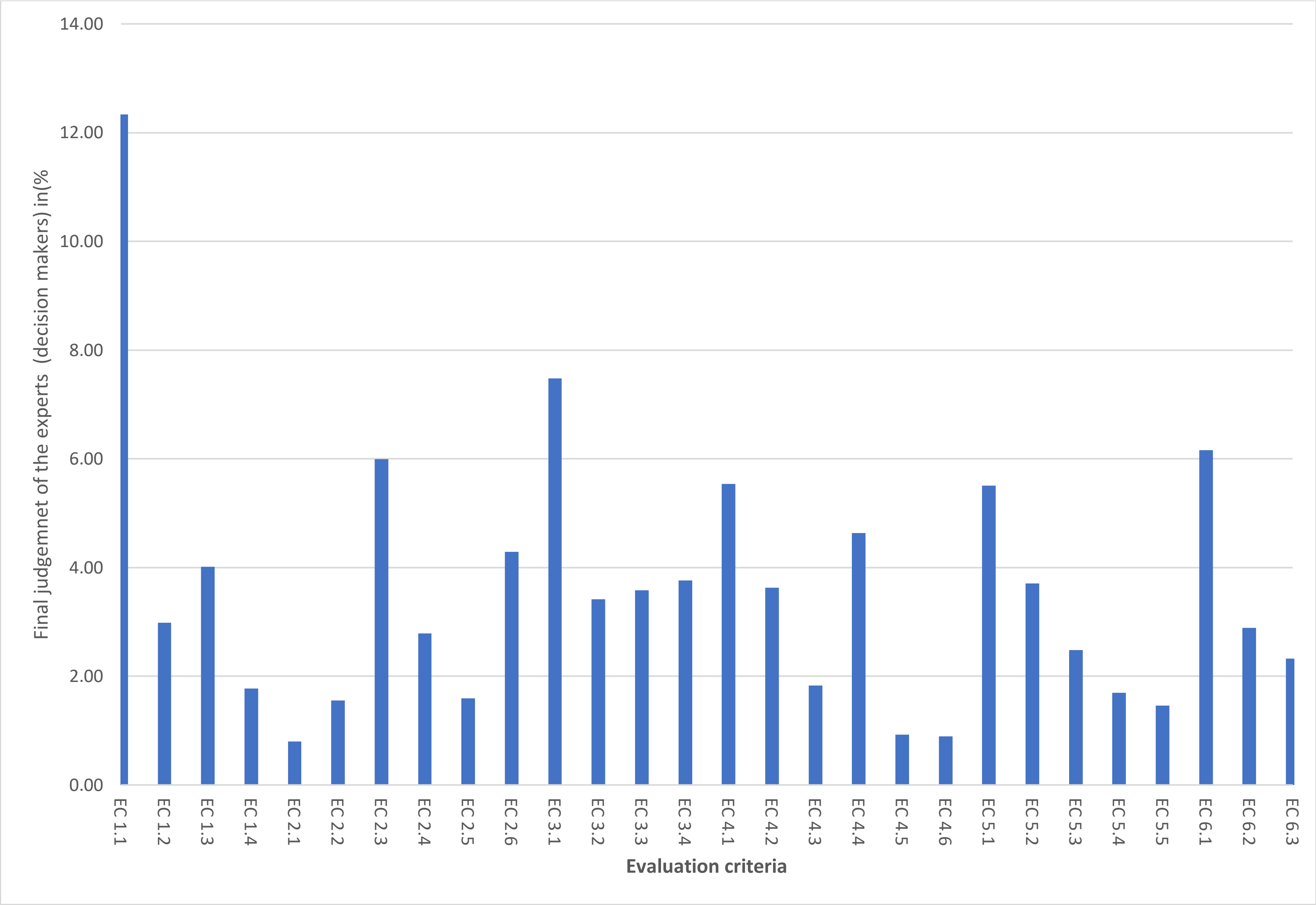

Appendix 6. Weights of all 28 evaluation criteria that were got from AHP.

Appendix 7. Description of climatological stations

Stations name (Class category)	Physical location		Mean Elevation (m)	Mean yearly rainfall (mm)	Observation duration	Proportion of missing values (%)	Mean annual temperature	
	Latitude	Longitude					Max (ºC)	Min (ºC)
Dire Dawa (1st class)	9.60	41.86	1045	647	1983-2020	9.12	32.8	19.0
Haramaya (1st class)	9.43	42.02	2025	816	1983-2020	12.92	24.05	9.74
Harar (1st class)	9.30	42.08	1977	801	1985-2020	18.01	23.0	16.0
Girawa (3rd class)	9.13	41.83	2470	958	1983-2017	14.83	22.0	13.0
Gursum (3rd class)	9.35	42.39	1937	840	1983-2017	8.74	27.2	12.8

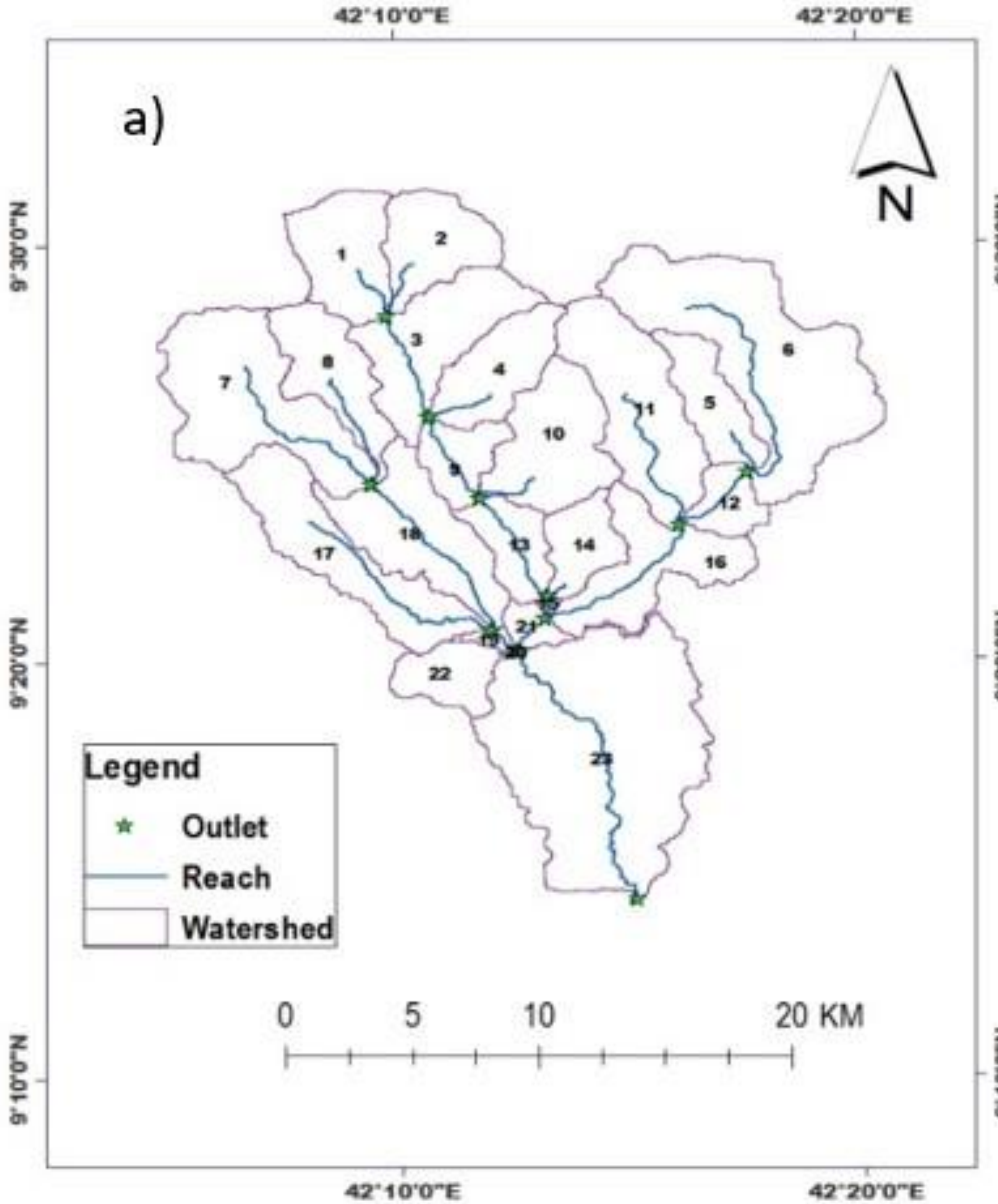

Appendix 8. Upper Erer subbasin watershed delineation map

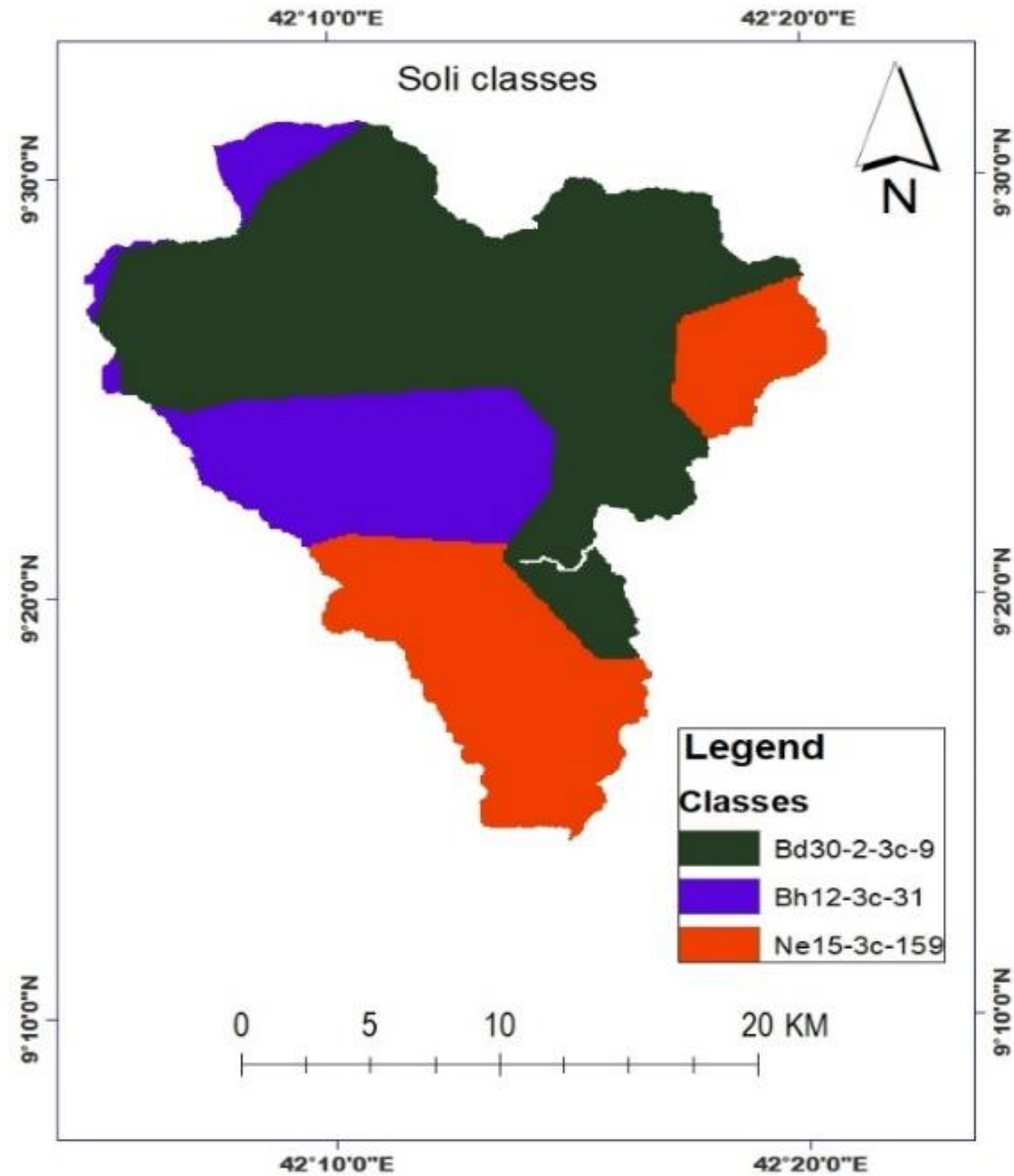

Appendix 9. **Soil types categories for the study area**

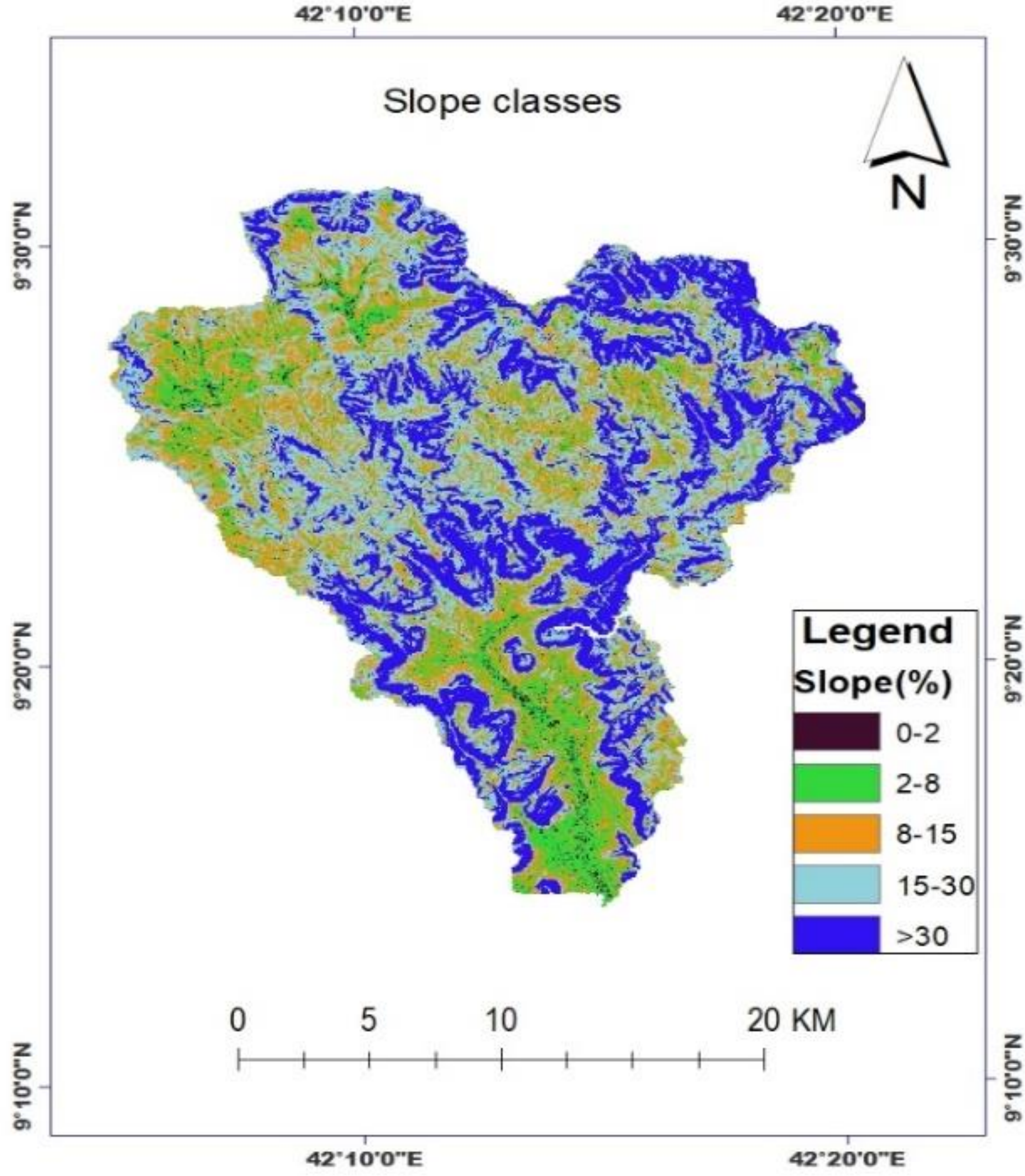

Appendix 10. Slope classes for the study area

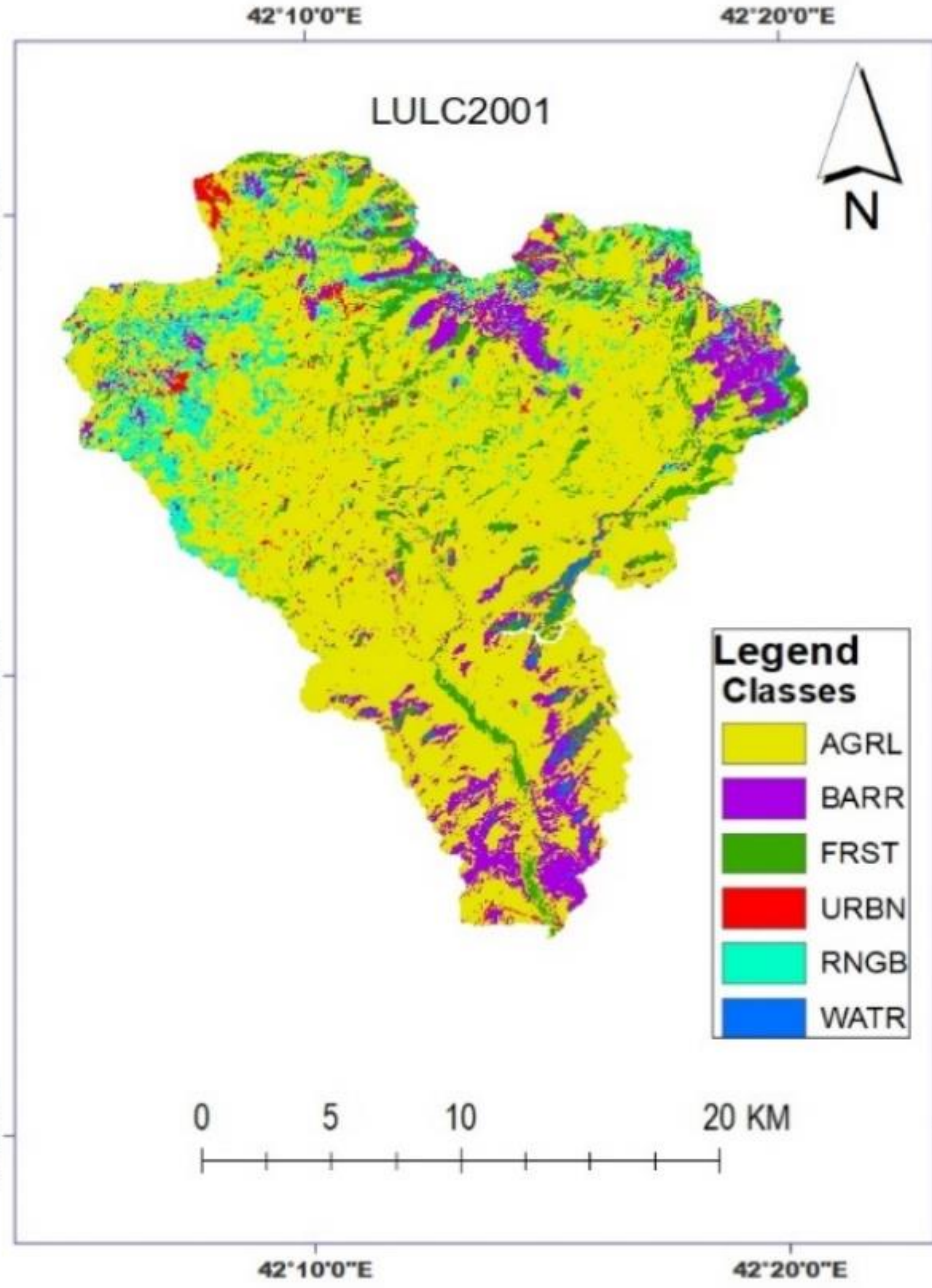

Appendix 11. **LULC maps for the year 2001**

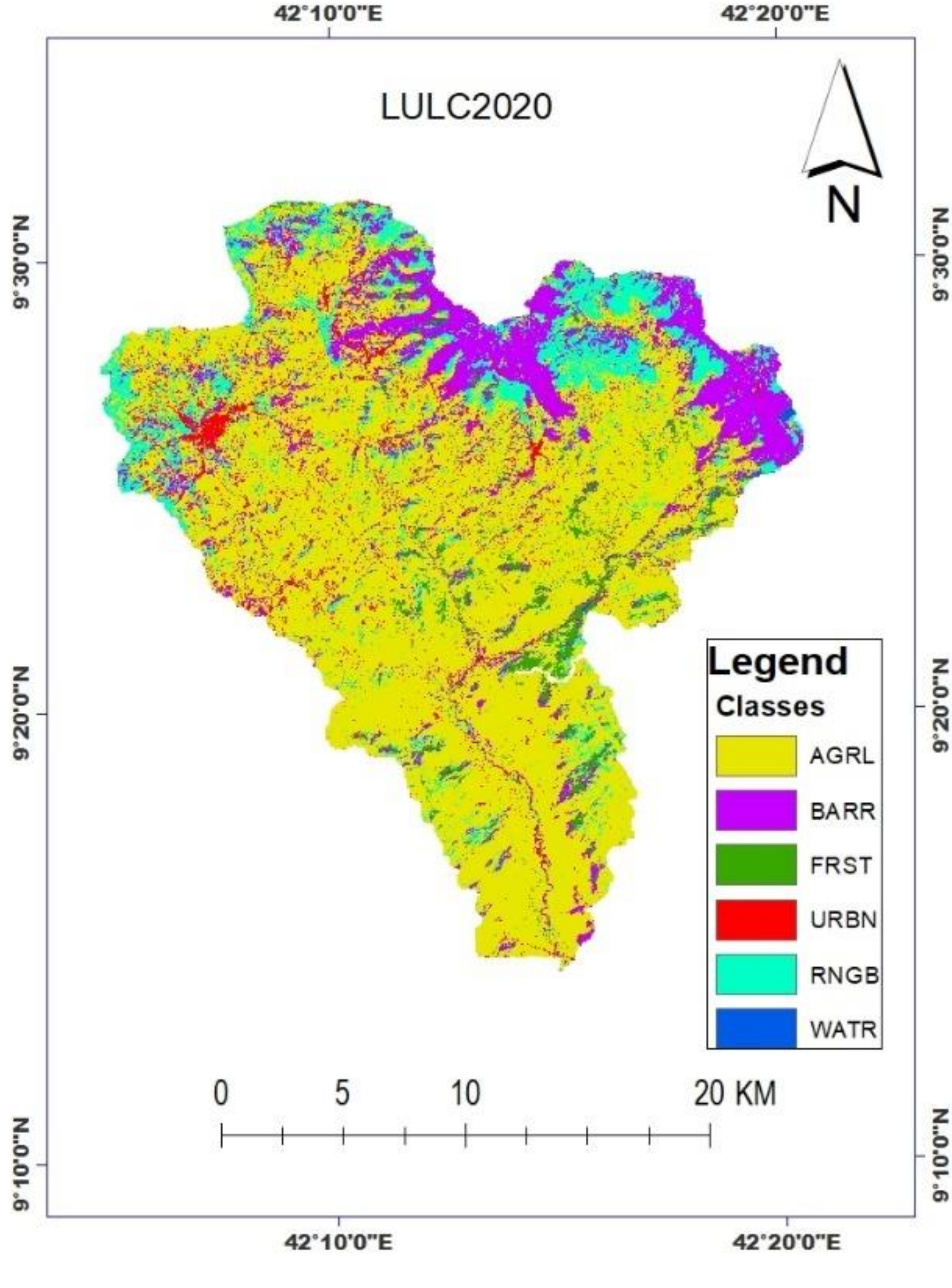

Appendix 12. LULC maps for the year 2020

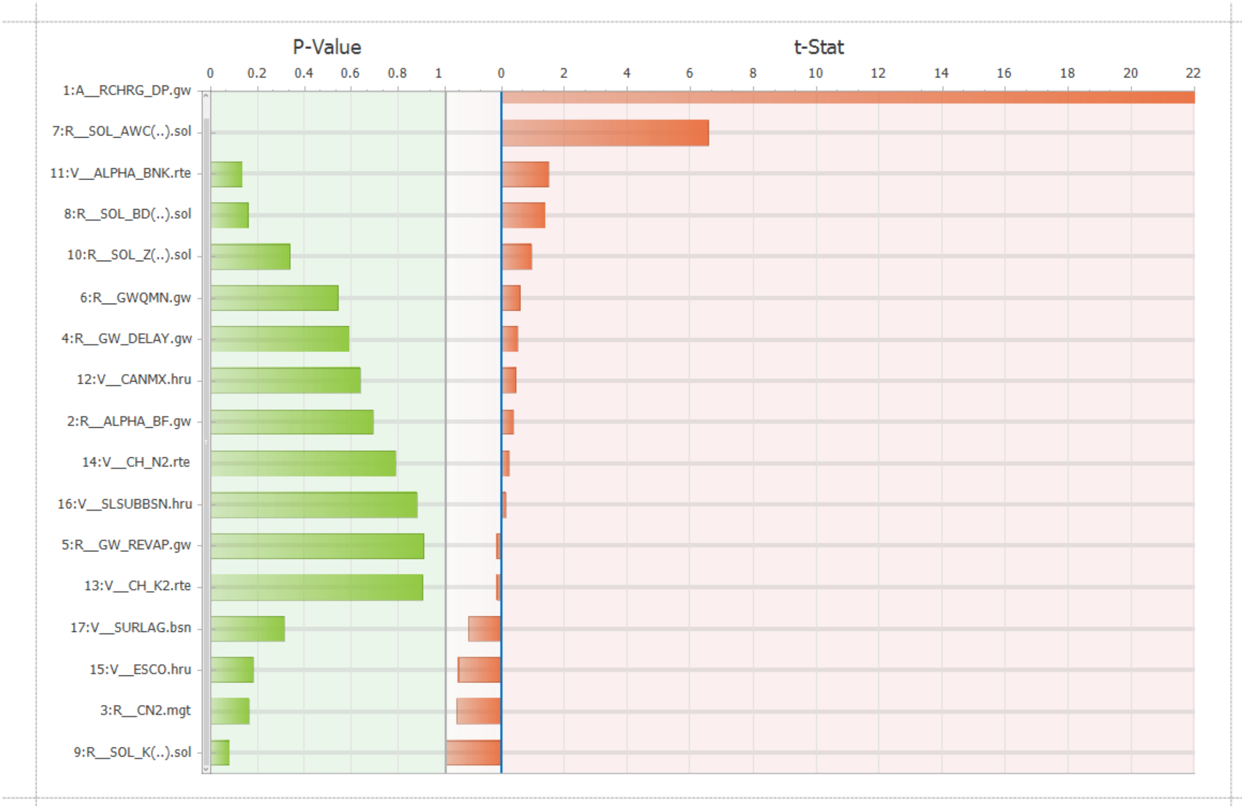

Appendix 13. Global sensitivity analysis results of parameters

Appendix 14. Sensitive parameter description and their values (default, fitted, minimum and maximum ranges). The abbreviations Min. and Max. denotes the minimum and maximum ranges, respectively.

Parameter Name	**Description (unit)**	**Default values**	**Final fitted values**	**Min. range**	**Max. range**
CN2_mgt	Initial-soil-conservation-service (SCS)-curve-number-2 (none)	65	72.5	35	98
SOL_AWC (1) _sol	Soil-water-available- capacity (millimeters H2O/mm soil)	0.092	0.097	0	1
SOL_K (1) _sol	Saturated-hydraulic-conductivity (millimeters /hrs.)	7.04	21.12	0	200
ESCO_hru	Soil-evaporation-compensation-factor (none)	0.95	0.92	0.01	1
EPCO_hru	Plant-uptake-compensation-factor (none)	1	0.98	0	1
GWQMN_gw	Threshold-water-level-in-shallow-aquifer-for-baseflow (millimeters)	1000	1300	0	5000
REVAPMN_gw	Threshold-depth-of-water-in-the-shallow-aquifer-for “revap.” to-occur (millimeters)	750	75	0	500
GW_REVAP_gw	Groundwater – ‘revap.’-coefficient (none)	0.02	0.018	0.02	0.2
SURLAG_bsn	Surface-runoff-lag-coefficient (none)	4	2.5	0.05	24
RCHRG_DP_gw	Deep-aquifer-percolation-fraction (none)	0.05	0.042	0	1

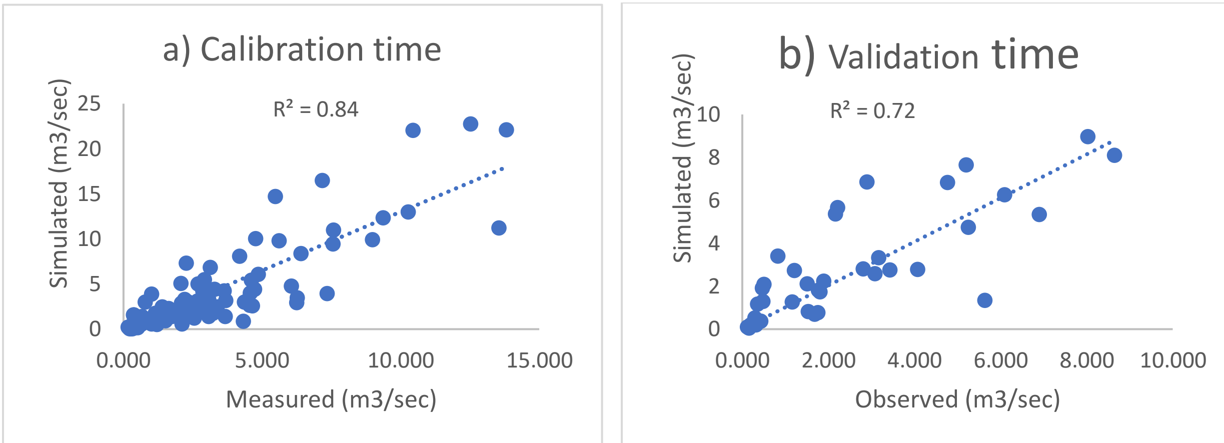

Appendix 15. Scatter plot of measured and predicted monthly streamflow for a) calibration and b) validation time.

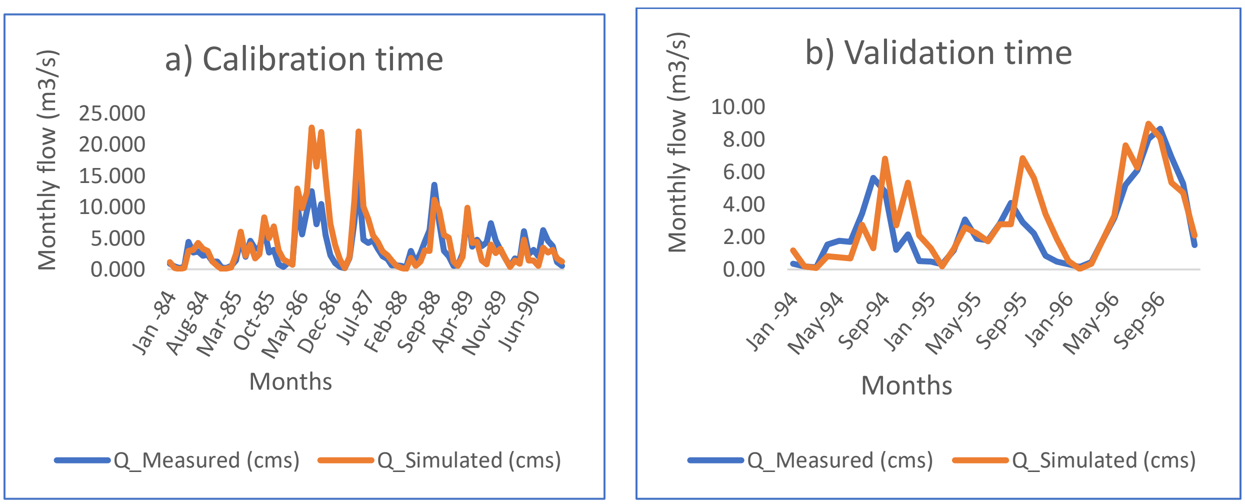

Appendix 16. Monthly runoff hydrograph for a) calibration and b) validation time

Appendix 17. Joint probability of rain days for daily, decadal, monthly and seasonal estimation

Number of combined stations	Combinations	Joint probability of rain days for daily (%)	Joint probability of rain days for decadal (%)	Joint probability of rain days for monthly (%)	Joint probability of rain days for Summer (%)	Joint probability of rain days for Spring (%)
5	Dire Dawa-Grawa-Gursum-Haramaya-Harar	2.52	25.37	39.47	68.42	67.42
4	Dire Dawa-Grawa-Gursum-Haramaya	3.22	30.48	47.15	73.68	76.32
4	Dire Dawa-Grawa-Gursum-Harar	2.97	30.48	47.15	73.68	76.32
4	Dire Dawa-Grawa-Haramaya-Harar	5.48	27.92	41.23	68.42	67.42
4	Dire Dawa-Gursum-Haramaya-Harar	3.49	29.39	44.08	71.05	70.05
4	Grawa-Gursum-Haramaya-Harar	3.92	29.53	42.76	71.05	70.05
3	Dire Dawa-Grawa-Gursum	4.05	36.55	55.92	84.21	86.84
3	Grawa-Gursum-Haramaya-	5.48	35.60	50.44	76.32	78.95
3	Gursum-Haramaya-Harar	6.06	35.01	48.90	73.68	73.35
3	Dire Dawa-Haramaya-Harar	8.14	35.45	50.00	78.95	76.32
3	Grawa-Haramaya-	9.16	33.48	46.05	71.05	71.02

Number of combined stations	Combinations	Joint probability of rain days for daily (%)	Joint probability of rain days for decadal (%)	Joint probability of rain days for monthly (%)	Joint probability of rain days for Summer (%)	Joint probability of rain days for Spring (%)
	Harar					
3	Dire Dawa-Gursum-Haramaya	4.65	35.60	52.85	76.32	78.95
3	Grawa-Gursum-Harar	5.52	36.26	51.97	81.58	81.36
2	Dire Dawa-Grawa	9.09	42.76	60.75	86.84	86.65
2	Dire Dawa-Gursum	7.04	43.27	62.50	86.84	89.24
2	Dire Dawa-Haramaya	10.60	44.96	61.40	86.84	84.21
3	Dire Dawa-Harar	10.10	44.15	61.40	89.47	86.84
2	Grawa-Gursum	8.51	43.27	60.53	86.84	89.47
2	Grawa-Haramaya	12.80	41.59	54.61	78.95	78.45
2	Grawa-Harar	13.03	42.25	56.80	81.58	81.26
2	Gursum-Haramaya	8.86	42.69	58.11	78.95	81.58
2	Gursum-Harar	9.62	43.64	59.43	84.21	84.01
2	Haramaya-Harar	15.30	44.30	57.68	81.58	78.95

Appendix 18. Joint arithmetic average areal rainfall estimation for daily, decadal, monthly and seasonal

Number of combined stations	Combinations	Joint arithmetic mean for daily (mm)	Joint arithmetic mean for decadal (mm)	Joint arithmetic mean for monthly (mm)	Joint arithmetic mean for Summer (mm)	Joint arithmetic mean for Spring (mm)
5	Dire Dawa-Grawa-Gursum-Haramaya-Harar	2.25	19.49	58.48	89.89	67.35
4	Dire Dawa-Grawa-Gursum-Haramaya	2.25	19.62	58.86	90.18	68.05
4	Dire Dawa-Grawa-Gursum-Harar	2.23	19.62	58.86	90.18	68.05
4	Dire Dawa-Grawa-Haramaya-Harar	2.21	19.25	57.76	89.79	65.39
4	Dire Dawa-Gursum-Haramaya-Harar	2.15	18.81	56.42	86.70	64.83
4	Grawa-Gursum-Haramaya-Harar	2.41	20.30	60.91	95.02	69.24
3	Dire Dawa-Grawa-Gursum	2.23	19.64	58.93	87.46	70.79
3	Grawa-Gursum-Haramaya-	2.48	20.75	62.24	97.10	70.81
3	Gursum-Haramaya-Harar	2.21	19.66	58.97	92.47	66.52
3	Dire Dawa-Haramaya-Harar	2.15	18.26	54.78	85.49	61.38
3	Grawa-Haramaya-	2.41	20.26	60.77	96.58	67.26

Number of combined stations	Combinations	Joint arithmetic mean for daily (mm)	Joint arithmetic mean for decadal (mm)	Joint arithmetic mean for monthly (mm)	Joint arithmetic mean for Summer (mm)	Joint arithmetic mean for Spring (mm)
	Harar					
3	Dire Dawa-Gursum-Haramaya	2.23	18.75	56.25	86.02	64.93
3	Grawa-Gursum-Harar	2.48	20.55	61.66	93.92	72.38
2	Dire Dawa-Grawa	2.31	19.24	57.73	86.03	68.59
2	Dire Dawa-Gursum	2.06	18.35	55.04	79.86	67.48
2	Dire Dawa-Haramaya	2.39	17.90	53.71	83.86	59.81
3	Dire Dawa-Harar	1.98	17.61	52.83	79.08	62.15
2	Grawa-Gursum	2.56	21.34	64.02	96.49	76.30
2	Grawa-Haramaya	2.48	20.90	62.69	100.49	68.62
2	Grawa-Harar	2.45	20.61	61.82	95.71	70.97
2	Gursum-Haramaya	2.36	20.00	60.00	94.32	67.52
2	Gursum-Harar	2.31	19.71	59.12	89.55	69.86
2	Haramaya-Harar	2.25	19.26	57.79	93.54	62.19

Appendix 19. Regression analysis for stage and observed discharge reading

No	H (m)	Qo (m3/sec)	H + a	Qs=c (h + a) ^n	(Qo-Qs) ^2
1	0.23	2.80	1.38	2.55	0.06
2	0.24	2.94	1.39	2.65	0.09
3	0.28	2.59	1.43	3.06	0.22
4	0.30	2.41	1.45	3.29	0.78
5	0.35	3.26	1.50	3.92	0.44
6	0.35	3.27	1.50	3.92	0.42
7	0.36	4.00	1.51	4.05	0.00
8	0.40	5.33	1.55	4.64	0.48
9	0.47	5.33	1.62	5.83	0.24
10	0.50	5.33	1.65	6.40	1.15
11	0.51	5.33	1.66	6.61	1.62
12	0.52	5.33	1.67	6.81	2.19
13	0.54	5.34	1.69	7.25	3.65
14	0.55	5.34	1.70	7.47	4.55
15	0.58	5.34	1.73	8.17	8.05
16	0.60	5.34	1.75	8.67	11.13
17	0.63	5.34	1.78	9.47	17.05
18	0.66	5.34	1.81	10.32	24.77
19	0.68	5.91	1.83	10.92	25.08
20	0.70	6.29	1.85	11.55	27.71
21	0.75	7.93	1.90	13.25	28.31
22	0.78	17.14	1.93	14.37	7.67
23	0.84	21.18	1.99	16.83	18.94
24	0.85	25.28	2.00	17.27	64.15
25	0.86	25.84	2.01	17.72	65.97
26	0.88	25.58	2.03	18.65	48.08
27	0.88	25.61	2.03	18.65	48.55
28	0.94	29.98	2.09	21.67	69.15
29	0.96	28.56	2.11	22.76	33.65
30	1.18	34.91	2.33	37.96	9.28
31	1.20	34.94	2.35	39.67	22.35
32	1.24	35.00	2.39	43.28	68.55
33	1.72	105.24	2.87	111.26	36.30
34	1.80	134.12	2.95	128.22	34.84

Appendix 20. SWAT output for historical period under bias corrected historical climate model data

SWAT May 26 VER 2020/Rev 681

General Input/Output section (file.cio):

7/1/2023 12:00:00 AM ARCGIS-SWAT interface AV

AVE ANNUAL BASIN VALUES

PRECIP = 1012.0 MM

SNOW FALL = 0.00 MM

SNOW MELT = 0.00 MM

SUBLIMATION = 0.00 MM

SURFACE RUNOFF Q = 68.11 MM

LATERAL SOIL Q = 77.85 MM

TILE Q = 0.00 MM

GROUNDWATER (SHAL AQ) Q = 111.81 MM

GROUNDWATER (DEEP AQ) Q = 8.11 MM

REVAP (SHAL AQ => SOIL/PLANTS) = 35.03 MM

DEEP AQ RECHARGE = 8.13 MM

TOTAL AQ RECHARGE = 156.34 MM

TOTAL WATER YLD = 265.89 MM

PERCOLATION OUT OF SOIL = 156.39 MM

ET = 709.2 MM

PET = 1971.7MM

TRANSMISSION LOSSES = 0.00 MM

SEPTIC INFLOW = 0.00 MM

TOTAL SEDIMENT LOADING = 48.07 T/HA

TILE FROM IMPOUNDED WATER = 0.000 (MM)

EVAPORATION FROM IMPOUNDED WATER = 0.000 (MM)

SEEPAGE INTO SOIL FROM IMPOUNDED WATER = 0.000 (MM)

OVERFLOW FROM IMPOUNDED WATER = 0.000 (MM)

Appendix 21. SWAT output for Projected period under RCP-4.5 climate model data

SWAT May 26 VER 2020/Rev 681

General Input/Output section (file.cio):

7/1/2023 12:00:00 AM ARCGIS-SWAT interface AV

AVE ANNUAL BASIN VALUES

PRECIP = 979.1 MM

SNOW FALL = 0.00 MM

SNOW MELT = 0.00 MM

SUBLIMATION = 0.00 MM

SURFACE RUNOFF Q = 64.50 MM

LATERAL SOIL Q = 77.71 MM

TILE Q = 0.00 MM

GROUNDWATER (SHAL AQ) Q = 102.26 MM

GROUNDWATER (DEEP AQ) Q = 7.57 MM

REVAP (SHAL AQ => SOIL/PLANTS) = 35.06 MM

DEEP AQ RECHARGE = 7.59 MM

TOTAL AQ RECHARGE = 145.89 MM

TOTAL WATER YLD = 252.04 MM

PERCOLATION OUT OF SOIL = 145.94 MM

ET = 691.0 MM

PET = 1981.5MM

TRANSMISSION LOSSES = 0.00 MM

SEPTIC INFLOW = 0.00 MM

TOTAL SEDIMENT LOADING = 45.59 T/HA

TILE FROM IMPOUNDED WATER = 0.000 (MM)

EVAPORATION FROM IMPOUNDED WATER = 0.000 (MM)

SEEPAGE INTO SOIL FROM IMPOUNDED WATER = 0.000 (MM)

OVERFLOW FROM IMPOUNDED WATER = 0.000 (MM)

Appendix 22. SWAT output for LULC-2001 under observed temperature and rainfall data

SWAT May 26 VER 2020/Rev 681

General Input/Output section (file.cio):

4/4/2023 12:00:00 AM ARCGIS-SWAT interface AV

AVE ANNUAL BASIN VALUES

PRECIP = 844.4 MM

SNOW FALL = 0.00 MM

SNOW MELT = 0.00 MM

SUBLIMATION = 0.00 MM

SURFACE RUNOFF Q = 75.82 MM

LATERAL SOIL Q = 63.85 MM

TILE Q = 0.00 MM

GROUNDWATER (SHAL AQ) Q = 85.17 MM

GROUNDWATER (DEEP AQ) Q = 5.41 MM

REVAP (SHAL AQ => SOIL/PLANTS) = 34.81 MM

DEEP AQ RECHARGE = 5.45 MM

TOTAL AQ RECHARGE = 129.68 MM

TOTAL WATER YLD = 230.25 MM

PERCOLATION OUT OF SOIL = 130.00 MM

ET = 574.2 MM

PET = 1934.0MM

TRANSMISSION LOSSES = 0.00 MM

SEPTIC INFLOW = 0.00 MM

TOTAL SEDIMENT LOADING = 54.92 T/HA

TILE FROM IMPOUNDED WATER = 0.000 (MM)

EVAPORATION FROM IMPOUNDED WATER = 0.000 (MM)

SEEPAGE INTO SOIL FROM IMPOUNDED WATER = 0.000 (MM)

OVERFLOW FROM IMPOUNDED WATER = 0.000 (MM)

Appendix 23. SWAT output for LULC-2020 under observed temperature and rainfall data

SWAT May 26 VER 2020/Rev 681

General Input/Output section (file.cio):

4/5/2023 12:00:00 AM ARCGIS-SWAT interface AV

AVE ANNUAL BASIN VALUES

PRECIP = 844.4 MM

SNOW FALL = 0.00 MM

SNOW MELT = 0.00 MM

SUBLIMATION = 0.00 MM

SURFACE RUNOFF Q = 80.39 MM

LATERAL SOIL Q = 65.03 MM

TILE Q = 0.00 MM

GROUNDWATER (SHAL AQ) Q = 97.78 MM

GROUNDWATER (DEEP AQ) Q = 5.97 MM

REVAP (SHAL AQ => SOIL/PLANTS) = 34.81 MM

DEEP AQ RECHARGE = 6.01 MM

TOTAL AQ RECHARGE = 143.16 MM

TOTAL WATER YLD = 249.18 MM

PERCOLATION OUT OF SOIL = 143.50 MM

ET = 555.0 MM

PET = 1934.0MM

TRANSMISSION LOSSES = 0.00 MM

SEPTIC INFLOW = 0.00 MM

TOTAL SEDIMENT LOADING = 71.43 T/HA

TILE FROM IMPOUNDED WATER = 0.000 (MM)

EVAPORATION FROM IMPOUNDED WATER = 0.000 (MM)

SEEPAGE INTO SOIL FROM IMPOUNDED WATER = 0.000 (MM)

OVERFLOW FROM IMPOUNDED WATER = 0.000 (MM)

Appendix 24. Average monthly hydrological components for references, future scenario (RCP-4.5 and RCP-8.5) in Upper Erer subbasin

MONTHS	RAINFALL (mm)	SURF Q (mm)	LAT Q (mm)	WATER YIELD (mm)	ET (mm)	PET (mm)
Reference period (1979-2014)						
Jan/	10.64	0.01	0.68	2.24	16.76	148.23
Feb/	31.61	1.28	1.75	3.61	22.9	150.68
Mar/	81.89	2.85	4.85	8.49	59.99	173.6
Apr/	159	15.89	10.57	30	103.34	161.52
May	117.53	7.97	8.47	25.57	117.66	174.24
Jun/	79.36	2.08	5.51	15.54	86.69	187.99
Jul/	141.46	8.22	9.15	21.58	78.2	178.04
Aug/	164.25	14.78	14.06	36.87	62.83	178.22
Sep/	132.16	11.63	13.25	47.94	62.45	166.18
Oct/	62.62	2.69	6.82	41.29	50.42	156.95
Nov/	17.85	0.4	1.8	23.67	28.09	151.36
Dec/	13.34	0.27	0.93	9.05	19.72	143.41
Projected period (2024-2070) under RCP-4.5 scenario						
Jan/	13.38	0.02	0.82	2.45	17.34	146.64
Feb/	28.45	1.43	1.52	3.53	20.97	152.51
Mar/	71.94	3.03	4.24	8.05	54.9	176.72
Apr/	153.62	13.76	10.3	27.1	103.03	162.11
May	110.15	6.71	7.64	22.03	114.55	175.09
Jun/	75.35	1.59	5.07	12.94	81.52	190.41
Jul/	135.22	6.05	8.67	17.93	76.76	176.78
Aug/	169.99	17.1	14.21	38.24	63.51	179.84
Sep/	132.18	12.06	13.32	47.28	63.54	166.16
Oct/	55.82	2.24	6.21	38.95	48.1	160.16
Nov/	22.71	0.61	2.12	23.53	28.16	150.5
Dec/	10.01	0.12	0.88	9.08	19.22	143.22
Projected period (2024-207) under RCP-8.5 scenario						
Jan/	13.38	0.02	0.85	2.47	17.31	146.64
Feb/	28.45	1.42	1.6	3.59	20.94	152.51
Mar/	71.94	3.02	4.42	8.22	54.83	176.72
Apr/	153.62	13.72	10.72	27.44	102.96	162.11
May	110.15	6.68	7.89	22.15	114.37	175.09
Jun/	75.35	1.58	5.25	13	81.33	190.41
Jul/	135.22	6.02	9.05	18.22	76.67	176.78
Aug/	169.99	17.03	14.75	38.6	63.48	179.84
Sep/	132.18	12.04	13.74	47.37	63.51	166.16
Oct/	55.82	2.24	6.35	38.67	48.06	160.16
Nov/	22.71	0.61	2.18	23.3	28.13	150.5
Dec/	10.01	0.12	0.9	8.98	19.19	143.22

Appendix 25. Average annual surface runoff and average daily water supply from the upper Erer River outlet and Harar town estimated average daily water demand.

Impact conditions	For LULC change		For Climate change		
Periods/ year under consideration	2001	2020	Historical	Future period	
				RCP-4.5	RCP-8.5
Surface runoff (mm)	75.82	80.39	68.11	64.50	64.72
Surface runoff (m^3/day)	96,800.32	102,634.9	86,956.87	82,347.94	82,628.82
Estimated average demand (m^3/day)				139,412.7 (source Table 3.1)	

Note the supply is much less than the estimated daily average demand for the year 2070 (around 139,412.7 m^3/day).